Muscle wasting

The role of the ubiquitin-proteasome pathway in muscle atrophy and remodeling

The study presented in this thesis was performed within the Nutrition and Toxicology Research Institute Maastricht (NUTRIM) which participates in the Graduate School VLAG (Food Technology, Agrobiotechnology, Nutrition and Health Sciences), accredited by the Royal Netherlands Academy of Arts and Sciences.

Coverdesign: Datawyse / Universitaire Pers Maastricht
Layout: Ronnie Minnaard
Printed by: Datawyse / Universitaire Pers Maastricht

ISBN-10: 90-5278-558-9
ISBN-13: 978-90-5278-558-5

Muscle wasting

The role of the ubiquitin-proteasome pathway in muscle atrophy and remodeling

PROEFSCHRIFT

ter verkrijging van de graad van doctor
aan de Universiteit Maastricht
op gezag van de Rector Magnificus,
Prof. mr. G.P.M.F. Mols
volgens het besluit van het College van Decanen,
in het openbaar te verdedigen
op donderdag 21 september om 12:00 uur

door

Ronnie Minnaard

geboren te Goes op 12 juli 1977

UNIVERSITAIRE PERS MAASTRICHT

Promotores:

Prof. dr. H. Kuipers
Prof. dr. A.J.M. Wagenmakers

Copromotores:

Dr. M.K.C. Hesselink
Dr. ir. M.R. Drost

Beoordelingscommissie:

Prof. dr. E.F.M. Wouters (voorzitter)
Dr. C. Dejong
Prof. dr. E.C.M. Mariman
Dr. O. Rooyackers (Karolinska University Hospital, Huddinge, Sweden)
Prof. dr. ir. W. Saris

Contents

1

General Introduction

Background

Skeletal muscle is the most abundant tissue in the human body accounting, for 40-45% of the total body weight. The main function of skeletal muscle is to provide power for locomotion and to keep posture. A decrease of skeletal muscle mass can therefore impair human movement, leading to difficulties in performing the activities of daily living. Moreover, skeletal muscle is the major site of metabolic activity. It accounts for a large part of glucose disposal from the circulation (either stored as glycogen or directly oxidized) and therefore it is a critical organ for regulating blood glucose levels. Skeletal muscle is also the major reservoir of protein (±50% of total body protein) and free amino-acids in the body. During periods of food deprivation muscle is the major source of amino acids (mainly glutamine and alanine) used for glucose production (gluconeogenesis) in the liver. During catabolic (inflammatory) diseases, such as sepsis, cancer and severe trauma, the decrease of muscle mass provides amino acids essential for wound healing and synthesis of antibodies and acute phase proteins. Although this loss of muscle protein is necessary to fight the underlying disease, an uncontrolled decrease of muscle mass can be very detrimental to the body, because of the essential functions of this tissue in locomotion and metabolism. In addition, a vital function like respiration is also supported by skeletal muscle function, making uncontrolled muscle wasting life threatening.

Muscle wasting occurs in several conditions, including sepsis, cancer, starvation, denervation, disuse, etc. Although the trigger for muscle wasting can be different in these conditions, muscle wasting always reflects an imbalance between protein synthesis and protein breakdown. A net loss of muscle protein will occur when muscle protein breakdown exceeds protein synthesis. Thus, muscle wasting can be caused by an increased protein breakdown, a decreased protein synthesis, or a combination of both. It has been shown that an increased muscle protein breakdown plays a crucial role in many conditions leading to muscle atrophy. A detailed knowledge of the cellular mechanisms that are responsible for the increased protein breakdown is critical to develop interventions for maintaining muscle mass during these conditions.

Proteolysis in conditions of muscle atrophy

Muscle proteins, like the proteins in other tissues, are constantly turning over, meaning that they are continuously degraded and newly synthesized. The rate of turnover varies greatly between different types of proteins. For example, some regulatory enzymes can have half-lives as short as 15 minutes, while it may take many weeks for the myofibrillar proteins actin and myosin to turn over once. It has become clear that the majority of eukaryotic cell proteins are degraded by the ubiquitin-proteasome (Ub-P) pathway. Besides the Ub-P pathway, muscle cells contain several other proteolytic pathways to carry out the degradation of specific classes of proteins. Lysosomal cathepsins, which mainly degrade membrane proteins and extracellular proteins (e.g. plasma proteins and hormones), form the most widely studied proteolytic pathway (1). Another proteolytic pathway active in skeletal muscle is the Ca^{2+}-dependent calpain system, of which the exact substrates are unknown (2).

Although a continuous breakdown of muscle proteins is required to ensure a constant protein turnover, an accelerated proteolysis is the major cause for muscle wasting in several conditions. In animal models, an increased rate of proteolysis has been observed in muscles atrophying as a result of sepsis (3, 4), fasting (5, 6), cancer (7, 8), denervation (6, 9) and disuse (10). In these experiments, proteolysis was measured by monitoring the tyrosine release from incubated muscles. In all of these catabolic states it was shown that incubating the muscles with inhibitors of lysosomal proteases and calpains did not significantly reduce the increased proteolysis. Depletion of ATP, however, completely normalized or greatly reduced the increased proteolysis. These studies suggested that an ATP-dependent, non-lysosomal proteolytic system accounted for a large part of the increased proteolysis in several conditions of muscle atrophy. It was only after specific inhibitors of the proteasome (11) became available that it could be demonstrated that most of the increased proteolysis in several catabolic states indeed occurred through the ATP-dependent Ub-P pathway (12-14). It must be noted that most studies in catabolic animal models use the tyrosine-release method, which gives a measure of the overall muscle proteolysis, as tyrosine occurs in all muscle proteins. Because the half-lives of muscle proteins vary from ~15 minutes to several weeks, proteolysis rates acquired with this method do not necessarily reflect the actual muscle protein wasting. The reason for this is that the rapid degradation of short-lived proteins may have a greater

impact on tyrosine release (typically measured over 2-3 h) than the slower degradation of long-lived proteins, like the very abundant myofibrillar proteins. An important observation in this respect was that proteasome inhibitors, but not inhibitors of other proteases, suppressed the increased 3-methylhistidine (3-MH) release from incubated septic muscles (15). The release of 3-MH reflects the breakdown of the myofibrillar proteins actin and myosin, as this amino acid only occurs in these two proteins (3-MH is formed by post-translational modification of histidine residues present in actin and myosin heavy chains). Therefore, this study demonstrated a major role for the Ub-P pathway in accelerating proteolysis of myofibrillar proteins during muscle atrophy (15).

Although there is a universal agreement that an increased activity of the Ub-P pathway is essential for the development of muscle atrophy, the important observation that this pathway cannot degrade intact myofibrils (16) suggests that other proteases have to be activated simultaneously to release actin and myosin from the myofibrils. There is evidence that both the calpains and caspase-3 can trigger this release of myofilaments in conditions of muscle atrophy (17, 18). In septic rats, it was found that the increased release of myofilaments from the myofibrils was inhibited by dantrolene (a substance which inhibits the release of calcium from intracellular stores) and that the gene expression of m-calpain, μ-calpain and the muscle-specific calpain p94 was increased in the muscles of these rats (19). Contradicting results have been obtained in muscles atrophying as a result of insulin deficiency or uremia. In these conditions it was shown that caspase-3, rather than calpains, accounted for the increased disassembly of myofibrils and subsequent degradation by the Ub-P pathway (20). At present, it is unclear whether the discrepancy in results is caused by the differing experimental conditions, or whether calpains and caspase-3 complement each other in the disassembly of myofibrils during conditions of muscle atrophy.

Ubiquitin-proteasome-dependent proteolysis

The Ub-P pathway is the major pathway responsible for protein breakdown in mammalian cells (21). This rather complex pathway can be roughly divided into two main steps. In the initial step, proteins are targeted for degradation by the covalent attachment of a chain of ubiquitin molecules.

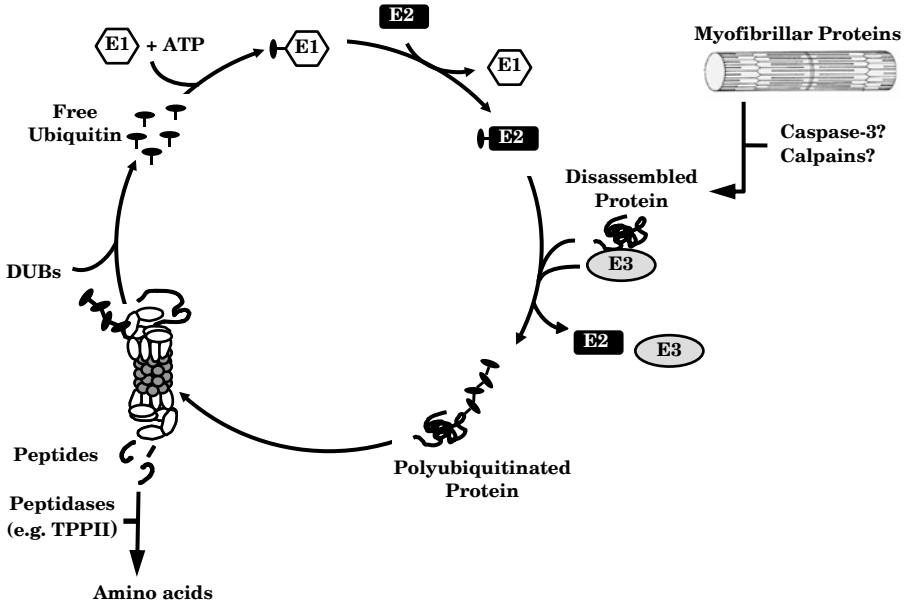

Figure 1: Sequence of events leading to the ubiquitination and subsequent degradation of (myofibrillar) proteins to amino acids. Firstly, ubiquitin is activated by a ubiquitin-activating enzyme (E1) and transferred to a ubiquitin-conjugating enzyme (E2). This E2 enzyme works together with an E3 ubiquitin protein ligase to bind a chain of ubiquitin molecules (polyubiquitination) to the target protein. To be degraded in the Ub-P pathway myofibrillar proteins first have to be released from the myofibrils, possibly through the action of calpains and/or caspase-3. As a result of polyubiquitination, the target protein is recognized by the 26S proteasome, which unfolds and degrades the protein to peptides. These peptides are then degraded to amino acids by several other peptidases (e.g. by TPPII – tripeptidyl peptidase II). The polyubiquitin chain is recycled to free ubiquitin by deubiquitinating enzymes (DUBs).

This process, termed ubiquitin conjugation, (or ubiquitination) is controlled by various ubiquitinating and deubiquitinating enzymes. In the second step, polyubiquitinated proteins are recognized and degraded by the 26S proteasome, a large multi-catalytic protein complex. A schematic overview of the degradation of (myofibrillar) proteins by the Ub-P pathway is given in Figure 1.

Ubiquitin conjugation

Ubiquitin is a protein comprising 76 amino acids and is extremely conserved in eukaryotic cells. Ubiquitin conjugation is a post-translational modification involved in proteolysis, but is also important in several other cellular processes, e.g. endocytosis of membrane proteins, transcriptional regulation, DNA repair and replication (22, 23). It has been shown that

proteins must be tagged by a chain of at least four ubiquitin molecules (polyubiquitination) in order to be recognized and degraded by the 26S proteasome (24). Although many cellular proteins are known to be substrates of the Ub-P pathway, the signals that mark these proteins for polyubiquitination and subsequent degradation are less well-known (reviewed in (25)). One such recognition signal is the presence of a bulky, hydrophobic N-terminal amino acid in the protein, leading to proteasomal degradation of the protein in a process termed the 'N-end rule pathway' (26). Phosphorylation is another important mechanism marking proteins for polyubiquitination (25). The conjugation of ubiquitin to target proteins is a complex process requiring action of three different classes of ubiquitinating enzymes. Firstly, the ubiquitin-activating enzyme (E1) uses ATP to activate and bind ubiquitin. This step renders ubiquitin active for the complete downstream ubiquitin conjugation pathway. Secondly, the activated ubiquitin is transferred to a ubiquitin conjugating enzyme (E2). Thirdly, ubiquitin protein ligases (E3s) are involved in the selective recognition and binding of protein substrates. These E3 enzymes also bind to E2 enzymes, thereby transferring ubiquitin from the E2 enzyme to a lysine residue on the protein substrate. A polyubiquitin chain is then formed by the binding of additional activated ubiquitin moieties to the preceding conjugated ubiquitin moiety. The ubiquitinating enzymes are organized in a hierarchical fashion, permitting the selective polyubiquitination of specific proteins. There is only one ubiquitin activating enzyme (E1), which supplies activated ubiquitin to a family of ubiquitin conjugating enzymes (E2s), containing approximately fifty members. Each of these E2 enzymes interacts with a specific subset of ubiquitin protein ligases (E3s), giving the ubiquitin-proteasome pathway its ability to very selectively target a vast number of different proteins (27).

The ubiquitin conjugation process is also controlled by the activity of deubiquitinating enzymes. Analogous to the E3 enzymes there are a lot of different deubiquitinating enzymes, which are only now beginning to be identified. Although the exact function of most deubiquitinating enzymes is unknown at present, several putative functions of these enzymes in proteasome-dependent proteolysis have been proposed (28). They have been proposed to help maintain free ubiquitin levels by releasing polyubiquitin chains from the 26S proteasome after degradation of the protein and by

recycling ubiquitin from poly-ubiquitin chains. Moreover, these enzymes may also deubiquitinate proteins mistakenly targeted for degra-dation.

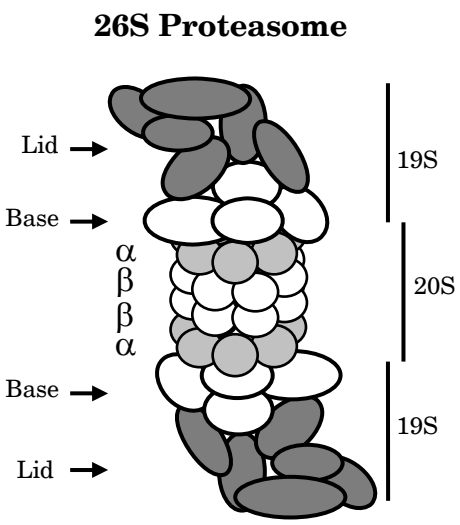

Figure 2: Schematic representation of the 26S proteasome and its subcomplexes. The composition of the 26S proteasome is described in the text.

The 26S Proteasome

The binding of a polyubiquitin chain marks proteins for degradation by the 26S proteasome, a large multicatalytic complex (~2500 kDa). The 26S proteasome consists of a large proteolytic core complex (20S proteasome) associated with two regulatory 19S proteasome complexes (see Figure 2). The 20S proteasome has a barrel-shaped form, consisting of a stack of four rings. Each ring is made up of seven subunits, with the α-subunits forming the outer rings and the β-subunits forming the inner rings. The proteolytic active sites of the 20S proteasome are located inside the cylinder on the β-subunits. The three main proteolytic activities of the 20S proteasome are the chymotrypsin-, trypsin- and caspase-like activities, each situated on different β-subunits (29). These activities cleave proteins after hydrophobic, basic and acidic amino acid residues, respectively, and hydrolyze proteins to peptides of typically 4-25 amino acids (30). The activity of additional peptidases is therefore required to completely degrade proteins to amino acids. By itself, the 20S proteasome cannot degrade proteins, as they are too large to pass the narrow opening in the α-subunits. It requires the binding of proteasome activators to open the catalytic channel by inducing a conformational change of the α-subunits. The most well known proteasome activator is the 19S proteasome complex, also called proteasome activator 700 (PA700). Two of these complexes bind to the 20S proteasome to form the 26S proteasome. Like the 20S proteasome, the 19S proteasome is composed of at least 18 different subunits (both ATPase and non-ATPase), organized in two subcomplexes named the base and the lid. The most important functions of

the 19S proteasome are to recognize polyubiquitinated proteins (24) and to unfold and translocate these proteins into the 20S proteasome (30-32).

The Ub-P pathway is regulated at different levels during muscle atrophy

As is shown in Figure 1, the degradation of a protein substrate by the Ub-P pathway occurs through a cascade of reactions eventually leading to polyubiquitination and subsequent degradation of the protein by the 26S proteasome. To gain insight into the role of the Ub-P pathway during muscle atrophy it is important to identify the components of the pathway that determine the rate of Ub-P dependent proteolysis. Identifying these rate-limiting steps is complicated, for they may vary between different catabolic conditions, and because the pathway contains numerous parallel Ub-conjugating pathways of different E2 and E3 enzymes to target specific muscle proteins for degradation. Despite these difficulties, the knowledge on the regulation of the Ub-P pathway during muscle atrophy has expanded considerably in the recent years, the most important aspects of which will be highlighted in this paragraph.

Ubiquitin conjugation

There are several lines of evidence which suggest that the enhanced Ub-P dependent proteolysis during muscle atrophy results from accelerated ubiquitin conjugation to protein substrates. Firstly, there are several studies which revealed that Ub-protein conjugates accumulate in muscles atrophying as a result of fasting, denervation (33), sepsis (34), cancer (8), and diabetes (35). These experiments suggest that an increased rate of Ub-conjugation to muscle proteins is an important condition for muscle atrophy. However, ensure that it indeed was an increased activation of the ubiquitination machinery (E1, E2 and E3 enzymes) and not a compromised degradation of these conjugates by the proteasome, causing the increased muscle levels of Ub-protein conjugates, experiments were performed in muscle extracts to measure the rate of conjugation of exogenous, I^{125}-labelled Ub to muscle proteins. These studies clearly showed that rates of Ub-conjugation were increased during muscle atrophy caused by sepsis, cancer, thyroid hormone treatment (36), diabetes (35) and burn-injury (37),

suggesting that this is an important mechanism responsible for the increased proteolysis in many conditions of muscle atrophy. However, the exact proteins that are ubiquitinated in skeletal muscle remain to be identified.

An important question still remained as to which specific enzymes of the very large numbers involved in Ub-conjugation are responsible for the activation of proteolysis during muscle atrophy. The 14 kDa E2 and E3α enzymes were the first candidates to be implicated in the atrophy process. These enzymes work together to ubiquitinate proteins that have bulky, hydrophobic or basic amino acids at their N-terminus, a process termed the N-end rule pathway (38, 39). In extracts from muscles atrophying as a result of cancer, sepsis and diabetes it was shown that the increased Ub-conjugation occurred largely through the N-end rule pathway (35, 36, 40). In addition, increases in the skeletal muscle mRNA expression of both 14 kDa E2 and E3α have been found in a large variety of catabolic conditions (41, 42), but attempts to correlate these mRNA levels with the levels of their respective proteins have failed (35, 43). An important role for the N-end rule pathway is also questioned by findings in 14 kDa E2 knock-out mice, which show similar rates of muscle atrophy and formation of ubiquitin conjugates as their wild-type littermates in response to starvation (44). Moreover, E3α knockouts are viable and only display a small decrease of muscle mass compared to their wild-type littermates (45).

In a very important study screening for markers of muscle atrophy, two muscle-specific E3-ligases have been identified, whose expression increased significantly in multiple models of muscle atrophy (46). These E3-ligases have been named Muscle Ring Finger1 (MuRF1) and Muscle Atrophy F-box (MAFbx). The MAFbx gene was simultaneously identified by another group, who named it atrogin-1 (47). MuRF1 and atrogin-1/MAFbx are considered to be general markers of muscle atrophy, because an increased expression of both genes has been shown in as many as 13 distinct models of muscle atrophy (48), including sepsis (49) and cancer cachexia (47, 50). Although no good antibodies have been available to determine whether increased MuRF1 and atrogin-1/MAFbx expression is also present at the protein level during muscle atrophy, strong evidence for a critical role of both genes is obtained from MuRF1 and MAFbx knock-out mice. These mice show a 36% and 56% sparing of muscle mass in response to denervation, respectively (46). Therefore, it is extremely important to identify the substrates of these E3-

ligases. It has been suggested that MuRF1 may act by targeting components of the contractile apparatus, because it has been shown to induce ubiquitination of troponin I in cardiomyocytes (51) and to bind to titin at the M-line (52). Recently, MyoD (53) and calcineurin (54) have been suggested as substrates of atrogin-1/MAFbx, but no clear link with muscle atrophy was made in these papers. Besides identifying the substrates of MuRF1 and atrogin-1/MAFbx, much effort has also been put in identifying the signaling routes that are involved in increasing the expression of these genes during muscle atrophy. However, as MuRF1$^{-/-}$ and MAFbx$^{-/-}$ mice only show a partial rescue of muscle mass during denervation (46), it is likely that other candidate genes (probably coding for an E3 Ub-ligase) exist, which are vital for muscle atrophy to occur.

The proteasome

The proteasome is another obvious candidate determining the increased rates of Ub-P dependent proteolysis during conditions of muscle atrophy, as the actual proteolysis takes place inside this protein complex. The findings that Ub-conjugates accumulate in muscles atrophying as a result of several catabolic conditions indicate that the breakdown of Ub-conjugated proteins by the proteasome may be the step determining the rate of Ub-P dependent proteolysis during muscle atrophy (42). Indeed, proteasome activities have been shown to increase in atrophying skeletal muscle in animal models of sepsis (55) and burn injury (56). In addition, increased proteasome activities have been observed in skeletal muscle of gastric cancer patients (57). It is likely that these increased proteasome activities reflect an increased activity of the proteasome itself and not an increase in the amount of proteasomes, because the increased muscle proteasome activities during sepsis (55) and glucocorticoid administration (58) have been found not to be accompanied by increased protein levels of 20S or 19S proteasome subunits. In contrast, studies in several catabolic models, including sepsis (4) and cancer cachexia (7, 8), have shown increased mRNA levels of 19S and 20S proteasome subunits in atrophying muscles (41, 50, 59). Except for one study reporting increased muscular protein levels of a proteasome subunit during cancer cachexia (8), the expression of 19S and 20S proteasome subunits at the protein level was either unchanged or not measured in studies on muscle atrophy (41, 55, 58). Together, these data suggest that there are other

mechanisms for increasing the proteolytic activity of the proteasome during muscle atrophy conditions. The binding of proteasome activators and inhibitors, the assembly of 20S and 19S proteasomes and post-translational modifications (e.g. phosphorylation) of specific proteasome subunits have been shown to be involved in the regulation of the proteolytic activity of the 26S proteasome (42). The role of these mechanisms during muscle atrophy conditions is unknown, however.

Signals activating the Ub-P pathway during conditions of muscle atrophy

Glucocorticoids

Circulating levels of glucocorticoids are increased in sepsis, fasting, insulin-dependent diabetes and several other catabolic conditions (60). Administration of glucocorticoids to rodents leads to muscle atrophy, either by inhibiting muscle protein synthesis (61) or by stimulating muscle protein breakdown (34, 58, 61). By using inhibitors of specific proteolytic pathways it was shown that the Ub-P pathway was responsible for the increased muscle proteolysis after glucocorticoid administration (58). In this study, stimulation of Ub-P dependent proteolysis by glucocorticoids was substantiated by increased mRNA levels for 19S and 20S proteasome subunits, increased Ub-conjugation rates and increased proteasome activity (58). In addition, treating septic rats with the glucocorticoid antagonist RU38486 inhibited the ATP-ubiquitin dependent total and myofibrillar proteolysis, concomitant with a blunted increase of muscle Ub levels (34). Also, it has been shown that RU38486 prevented the increased expression of the critical E3-ligases MuRF1 and atrogin-1/MAFbx during sepsis in rats (49). Likewise, it was shown that adrenalectomy prevented the increased protein breakdown and activation of the Ub-P pathway during fasting (5), insulin-dependent diabetes (62) and acidosis (63, 64). Since it was shown in diabetic and acidotic adrenalectomized rats that giving a high (but physiologic) dose of glucocorticoids could restore the increased proteolysis and activation of the Ub-P pathway, it was concluded that glucocorticoids are necessary but not sufficient to stimulate (Ub-P dependent) proteolysis during conditions of muscle atrophy (62-64).

Cytokines

During sepsis several proinflammatory cytokines have been shown to be involved in the development of muscle atrophy. Cytokines are released by activated macrophages during phagocytosis of bacteria and endotoxins and aid in eliciting host defense responses to invading pathogens, including fever and the production of acute phase proteins. Although the exact origin is unknown, increased levels of circulating proinflammatory mediators are also found in cancer patients and have been implicated in the development of muscle atrophy (65). In rats it has been shown that repeated administration of TNFα, IL-1 and IL-6 alone induced significant muscle atrophy (66-69). Although these cytokines can act by decreasing rates of protein synthesis (70), there is a significant amount of evidence showing that muscle protein breakdown is stimulated by these cytokines (71, 72). Moreover, it has been shown in both sepsis and cancer cachexia that the administration of TNFα antibodies or agents which interfere with TNFα production (xanthine derivatives) suppressed the increased skeletal muscle proteolysis, presumably through a suppressed activation of the Ub-P pathway (73, 74). These observations raise the question as to which are the signals that activate the Ub-P pathway in response to the binding of these cytokines to their cell-surface receptors. Although these signals are just beginning to be identified, both *in vitro* and *in vivo* data implicate the transcription factor NF-κB in stimulating the activity of the Ub-P pathway (75, 76). NF-κB represents a family of transcription factors that mediate a variety of cellular processes, including inflammation, apoptosis and differentiation (77). Under normal conditions NF-κB is inactive and located in the cytoplasm bound to its inhibitory protein IκBα. When TNFα binds to its receptor a cascade of events is initiated resulting in the phosphorylation, ubiquitination and degradation of the inhibitory IκBα protein by the 26S proteasome. This allows NF-κB to enter the nucleus, where it increases the transcription of many genes (78), including many inflammatory ones, making NF-κB a major regulator of inflammatory mediators. Recently, evidence is accumulating that NF-κB is also involved in regulating muscle atrophy (79). Studies in muscle cells showed that TNFα inhibits myocyte differentiation through activation of NF-κB, suggesting that this contributes to muscle atrophy (80, 81). More direct evidence eminates from studies showing that NF-κB can interfere with muscle proteolysis, presumably by regulating the Ub-P pathway. It has been shown in muscle cells that NF-κB

activation is required for the cytokine-induced loss of skeletal muscle proteins (82, 83) and that NF-κB activation is responsible for an increase in Ub-conjugating activity and upregulation of the Ub-conjugating E2 enzyme UbcH2 (76). Recent *in vivo* evidence shows that NF-κB plays an important role in the development of muscle atrophy by activating the Ub-P pathway (75). In this study, NF-κB was selectively activated or inhibited in skeletal muscle of transgenic mice. It was shown that continuous activation of NF-κB caused significant muscle atrophy, partly by increasing the expression of MuRF1 (75). Moreover, muscle atrophy was shown to be accompanied by increased rates of Ub-P dependent proteolysis. Continuous inhibition of NF-κB reduced the muscle atrophy during denervation and cancer cachexia, lending further support for a critical role of NF-κB signaling in the development of muscle atrophy in these models (75).

Aims & outline of this thesis

The general aim of this thesis was to get insight into the role and functioning of the ubiquitin-proteasome pathway in muscle wasting during sepsis and cancer.

For this purpose we aimed to characterize the time-course of muscle atrophy and loss of muscle function in the zymosan sepsis-model in **chapter 2**. Zymosan injection leads to an acute septic state, characterized by rapid muscle wasting. This acute phase is followed by a slow recovery. Our next aim was to study the rate at which two key steps in Ub-P dependent proteolysis, e.g. ubiquitin-conjugation and protein degradation by the proteasome, proceeded during the acute septic phase and subsequent recovery (**chapter 3**). As there is ample data from animal experiments suggesting that the Ub-P pathway is involved in muscle atrophy due to several catabolic conditions, we aimed to translate these findings to the human setting of non-small cell cancer (NSCLC) patients in **chapter 6**. Substantial weight loss occurs in sixty percent of lung cancer patients and cancer cachexia has been associated with a poor prognosis and lower responses to chemotherapy and radiation treatment. In experimental models of cancer cachexia, (pro)inflammatory mediators and the transcription factor NF-κB have been implicated in the development of muscle atrophy, at least partly by activating the Ub-P pathway. In muscle biopsies of a group of newly diagnosed NSCLC patients we investigated

whether critical steps in the Ub-P pathway were activated, and whether this was related to levels of systemic (pro)inflammatory mediators and a muscular activation of the transcription factor NF-κB.

Most studies on proteolysis focus on its role during catabolic periods, while its role during periods of anabolism has not been investigated thoroughly. For this reason, a unilateral high-resistance exercise protocol was applied to rats in **chapter 5**. Similar exercise protocols have been shown to lead to hypertrophy when applied repeatedly. In this chapter, we aimed to investigate the acute effect of high-resistance exercise on mixed-muscle proteolysis and on the activity of the Ub-P pathway.

The uncoupling protein-3 (UCP3) has been implicated in the process of cachexia due to its presumed role in regulating energy expenditure. Recently, however, it has been hypothesized that UCP3 is involved in the modulation of mitochondrial lipotoxicity rather than in the modulation of energy expenditure. In **chapter 4**, we aimed to explore this hypothesis in a cachectic setting, for which purpose we again used the zymosan sepsis model in rats.

References

1. Bechet D, Tassa A, Taillandier D, Combaret L, and Attaix D. Lysosomal proteolysis in skeletal muscle. Int J Biochem Cell Biol 37: 2098-2114, 2005.
2. Goll DE, Thompson VF, Li H, Wei W, and Cong J. The calpain system. Physiol Rev 83: 731-801, 2003.
3. Tiao G, Fagan JM, Samuels N, James JH, Hudson K, Lieberman M, Fischer JE, and Hasselgren PO. Sepsis stimulates nonlysosomal, energy-dependent proteolysis and increases ubiquitin mRNA levels in rat skeletal muscle. J Clin Invest 94: 2255-2264, 1994.
4. Voisin L, Breuille D, Combaret L, Pouyet C, Taillandier D, Aurousseau E, Obled C, and Attaix D. Muscle wasting in a rat model of long-lasting sepsis results from the activation of lysosomal, Ca2+ -activated, and ubiquitin-proteasome proteolytic pathways. J Clin Invest 97: 1610-1617, 1996.
5. Wing SS and Goldberg AL. Glucocorticoids activate the ATP-ubiquitin-dependent proteolytic system in skeletal muscle during fasting. Am J Physiol 264: E668-676, 1993.
6. Medina R, Wing SS, Haas A, and Goldberg AL. Activation of the ubiquitin-ATP-dependent proteolytic system in skeletal muscle during fasting and denervation atrophy. Biomed Biochim Acta 50: 347-356, 1991.
7. Temparis S, Asensi M, Taillandier D, Aurousseau E, Larbaud D, Obled A, Bechet D, Ferrara M, Estrela JM, and Attaix D. Increased ATP-ubiquitin-dependent proteolysis in skeletal muscles of tumor-bearing rats. Cancer Res 54: 5568-5573, 1994.

8. Baracos VE, DeVivo C, Hoyle DH, and Goldberg AL. Activation of the ATP-ubiquitin-proteasome pathway in skeletal muscle of cachectic rats bearing a hepatoma. Am J Physiol 268: E996-1006, 1995.
9. Furuno K, Goodman MN, and Goldberg AL. Role of different proteolytic systems in the degradation of muscle proteins during denervation atrophy. J Biol Chem 265: 8550-8557, 1990.
10. Taillandier D, Aurousseau E, Meynial-Denis D, Bechet D, Ferrara M, Cottin P, Ducastaing A, Bigard X, Guezennec CY, Schmid HP, et al. Coordinate activation of lysosomal, Ca 2+-activated and ATP-ubiquitin- dependent proteinases in the unweighted rat soleus muscle. Biochem J 316: 65-72, 1996.
11. Kisselev AF and Goldberg AL. Proteasome inhibitors: from research tools to drug candidates. Chem Biol 8: 739-758, 2001.
12. Bailey JL, Wang X, England BK, Price SR, Ding X, and Mitch WE. The acidosis of chronic renal failure activates muscle proteolysis in rats by augmenting transcription of genes encoding proteins of the ATP-dependent ubiquitin-proteasome pathway. J Clin Invest 97: 1447-1453, 1996.
13. Tawa NE, Odessey R, and Goldberg AL. Inhibitors of the proteasome reduce the accelerated proteolysis in atrophying rat skeletal muscles. J Clin Invest 100: 197-203., 1997.
14. Price SR, Bailey JL, Wang X, Jurkovitz C, England BK, Ding X, Phillips LS, and Mitch WE. Muscle wasting in insulinopenic rats results from activation of the ATP-dependent, ubiquitin-proteasome proteolytic pathway by a mechanism including gene transcription. J Clin Invest 98: 1703-1708, 1996.
15. Hobler SC, Tiao G, Fischer JE, Monaco J, and Hasselgren PO. Sepsis-induced increase in muscle proteolysis is blocked by specific proteasome inhibitors. Am J Physiol 274: R30-37, 1998.
16. Solomon V and Goldberg AL. Importance of the ATP-ubiquitin-proteasome pathway in the degradation of soluble and myofibrillar proteins in rabbit muscle extracts. J Biol Chem 271: 26690-26697, 1996.
17. Hasselgren PO, Menconi MJ, Fareed MU, Yang H, Wei W, and Evenson A. Novel aspects on the regulation of muscle wasting in sepsis. Int J Biochem Cell Biol 37: 2156-2168, 2005.
18. Du J, Hu Z, and Mitch WE. Molecular mechanisms activating muscle protein degradation in chronic kidney disease and other catabolic conditions. Eur J Clin Invest 35: 157-163, 2005.
19. Williams AB, Decourten-Myers GM, Fischer JE, Luo G, Sun X, and Hasselgren PO. Sepsis stimulates release of myofilaments in skeletal muscle by a calcium-dependent mechanism. Faseb J 13: 1435-1443, 1999.
20. Du J, Wang X, Miereles C, Bailey JL, Debigare R, Zheng B, Price SR, and Mitch WE. Activation of caspase-3 is an initial step triggering accelerated muscle proteolysis in catabolic conditions. J Clin Invest 113: 115-123, 2004.
21. Rock KL, Gramm C, Rothstein L, Clark K, Stein R, Dick L, Hwang D, and Goldberg AL. Inhibitors of the proteasome block the degradation of most cell proteins and the generation of peptides presented on MHC class I molecules. Cell 78: 761-771, 1994.
22. Polo S, Confalonieri S, Salcini AE, and Di Fiore PP. EH and UIM: endocytosis and more. Sci STKE 2003: re17, 2003.
23. Sun L and Chen ZJ. The novel functions of ubiquitination in signaling. Curr Opin Cell Biol 16: 119-126, 2004.

24. Thrower JS, Hoffman L, Rechsteiner M, and Pickart CM. Recognition of the polyubiquitin proteolytic signal. Embo J 19: 94-102, 2000.
25. Pickart CM. Mechanisms underlying ubiquitination. Annu Rev Biochem 70: 503-533, 2001.
26. Varshavsky A. The N-end rule: functions, mysteries, uses. Proc Natl Acad Sci U S A 93: 12142-12149, 1996.
27. Pickart CM. Back to the future with ubiquitin. Cell 116: 181-190, 2004.
28. Wing SS. Deubiquitinating enzymes--the importance of driving in reverse along the ubiquitin-proteasome pathway. Int J Biochem Cell Biol 35: 590-605, 2003.
29. Orlowski M and Wilk S. Catalytic activities of the 20 S proteasome, a multicatalytic proteinase complex. Arch Biochem Biophys 383: 1-16, 2000.
30. Voges D, Zwickl P, and Baumeister W. The 26S proteasome: a molecular machine designed for controlled proteolysis. Annu Rev Biochem 68: 1015-1068, 1999.
31. Navon A and Goldberg AL. Proteins are unfolded on the surface of the ATPase ring before transport into the proteasome. Mol Cell 8: 1339-1349, 2001.
32. Kohler A, Cascio P, Leggett DS, Woo KM, Goldberg AL, and Finley D. The axial channel of the proteasome core particle is gated by the Rpt2 ATPase and controls both substrate entry and product release. Mol Cell 7: 1143-1152, 2001.
33. Wing SS, Haas AL, and Goldberg AL. Increase in ubiquitin-protein conjugates concomitant with the increase in proteolysis in rat skeletal muscle during starvation and atrophy denervation. Biochem J 307 (Pt 3): 639-645, 1995.
34. Tiao G, Fagan J, Roegner V, Lieberman M, Wang JJ, Fischer JE, and Hasselgren PO. Energy-ubiquitin-dependent muscle proteolysis during sepsis in rats is regulated by glucocorticoids. J Clin Invest 97: 339-348, 1996.
35. Lecker SH, Solomon V, Price SR, Kwon YT, Mitch WE, and Goldberg AL. Ubiquitin conjugation by the N-end rule pathway and mRNAs for its components increase in muscles of diabetic rats. J Clin Invest 104: 1411-1420, 1999.
36. Solomon V, Baracos V, Sarraf P, and Goldberg AL. Rates of ubiquitin conjugation increase when muscles atrophy, largely through activation of the N-end rule pathway. Proc Natl Acad Sci U S A 95: 12602-12607, 1998.
37. Solomon V, Madihally S, Yarmush M, and Toner M. Insulin suppresses the increased activities of lysosomal cathepsins and ubiquitin conjugation system in burn-injured rats. J Surg Res 93: 120-126, 2000.
38. Varshavsky A. The N-end rule. Cold Spring Harb Symp Quant Biol 60: 461-478, 1995.
39. Bachmair A, Finley D, and Varshavsky A. In vivo half-life of a protein is a function of its amino-terminal residue. Science 234: 179-186, 1986.
40. Solomon V, Lecker SH, and Goldberg AL. The N-end rule pathway catalyzes a major fraction of the protein degradation in skeletal muscle. J Biol Chem 273: 25216-25222, 1998.
41. Jagoe RT and Goldberg AL. What do we really know about the ubiquitin-proteasome pathway in muscle atrophy? Curr Opin Clin Nutr Metab Care 4: 183-190, 2001.
42. Attaix D, Combaret L, Kee AJ, and Taillandier D. Mechanisms of ubiquitination and proteasome-dependent proteolysis in skeletal muscle. Molecular Nutrition (J Zempleni, H Daniels eds) CAB International, Wallingford, Oxon, UK: 219-235, 2003.
43. Hobler SC, Wang JJ, Williams AB, Melandri F, Sun X, Fischer JE, and Hasselgren PO. Sepsis is associated with increased ubiquitinconjugating enzyme E214k mRNA in skeletal muscle. Am J Physiol 276: R468-473, 1999.

44. Adegoke OA, Bedard N, Roest HP, and Wing SS. Ubiquitin-conjugating enzyme E214k/HR6B is dispensable for increased protein catabolism in muscle of fasted mice. Am J Physiol Endocrinol Metab 283: E482-489, 2002.
45. Kwon YT, Xia Z, Davydov IV, Lecker SH, and Varshavsky A. Construction and analysis of mouse strains lacking the ubiquitin ligase UBR1 (E3alpha) of the N-end rule pathway. Mol Cell Biol 21: 8007-8021, 2001.
46. Bodine SC, Latres E, Baumhueter S, Lai VK, Nunez L, Clarke BA, Poueymirou WT, Panaro FJ, Na E, Dharmarajan K, Pan ZQ, Valenzuela DM, DeChiara TM, Stitt TN, Yancopoulos GD, and Glass DJ. Identification of ubiquitin ligases required for skeletal muscle atrophy. Science 294: 1704-1708, 2001.
47. Gomes MD, Lecker SH, Jagoe RT, Navon A, and Goldberg AL. Atrogin-1, a muscle-specific F-box protein highly expressed during muscle atrophy. Proc Natl Acad Sci U S A 98: 14440-14445, 2001.
48. Glass DJ. Skeletal muscle hypertrophy and atrophy signaling pathways. Int J Biochem Cell Biol 37: 1974-1984, 2005.
49. Wray CJ, Mammen JM, Hershko DD, and Hasselgren PO. Sepsis upregulates the gene expression of multiple ubiquitin ligases in skeletal muscle. Int J Biochem Cell Biol 35: 698-705, 2003.
50. Lecker SH, Jagoe RT, Gilbert A, Gomes M, Baracos V, Bailey J, Price SR, Mitch WE, and Goldberg AL. Multiple types of skeletal muscle atrophy involve a common program of changes in gene expression. Faseb J 18: 39-51, 2004.
51. Kedar V, McDonough H, Arya R, Li HH, Rockman HA, and Patterson C. Muscle-specific RING finger 1 is a bona fide ubiquitin ligase that degrades cardiac troponin I. Proc Natl Acad Sci U S A 101: 18135-18140, 2004.
52. McElhinny AS, Kakinuma K, Sorimachi H, Labeit S, and Gregorio CC. Muscle-specific RING finger-1 interacts with titin to regulate sarcomeric M-line and thick filament structure and may have nuclear functions via its interaction with glucocorticoid modulatory element binding protein-1. J Cell Biol 157: 125-136, 2002.
53. Tintignac LA, Lagirand J, Batonnet S, Sirri V, Leibovitch MP, and Leibovitch SA. Degradation of MyoD mediated by the SCF (MAFbx) ubiquitin ligase. J Biol Chem 280: 2847-2856, 2005.
54. Li HH, Kedar V, Zhang C, McDonough H, Arya R, Wang DZ, and Patterson C. Atrogin-1/muscle atrophy F-box inhibits calcineurin-dependent cardiac hypertrophy by participating in an SCF ubiquitin ligase complex. J Clin Invest 114: 1058-1071, 2004.
55. Hobler SC, Williams A, Fischer D, Wang JJ, Sun X, Fischer JE, Monaco JJ, and Hasselgren PO. Activity and expression of the 20S proteasome are increased in skeletal muscle during sepsis. Am J Physiol 277: R434-440, 1999.
56. Fang CH, Li BG, Fischer DR, Wang JJ, Runnels HA, Monaco JJ, and Hasselgren PO. Burn injury upregulates the activity and gene expression of the 20 S proteasome in rat skeletal muscle. Clin Sci (Lond) 99: 181-187, 2000.
57. Bossola M, Muscaritoli M, Costelli P, Grieco G, Bonelli G, Pacelli F, Rossi Fanelli F, Doglietto GB, and Baccino FM. Increased muscle proteasome activity correlates with disease severity in gastric cancer patients. Ann Surg 237: 384-389, 2003.
58. Combaret L, Taillandier D, Dardevet D, Bechet D, Ralliere C, Claustre A, Grizard J, and Attaix D. Glucocorticoids regulate mRNA levels for subunits of the 19 S regulatory complex of the 26 S proteasome in fast-twitch skeletal muscles. Biochem J 378: 239-246, 2004.

59. Attaix D and Taillandier D. The critical role of the ubiquitin-proteasome pathway in muscle wasting in comparison to lysosomal and Ca2+-dependent systems. Adv Mol Cell Biol 27: 235-266, 1998.
60. Hasselgren PO. Glucocorticoids and muscle catabolism. Curr Opin Clin Nutr Metab Care 2: 201-205, 1999.
61. Dardevet D, Sornet C, Taillandier D, Savary I, Attaix D, and Grizard J. Sensitivity and protein turnover response to glucocorticoids are different in skeletal muscle from adult and old rats. Lack of regulation of the ubiquitin-proteasome proteolytic pathway in aging. J Clin Invest 96: 2113-2119, 1995.
62. Mitch WE, Bailey JL, Wang X, Jurkovitz C, Newby D, and Price SR. Evaluation of signals activating ubiquitin-proteasome proteolysis in a model of muscle wasting. Am J Physiol 276: C1132-1138, 1999.
63. Price SR, England BK, Bailey JL, Van Vreede K, and Mitch WE. Acidosis and glucocorticoids concomitantly increase ubiquitin and proteasome subunit mRNAs in rat muscle. Am J Physiol 267: C955-960, 1994.
64. May RC, Bailey JL, Mitch WE, Masud T, and England BK. Glucocorticoids and acidosis stimulate protein and amino acid catabolism in vivo. Kidney Int 49: 679-683, 1996.
65. Argiles JM, Busquets S, and Lopez-Soriano FJ. The pivotal role of cytokines in muscle wasting during cancer. Int J Biochem Cell Biol 37: 1609-1619, 2005.
66. Goodman MN. Interleukin-6 induces skeletal muscle protein breakdown in rats. Proc Soc Exp Biol Med 205: 182-185, 1994.
67. Flores EA, Bistrian BR, Pomposelli JJ, Dinarello CA, Blackburn GL, and Istfan NW. Infusion of tumor necrosis factor/cachectin promotes muscle catabolism in the rat. A synergistic effect with interleukin 1. J Clin Invest 83: 1614-1622, 1989.
68. Fong Y, Moldawer LL, Marano M, Wei H, Barber A, Manogue K, Tracey KJ, Kuo G, Fischman DA, Cerami A, and et al. Cachectin/TNF or IL-1 alpha induces cachexia with redistribution of body proteins. Am J Physiol 256: R659-665, 1989.
69. Ling PR, Schwartz JH, and Bistrian BR. Mechanisms of host wasting induced by administration of cytokines in rats. Am J Physiol 272: E333-339, 1997.
70. Cooney RN, Kimball SR, and Vary TC. Regulation of skeletal muscle protein turnover during sepsis: mechanisms and mediators. Shock 7: 1-16, 1997.
71. Goodman MN. Tumor necrosis factor induces skeletal muscle protein breakdown in rats. Am J Physiol 260: E727-730, 1991.
72. Lecker SH, Solomon V, Mitch WE, and Goldberg AL. Muscle protein breakdown and the critical role of the ubiquitin- proteasome pathway in normal and disease states. J Nutr 129: 227S-237S, 1999.
73. Costelli P, Carbo N, Tessitore L, Bagby GJ, Lopez-Soriano FJ, Argiles JM, and Baccino FM. Tumor necrosis factor-alpha mediates changes in tissue protein turnover in a rat cancer cachexia model. J Clin Invest 92: 2783-2789, 1993.
74. Combaret L, Tilignac T, Claustre A, Voisin L, Taillandier D, Obled C, Tanaka K, and Attaix D. Torbafylline (HWA 448) inhibits enhanced skeletal muscle ubiquitin-proteasome-dependent proteolysis in cancer and septic rats. Biochem J 361: 185-192, 2002.
75. Cai D, Frantz JD, Tawa NE, Jr., Melendez PA, Oh BC, Lidov HG, Hasselgren PO, Frontera WR, Lee J, Glass DJ, and Shoelson SE. IKKbeta/NF-kappaB activation causes severe muscle wasting in mice. Cell 119: 285-298, 2004.

76. Li YP, Lecker SH, Chen Y, Waddell ID, Goldberg AL, and Reid MB. TNF-alpha increases ubiquitin-conjugating activity in skeletal muscle by up-regulating UbcH2/E220k. Faseb J 17: 1048-1057, 2003.
77. Baldwin AS, Jr. The NF-kappa B and I kappa B proteins: new discoveries and insights. Annu Rev Immunol 14: 649-683, 1996.
78. Pahl HL. Activators and target genes of Rel/NF-kappaB transcription factors. Oncogene 18: 6853-6866, 1999.
79. Jackman RW and Kandarian SC. The molecular basis of skeletal muscle atrophy. Am J Physiol Cell Physiol 287: C834-843, 2004.
80. Langen RC, Schols AM, Kelders MC, Wouters EF, and Janssen-Heininger YM. Inflammatory cytokines inhibit myogenic differentiation through activation of nuclear factor-kappaB. Faseb J 15: 1169-1180, 2001.
81. Guttridge DC, Mayo MW, Madrid LV, Wang CY, and Baldwin AS, Jr. NF-kappaB-induced loss of MyoD messenger RNA: possible role in muscle decay and cachexia. Science 289: 2363-2366, 2000.
82. Li YP and Reid MB. NF-kappaB mediates the protein loss induced by TNF-alpha in differentiated skeletal muscle myotubes. Am J Physiol Regul Integr Comp Physiol 279: R1165-1170, 2000.
83. Ladner KJ, Caligiuri MA, and Guttridge DC. Tumor necrosis factor-regulated biphasic activation of NF-kappa B is required for cytokine-induced loss of skeletal muscle gene products. J Biol Chem 278: 2294-2303, 2003.

2

Skeletal muscle wasting and contractile performance in septic rats

R. Minnaard, M.R. Drost, A.J.M. Wagenmakers,
G.P. van Kranenburg, H. Kuipers, and M.K.C. Hesselink

Muscle & Nerve 31: 339-348, 2005

Abstract

We investigated the temporal effects of sepsis on muscle wasting and muscle function in order to study the contribution of muscle wasting to the decline in muscle function. Moreover, we studied the fiber type specificity of this muscle wasting. Sepsis was induced by injecting rats intraperitoneally with a zymosan suspension. At 2 hours and at 2, 6 and 11 days after injection, muscle function was measured using *in situ* electrical stimulation. Zymosan injection induced severe muscle wasting compared to pair-fed and *ad libitum* fed controls. At 6 days, isometric force-generating capacity was drastically reduced in zymosan-treated rats. We conclude that this was fully accounted for by the reduction of muscle mass. At day 6 we also observed increased activity of the 20S proteasome in gastrocnemius but not soleus muscle from septic rats. In tibialis anterior but not in soleus, muscle wasting occurred in a fiber-type specific fashion, i.e. the reduction in CSA was significantly smaller in type 1 than in type 2A and 2B/X fibers. These findings suggest that both the inherent function of a muscle and the muscle fiber type distribution affect the responsiveness to catabolic signals.

Introduction

Patients with severe sepsis frequently develop extensive muscle wasting and weakness. This weakness may involve the respiratory muscles and can be life threatening. Skeletal muscle wasting and a loss of muscle excitability are the most important factors contributing to the development of muscle weakness (1), but their relative contribution during sepsis is unclear.

In animal models, endotoxin administration elicits a rapid decrease in *in vitro* force-generating capacity of both respiratory and limb striated muscles before a significant loss of muscle mass is present (2-4). Marked reductions (i.e. less negativity) also occur in the muscle resting membrane potential (RMP) within 1 hour after endotoxin administration (5). These findings in animals are consistent with the 25% reduction in RMP observed in critically ill patients in the intensive care unit (6). A derangement in RMP affects the excitability of the muscle. Altogether, the acute findings in endotoxin models of critical illness (decreased RMP and no significant loss of muscle mass) support an important role for decreased excitability in the observed muscle weakness.

Experimentally, sepsis can also be induced by injections with zymosan, a potent stimulator of the alternative pathway of the complement system and of macrophages. Intraperitoneal injection with zymosan results in an acute local inflammatory response (peritonitis). This local peritonitis triggers a systemic response resulting in clinical sepsis, defined as the host response to invasion of foreign micro-organisms (7, 8). In addition, a septic response can also be triggered by non-infective stimuli, as is the case following zymosan injection. As a result, signs traditionally associated with infection (e.g. tachycardia, fever, increased respiratory rate, hypophagia) are also apparent in zymosan-injected rats.

As endotoxin studies demonstrated acute changes in contractile performance, we hypothesized that zymosan injection leads to an acute phase of sepsis in which contractility is deranged while muscle mass is unchanged. This acute phase is then followed by a phase in which a reduction of muscle mass causes a further deterioration of contractile performance. To investigate this hypothesis we measured contractile performance (tetanic peak force, force-frequency relation) at several points (2h, 2d, 6d, and 11d) after zymosan injection. Since zymosan injection lowers food intake significantly, pair-fed rats were also included.

Earlier work on muscle wasting in septic or burn-injured rats has shown a greater increase in both total and myofibrillar protein breakdown in the extensor digitorum longus muscle (EDL), which contains predominantly fast glycolytic fibers (type 2A and 2B/X), than in the soleus muscle (SOL), which contains predominantly slow oxidative, type 1 fibers (9, 10). These results have been used to conclude that type 2 muscle fibers are more vulnerable to wasting than type 1 fibers. Therefore, the second aim of this study was to investigate whether the difference in susceptibility to muscle wasting between distinct muscle fibers was also present within one muscle. To this end we examined the individual tibialis anterior (TA) and SOL fiber cross-sectional area (CSA) in relation to fiber-type at different times after zymosan injection.

Muscle wasting during sepsis is mainly caused by increased proteolysis through the ATP-dependent ubiquitin-proteasome system (11-13). To test the involvement of the ubiquitin-proteasome system in zymosan-induced muscle wasting and to test a putative fiber-type specific regulation, we assessed the 20S proteasome activity in both the “white” gastrocnemius lateralis muscle (GL) and the “red” SOL. In addition, we determined the protein level of the 20S proteasome C8 subunit in the GL, SOL and TA muscles.

Methods

Animals and experimental design

The experiments were approved by the animal experimental committee of Maastricht University. Rats were individually housed (12h dark-light cycle, 21-22 °C and 50-60% humidity) and were allowed to acclimatize for at least 1 week prior to the experiments. In the experiments we used the zymosan model as described by Rooyackers et al. (14), which is a modified version of the original zymosan model (15). Ten-week-old, male Wistar rats with an average body mass of 300 g were given an aseptic intraperitoneal injection of zymosan (30 mg/ 100 g body mass) suspended in liquid paraffin (25 mg/ml). Prior to the experiments, a pilot experiment was performed to determine the desired zymosan dose (2d period of acute illness, mortality ± 20%). A Yellowline homogenizer (IKA Works, Wilmington, NC) was used to make a homogeneous zymosan suspension, after which the suspension was sterilized by incubation at 100°C for 90 minutes. Four groups of rats (n = 10)

were injected with the zymosan suspension. Food intake and body mass were recorded daily. Rats were tested at 2h, 2d, 6d, and 11d after zymosan injection. In each group, the muscle force-generating capacity was studied using *in situ* electrical stimulation. After this, the TA, EDL, SOL and gastrocnemius complex (GC) muscles of the non-exercised leg were carefully dissected, weighed, and frozen in melting 2-methylbutane, after which the rats were sacrificed by cervical dislocation. Muscles were frozen promptly after dissection. Since zymosan injection affects food intake, control rats were pair-fed to the 2, 6, and 11 d zymosan rats. An *ad libitum* fed control group, which was sacrificed at day 11, was also included.

Isometric torque measurements

Muscle function data were obtained by inducing isometric contractions of the dorsiflexor muscles while recording muscle torque (which is proportional to force). An illustrated description of the experimental arrangement can be found in Drost et al (16).

Rats were anaesthetized using a subcutaneous injection of ketamine (100 mg/kg body mass) and xylazine (10 mg/kg). A small longitudinal incision was made about 2 mm dorsal of the head of the fibula to expose the peroneal nerve. A bipolar, platinum hook electrode was carefully attached to the nerve to allow for electrical stimulation of the dorsiflexor muscles with the pulse generator. The rats were placed on the platform in a sideways position and their left foot was fixed tightly to the footplate. Hip fixation was achieved with a tail fixation unit. The footplate was fixed at an ankle angle of 90°, which corresponds to the optimal muscle fiber length (16). Supramaximal stimulation was defined as the current at which an increment in current was no longer paralleled by an increment in torque (typically ~ 1.0 mA). The stimulation protocol consisted of the following series of consecutive 400 ms pulse trains (pulse duration 0.5 ms, interval 15 s) at different stimulation frequencies: 1, 15, 40, 67, 100, 125, and 167 Hz.

Fiber cross-sectional area quantitation

Frozen TA and SOL tissue was cryosectioned at –20°C using a cryostat (CM3050, Leica, Nussloch, Germany) and cut midbelly, perpendicular to the muscle fiber axis. Transverse muscle sections (4 μm) were cut and thaw-

mounted on uncoated glass slides. The sections were air-dried for 2 h at room temperature and stored at –80°C until further analysis. Before staining, the sections were thawed and air-dried for 30 min at room temperature. Sections were pre-incubated for 5 min in 0.5% Triton X-100/PBS, followed by 5 min in phospate-buffered saline (PBS). After each of the following steps the sections were washed 3 times for 5 min in PBS. Sections were incubated for 1 h at room temperature with a mix of a rabbit polyclonal laminin antibody (1:100; Sigma, Zwijndrecht, The Netherlands), a mouse monoclonal myosin heavy chain (MHC) type 1 antibody (A4.840, Developmental Studies Hybridoma Bank; IgM subtype; 1:25) and a monoclonal MHC type 2A antibody (N2.261, Developmental Studies Hybridoma Bank; IgG subtype; 1:25), diluted in PBS. Subsequently, sections were incubated for 1 h at room temperature with a mix of an Alexa350-conjugated goat anti-rabbit Ig (GARIgG-Alexa350; 1:130; Molecular Probes, Invitrogen, Breda, The Netherlands), an Alexa555-conjugated goat anti-mouse IgM (GAMIgM-Alexa 555; 1:400; Molecular Probes) and a fluorescein isothiocyanate (FITC)-conjugated goat anti-mouse IgG (GAMIgGFITC; 1:80; Southern Biotechnology Associates, Birmingham, AL) antibody, diluted in PBS. Thereafter, sections were covered with a coverslip using Mowiol (Hoechst, Frankfurt, Germany).

All sections were examined using a Nikon E800 fluorescence microscope (Uvikon, Bunnik, The Netherlands). Digitally captured images were processed and analysed using Lucia 4.8 software (Nikon, Düsseldorf, Germany). Since we aimed to examine fiber-type specific muscle wasting, images were captured from the mixed fiber-type portion of TA and from

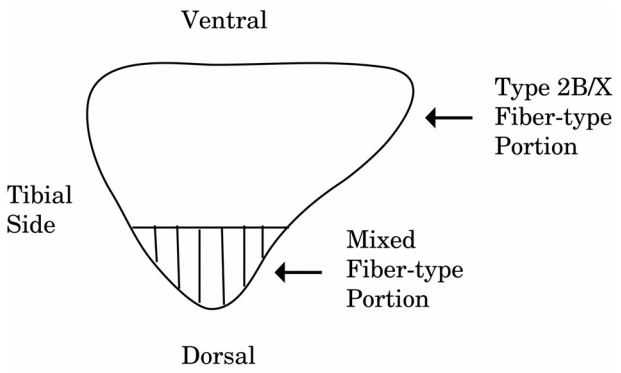

Figure 2: Representation of a TA muscle at the level of transverse sectioning.

SOL. The mixed fiber-type portion of TA is the most dorsal part of the muscle (17) (Figure 1). At least 100 muscle fibers were examined per muscle using laminin (a basement membrane protein) as a marker for cell boundary. Hereafter, the fiber CSA and MHC1 and 2A abundance were quantitated for each fiber. Fibers were classified as MHC type 1, 2A or 2B/X, based on their MHC (1/2A) content. Since at day 6 the greatest reduction in muscle mass was present in the zymosan group, muscle fiber-type specific wasting was analyzed at this time-point.

Isolation of 20S proteasomes and measurement of proteolytic activity

The 20S proteasome proteolytic activity was measured in the control rats, the 6-d zymosan rats and the 6-d pair-fed rats. Measurements were performed on both GL (predominantly fast-twitch fibers; n=8-10 per group) and SOL (predominantly slow-twitch fibers). Soleus muscles (n=8-10) were pooled in order to get a sufficient yield of muscle to perform the assay. To isolate the 20S proteasomes, muscles were homogenized in 10 vol of ice-cold buffer (pH 7.5), containing 50 mM Tris, 5 mM $MgCl_2$, 250 mM sucrose and protease inhibitors (10 μg/ml antipain, aprotinin, leupeptin and pepstatin A, 1 mM DTT and 0.2 mM PMSF) using a Yellow line homogenizer (IKA Works, Wilmington, NC). The proteasomes were isolated essentially according to Dahlmann et al. (18) and Hobler et al. (19). Adding MG132 to the reaction resulted in complete inhibition of the proteasome proteolytic activity, indicating succesful isolation of proteasomes without the presence of significant amounts of other proteases.
The proteolytic activity of the 20S proteasomes was determined fluorometrically by measuring the activity against the fluorogenic substrates succinyl-leu-leu-val-tyr-7-amido-4-methylcoumarin (Suc-LLVY-AMC; SIGMA) and t-butoxycarbonyl-leu-arg-arg-7-amido-4-methylcoumarin (Boc-LRR-AMC; Affiniti Research Products, Exeter, UK). These substrates are preferentially hydrolyzed by the chymotrypsin-like and trypsin-like activities of the 20S proteasome, respectively.

Measurement of 20S proteasome C8 subunit protein levels

Protein levels of the 20S proteasome C8 subunit were determined in both the proteasome preparations of GL and SOL, and in soluble protein

fractions of TA. Measurements were performed in the control, 6-d zymosan and 6-d pair-fed rats.
For the preparation of the soluble protein fraction, TA muscles were homogenized in 4 ml ice-cold buffer (pH 7.5), containing 50 mM Tris, 1 mM EDTA, 1 mM DTT, 1 mM PMSF, 10 μg/ml pepstatin A and 10 μg/ml leupeptin, using a Yellow line homogenizer (IKA Works). Homogenates were centrifuged at 10,000 g, 4 °C for 10 min and the resulting supernatants were centrifuged at 100,000 g, 4 °C for 1h. The supernatants contain the soluble proteins. The protein concentration of the soluble protein fraction was determined using the Bio-Rad protein assay.
Both the proteasome and soluble protein fractions (20 μg) were subjected to routine Western blotting using 12% SDS-polyacrylamide gels and an antibody against the 20S proteasome subunit C8 (MCP72; mouse monoclonal; 1:10,000; Affiniti). Chemiluminescence was performed using a Super Signal West Dura extended kit (Pierce, Rockford, IL) and the blots were exposed to Hyperfilm ECL (Amersham Biosciences, Roosendaal, The Netherlands). Protein bands were quantified using densitometry.

Statistics

Results are presented as means ± SEM. The zymosan, pair-fed, and control group data were compared using ANOVA. Differences were located using the Scheffé post-hoc test. Significance was set at $P < 0.05$.

Results

Body and muscle mass

Zymosan injection induced an acute peritonitis, with symptoms of severe illness being present in all rats during the first 2 days after injection. Symptoms included lethargy, hypophagia, hyperventilation, tachycardia, fever, diarrhea and loss of hemorrhagic fluid from the nose. There was a mortality of 20% in this acute phase. Zymosan injection significantly reduced food intake from ~20 g/day to an average of 1 g/day on day 1 and 2, after which it gradually increased to 75% of normal intake on day 8 (Figure 2A), and then remained constant. Both the zymosan and pair-fed groups showed a large loss of body mass (Figure 2B). Both groups of rats started to regain body mass between days 5 and 11. There were no significant

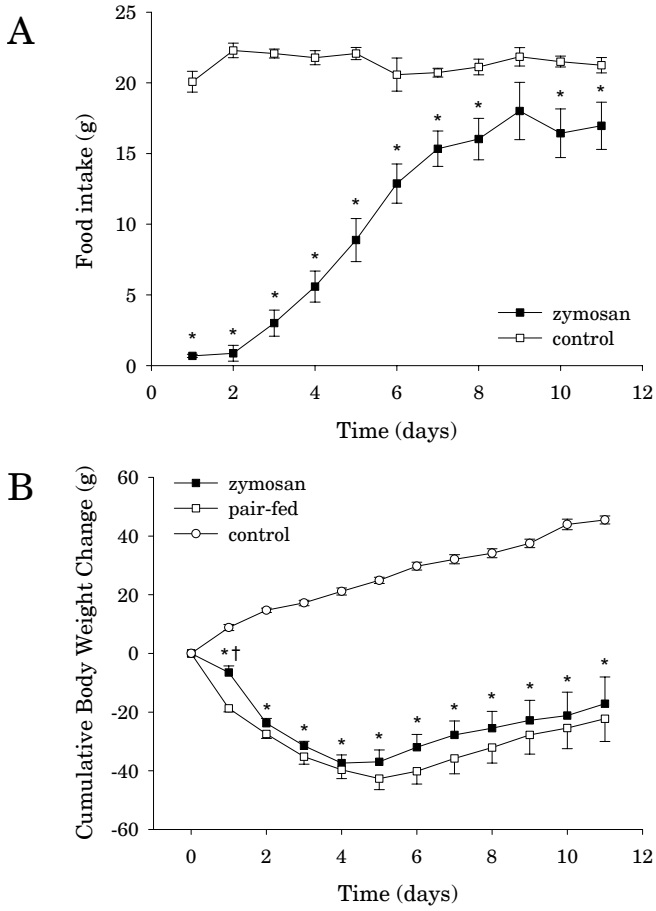

Figure 2: (A) Food intake of zymosan-treated and *ad libitum* fed control rats. **(B)** Cumulative change in body mass of zymosan treated, pair-fed control and *ad libitum* fed control rats.
* P<0.05 vs. *ad libitum* fed control rats, † P<0.05 vs. pair-fed controls.

differences in body mass between the zymosan and the pair-fed group. No catch-up growth was observed in either group.

Muscle mass of the main dorsiflexor (TA) and plantarflexor (GC) muscles are shown in Table 1. TA muscle mass significantly declined (compared to pair-fed and *ad libitum* fed controls) as soon as 2 days after zymosan injection and up to 66 ± 2.6 % of control values at day 6. The pair-fed group showed a similar but less pronounced response. On day 11, TA muscle mass started to regain in both groups. The observation that on day 11 TA muscle mass was still considerably lower than in controls corresponds with the absence of catch-up growth on day 11. In both groups GC muscle mass follows the same pattern of wasting (and recovery) as the TA muscle.

Table 1: Initial body mass and lower hindlimb muscle mass in the different experimental groups.

		Initial body mass (g)	TA muscle mass (mg)	GC muscle mass (mg)
	control	262 ± 1.2	610 ± 9.1	1952 ± 27
2 h	zymosan	305 ± 3.5*	617 ± 19	1891 ± 33
2 d	zymosan	313 ± 11.8*	518 ± 22*†	1644 ± 80*†
	pair-fed	320 ± 6.1*	604 ± 14	1961 ± 32
6 d	zymosan	306 ± 6.5*	444 ± 15*†	1441 ± 60*†
	pair-fed	295 ± 4.1*	545 ± 11*	1736 ± 25*
11 d	zymosan	304 ± 5.3	522 ± 23*†	1680 ± 86*†
	pair-fed	301 ± 5.1	611 ± 12	1929 ± 55

* $P<0.05$ vs. *ad libitum* fed control rats
† $P<0.05$ vs. pair-fed rats.

Contractility

In the experimental groups, dorsiflexor muscle function was determined by measuring the maximal isometric torque during a tetanic contraction (tetanic peak force). Maximal isometric torques (stimulation frequency, 167 Hz) are shown in Table 2, where torques are presented both as absolute values and as values normalized on muscle mass, i.e., maximal torques over the sum of TA and EDL muscle mass (g). Until day 6, significant differences in torque between the control, pair-fed, and zymosan groups were absent. On day 6, zymosan rats showed a marked reduction in torque compared to the pair-fed and control rats (Figure 3A). On day 11 the torque generated by the zymosan rats gradually recovered, but still was significantly lower than in the pair-fed and control rats.
Normalization on muscle mass abolished all differences in maximal torque between the experimental groups (Table 2). At all timepoints, tetanic (Figure 3B) as well as submaximal stimulation frequencies (data not shown) resulted in similar torque traces between the groups.

Muscle wasting and fiber type

Figure 4 shows immunofluorescent stainings of TA and SOL from all groups, sampled at day 6, with corresponding CSAs shown in Table 3. CSAs for the zymosan and pair-fed groups are expressed as relative differences from control values. The reduction in TA fiber CSA was most pronounced following zymosan (31% reduction) and was almost completely accounted for by the reduced CSA in the type 2A and 2B fibers. This fiber-type specific

Table 2: Maximal and normalized isometric torques in the different experimental groups.

		Torque (N·mm)	Normalized Torque (Nmm·g muscle^{-1})
	control	43.4 ± 1.7	56.3 ± 1.8
2 h	zymosan	42.4 ± 1.1	55.0 ± 0.9
2 d	zymosan	39.3 ± 2.7	60.3 ± 2.3
2 d	pair-fed	43.7 ± 2.2	57.5 ± 2.2
6 d	zymosan	32.4 ± 1.8*†	55.4 ± 2.7
6 d	pair-fed	38.9 ± 1.2	56.1 ± 2.0
11 d	zymosan	37.5 ± 1.6*†	57.1 ± 2.1
11 d	pair-fed	44.8 ± 1.7	58.4 ± 0.9

* P<0.05 vs. *ad libitum* fed control rats
† P<0.05 vs. pair-fed controls.

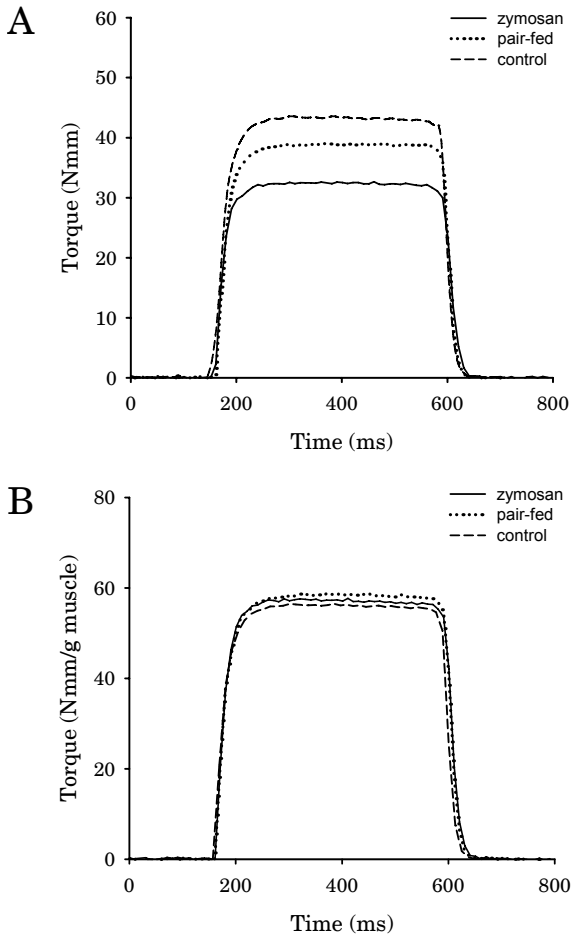

Figure 3: (A) Maximal isometric torques and **(B)** normalized isometric torques at day 6 using a stimulation frequency of 167 Hz in the zymosan (n=7), pair-fed (n=7) and *ad libitum* fed control (n=8) groups.

wasting effect was absent in the pair-fed group. In the SOL muscle, the reduction in CSA was less prominent than in the TA muscle. Importantly, in SOL the reduction in CSA in both the zymosan and pair-fed groups did not occur in a fiber-type specific fashion.

20S proteasome activity and protein level

Figures 5A and 5B show a nearly twofold increase in the 20S proteasome chymotrypsin-like and trypsin-like activities in GL from the 6-d zymosan group compared to pair-fed and control GL muscles. Such an effect was not present in SOL, which supports a fiber-type specific regulation of proteasome activity by zymosan. Protein levels of the 20S proteasome C8 subunit in proteasome preparations of the GL were similar in all groups, indicating that increased specific activity of the proteasome and not an increase in 20S protein content is responsible for the observed differences. In line with this, C8 subunit protein levels in soluble fractions of the TA muscle were similar in all groups (Figure 6A).

Table 3: Relative reduction of TA and SOL muscle fiber CSA at day 6.

		Type 1 fiber CSA	Type 2A fiber CSA	Type 2B/X fiber CSA	Mean fiber CSA
TA 6 d	control	901 ± 37 μm²	1138 ± 78 μm²	1898 ± 97 μm²	1469 ± 70 μm²
	zymosan	21 ± 1.9 %[A,B]	34 ± 3.5 %	34 ± 4.7 %†	31 ± 4.2 %†
	pair-fed	14 ± 4.1 %	27 ± 4.6 %	14 ± 7.1 %	14 ± 5.6 %
SOL 6 d	control	2548 ± 90 μm²	2010 ± 97 μm²	-	2445 ± 93 μm²
	zymosan	22 ± 4.0 %	28 ± 4.8 %†	-	22 ± 3.8 %
	pair-fed	13 ± 3.7 %	3.4 ± 4.7 %	-	12 ± 4.1 %

Zymosan and pair-fed control values are presented as % reduction compared to control fibers. As a reference, control values are presented as absolute values.
[A] P<0.05 vs. type 2A fibers
[B] P<0.05 vs. type 2B/X fibers
† P<0.05 vs. pair-fed controls

Discussion

In the present study, zymosan injection induced massive muscle wasting, with the most prominent loss of mass at 6 days after injection in the TA and GC. At all time points, muscle wasting was more severe in the zymosan

than in the pair-fed group, indicating that food restriction only partially explains the sepsis-induced wasting.

At 2 h and 2 d, maximal isometric torque was similar in all groups. From this we conclude that zymosan injection does not lead to an acute deterioration of muscle function. This observation is in contrast with studies in endotoxin models reporting an acute endotoxin- induced decrease of maximum force upon *in vitro* electrical stimulation of chemically skinned muscle fibers or muscle strips (2-4, 20, 21). Increased production of oxygen-derived free radicals was proposed to cause alterations in the muscle contractile properties, but the precise mechanism has not been elucidated. In addition, a reduced RMP has been linked to a decline in contractile performance, as it was shown in dogs that endotoxins lower the muscle RMP within several hours after administration (5). In an *in vitro* study with healthy rat muscles, adding TNFα to the incubation medium indeed lowered the RMP, hence affecting muscle contractility (22). *In vivo*, however, we failed to identify any signs pointing towards an alteration of the RMP. There were no differences in time to peak-force across all conditions, and muscles responded similarly to the different stimulation frequencies applied.

Six days after zymosan administration, dorsiflexor muscle torque was decreased in the zymosan and pair-fed rats, with a significantly greater effect in the zymosan group. Normalization of torques on muscle mass indicated that the decrease in muscle torque in both the zymosan and pair-fed rats is accounted for by the loss of muscle mass. The same is true for the 11-d groups. Eleven days after injection, zymosan rats still generated lower torques than pair-fed controls, but this effect again disappeared after normalization. The discrepancy of these findings with those of an earlier study from our laboratory (23), in which plantarflexor muscle function was studied in the zymosan model, is not clear. A significant decline of muscle function was reported 6 d after zymosan injection, of which only a small part could be explained by a loss of muscle mass. In that study (23) the mortality rate, food intake, body mass, and muscle mass showed a similar response to zymosan as in our study. At present, we cannot exclude the possibility that the difference in muscle group studied accounts for the discrepancy. We feel, however, that other, as of yet unidentified factors may account for the conflicting results. It should also be noted that this is a short-term model

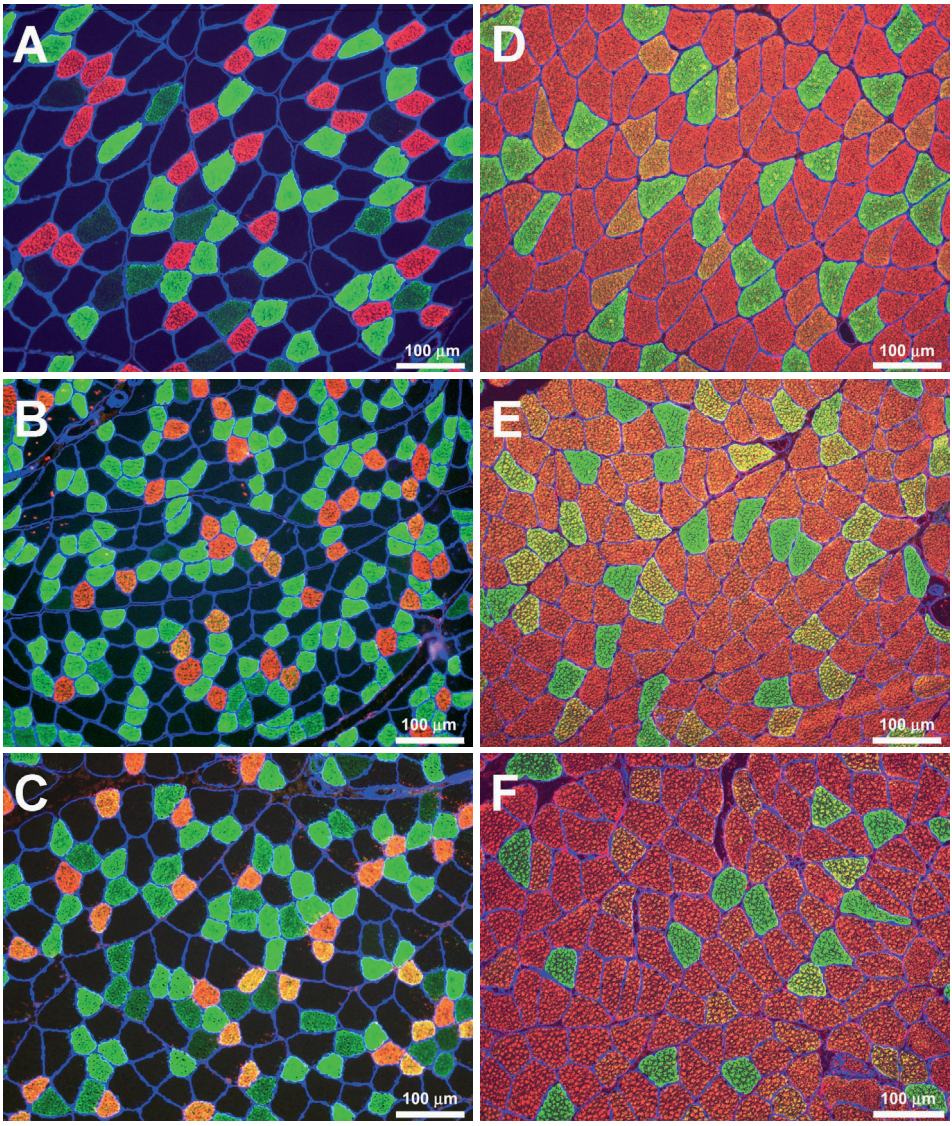

Figure 4: Staining of laminin (blue), MHC type 1 (red) and MHC type 2A (green) in samples of TA (left panels) and SOL (right panels) taken at day 6. Control sections are shown in **A** and **D**, zymosan-treated rats in **B** and **E**, and pair-fed controls in **C** and **F**. Non-stained fibers in the TA sections were classified as type 2B/X.

and that exposure to sepsis for longer than 11 days may result in neuropathy and concomitant alterations in excitability.

Muscle wasting during sepsis is mainly caused by an increased ubiquitin-proteasome dependent proteolysis. Both human and animal studies provided considerable evidence that sepsis results in an endogenous

increase in glucocorticoids, which is (partly) responsible for the activation of the ubiquitin-proteasome pathway (24-27), where proteins are targeted for degradation by covalent attachment of a chain of ubiquitin molecules (ubiquitin conjugation), with subsequent recognition and degradation by the 26S proteasome, a large multi-catalytic protein complex. The central core of this complex is referred to as the 20S proteasome and contains the actual proteolytic activity. Many components of this pathway have been implicated in its activation during sepsis, including increased ubiquitin conjugation rates, increased levels of mRNAs encoding for multiple components of the system (e.g., ubiquitin, 14 kDa-E2 and 19S and 20S subunits) and increased proteasome activity (11, 13, 19, 24, 28). Our finding of an increased 20S proteasome activity in GL 6 days after zymosan treatment supports a role

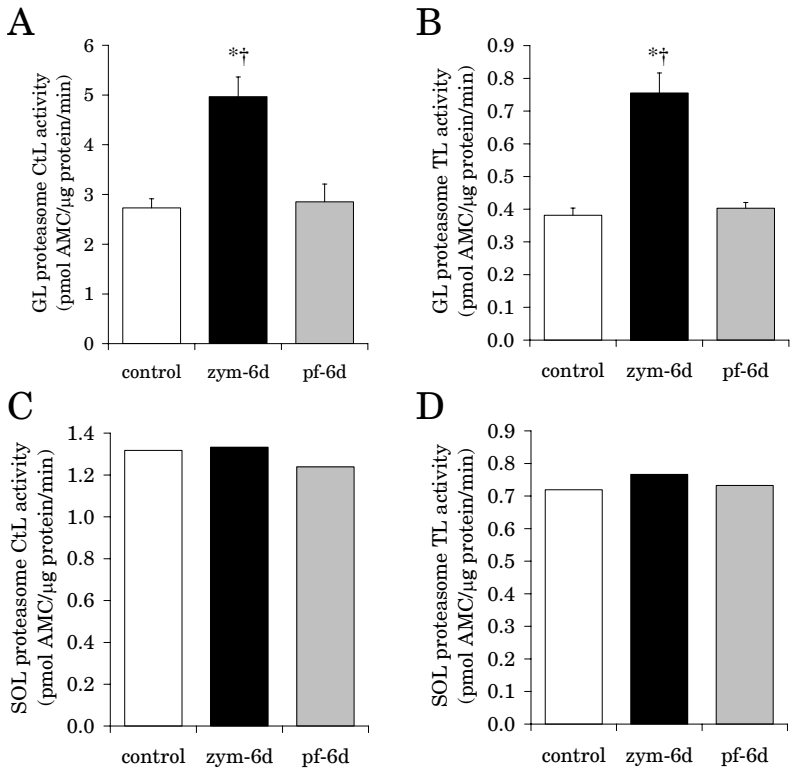

Figure 5: Chymotrypsin-like (CtL) proteasome activity and trypsin-like (TL) proteasome activity in 20S proteasome preparations from GL (A and B) and SOL (C and D). Activities against Suc-LLVY-AMC (chymotrypsin-like) and Boc-LRR-AMC (trypsin-like) are presented as pmol of AMC/μg protein/min. Values are presented for the control group (open bar), 6d zymosan group (black bars) and 6d pair-fed group (grey bars). Data on the soleus activities are based on pooled muscles (8-10 muscles per pool).
* P<0.05 vs. *ad libitum* fed control rats, † P<0.05 vs. pair-fed controls.

for the ubiquitin-proteasome system in the muscle wasting induced by zymosan. Because 20S proteasome subunit C8 protein levels are unchanged, it is highly likely that it is the specific activity of the 20S proteasome that is upregulated by zymosan.

The CSA of fibers from the mixed fiber-type portion of TA and from SOL was examined after classification of fibers as either MHC1, 2A, or 2B/X. Muscle samples from the 6-d experimental groups were analyzed, because the largest reduction of muscle mass was present at this time. These data show that muscle wasting during sepsis occurs in a fiber-type specific fashion in TA but not in SOL. Our finding of a differential regulation of 20S proteasome activity supports this fiber-type specific effect of zymosan. Six days after zymosan injection, 20S proteasome activity was significantly increased in GL (predominantly fast-twitch fibers), whereas no changes were found in SOL (predominantly slow-twitch fibers). Slow-twitch muscles indeed have been reported to be more resistant to wasting induced by sepsis (9, 10, 29-32) or fasting (33, 34) than fast-twitch muscles. Most of these observations point to differential regulation of proteolysis during sepsis, although there is also evidence for differentially regulated protein synthesis. It was shown that sepsis (9, 31) and burn injury (10, 32) stimulated total and myofibrillar protein breakdown to a greater extent in muscles primarily

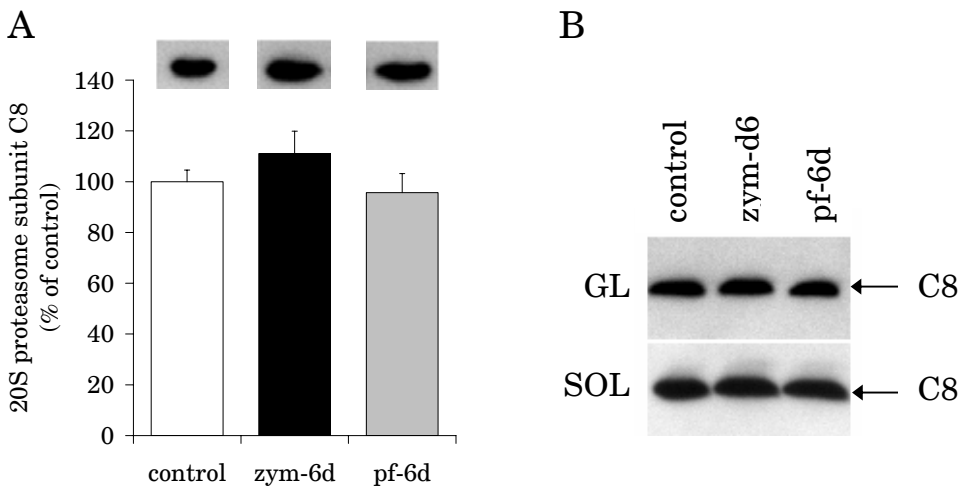

Figure 6: (A) 20S proteasome C8 subunit protein levels determined in soluble protein fractions of the TA of control (n=10), 6 d zymosan (n=8) and 6 d pair-fed (n=8) rats. **(B)** Representative 20S proteasome C8 subunit immunoblots from proteasome preparations of the GL and SOL. No statistical significant differences were detected.

composed of fast-twitch fibers (EDL) than slow-twitch fibers (SOL). Reverse observations were made for protein synthesis, showing that sepsis caused a greater inhibition of protein synthesis in fast glycolytic muscles than in slow oxidative muscles (29). This was attributed to a reduced translational efficiency in fast muscles (29, 30). A difference in the sensitivity to glucocorticoids between "red" and "white" muscles has also been suggested as a mechanism for the differential regulation of muscle protein turnover, as dexamethasone (a glucocorticoid) stimulated proteolysis to a greater extent in fast-twitch than in slow-twitch muscle (35).

In contrast with sepsis, unloading results in a greater muscle wasting in the slow SOL, compared to the faster EDL and GC (36, 37). The fact that the anti-gravity SOL responds to a greater extent to unloading suggests that the function of a muscle greatly influences the wasting response to a catabolic stimulus. In addition to previous reports, we show a fiber-type specific response to a catabolic condition even within one muscle. This demonstrates that, besides muscle function, muscle fiber-type is an important factor that should be taken into account when studying muscle protein metabolism.

In conclusion, this study shows that zymosan injection has no acute effects on muscle contractile performance. At six days after injection a pronounced decline in muscle force-generating capacity is present, which is totally accounted for by loss of muscle mass. The increased activity of the 20S proteasome at this time point parallels the loss of muscle mass. Finally, our results show that in the TA muscle, sepsis-induced muscle wasting is more pronounced in both type 2A and type 2B/X MHC fibers than in type 1 MHC fibers. This fiber-type specific wasting effect is not present in the soleus muscle, nor did we observe increased activity of the 20S proteasome in the soleus muscle.

Acknowledgements

The antibodies against myosin heavy chain type 1 and 2A (referred to as A4.480 and N2.261, respectively) used in the present study were developed by Dr. Blau and were obtained from the Developmental Studies Hybridoma Bank, developed under the auspices of the NICHD and maintained by the University of Iowa, Department of Biological Sciences, USA.

References

1. Wagenmakers AJ. Muscle function in critically ill patients. Clin Nutr 20: 451-454., 2001.
2. Callahan LA, Nethery D, Stofan D, DiMarco A, and Supinski G. Free radical-induced contractile protein dysfunction in endotoxin-induced sepsis. Am J Respir Cell Mol Biol 24: 210-217, 2001.
3. el-Dwairi Q, Comtois A, Guo Y, and Hussain SN. Endotoxin-induced skeletal muscle contractile dysfunction: contribution of nitric oxide synthases. Am J Physiol 274: C770-779, 1998.
4. Supinski G, Nethery D, Stofan D, and DiMarco A. Comparison of the effects of endotoxin on limb, respiratory, and cardiac muscles. J Appl Physiol 81: 1370-1378, 1996.
5. Gibson WH, Cook JJ, Gatipon G, and Moses ME. Effect of endotoxin shock on skeletal muscle cell membrane potential. Surgery 81: 571-577, 1977.
6. Cunningham JN, Carter NW, Rector FC, and Seldin DW. Resting transmembrane potential difference of skeletal muscle in normal subjects and severely ill patients. J Clin Invest 50: 49-59, 1971.
7. Schein M, Wittmann DH, Wise L, and Condon RE. Abdominal contamination, infection and sepsis: a continuum. Br J Surg 84: 269-272, 1997.
8. Vincent JL. Sepsis definitions. Lancet Infect Dis 2: 135, 2002.
9. Hasselgren PO, James JH, Benson DW, et al. Total and myofibrillar protein breakdown in different types of rat skeletal muscle: effects of sepsis and regulation by insulin. Metabolism 38: 634-640, 1989.
10. Chai J, Wu Y, and Sheng Z. The relationship between skeletal muscle proteolysis and ubiquitin-proteasome proteolytic pathway in burned rats. Burns 28: 527-533, 2002.
11. Attaix D and Taillandier D. The critical role of the ubiquitin-proteasome pathway in muscle wasting in comparison to lysosomal and Ca^{2+}-dependent systems. Adv Mol Cell Biol 27: 235-266, 1998.
12. Hasselgren PO. Pathways of muscle protein breakdown in injury and sepsis. Curr Opin Clin Nutr Metab Care 2: 155-160, 1999.
13. Voisin L, Breuille D, Combaret L, et al. Muscle wasting in a rat model of long-lasting sepsis results from the activation of lysosomal, Ca^{2+} -activated, and ubiquitin-proteasome proteolytic pathways. J Clin Invest 97: 1610-1617, 1996.
14. Rooyackers OE, Saris WH, Soeters PB, and Wagenmakers AJ. Prolonged changes in protein and amino acid metabolism after zymosan treatment in rats. Clin Sci (Lond) 87: 619-626, 1994.
15. Goris RJ, Boekholtz WK, van Bebber IP, Nuytinck JK, and Schillings PH. Multiple-organ failure and sepsis without bacteria. An experimental model. Arch Surg 121: 897-901, 1986.
16. Drost MR, Maenhout M, Willems PJ, Oomens CW, Baaijens FP, and Hesselink MK. Spatial and temporal heterogeneity of superficial muscle strain during in situ fixed-end contractions. J Biomech 36: 1055-1063, 2003.
17. Deveci D and Egginton S. Differing mechanisms of cold-induced changes in capillary supply in m. tibialis anterior of rats and hamsters. J Exp Biol 205: 829-840, 2002.
18. Dahlmann B, Kuehn L, Rutschmann M, and Reinauer H. Purification and characterization of a multicatalytic high-molecular-mass proteinase from rat skeletal muscle. Biochem J 228: 161-170, 1985.
19. Hobler SC, Williams A, Fischer D, et al. Activity and expression of the 20S proteasome are increased in skeletal muscle during sepsis. Am J Physiol 277: R434-440, 1999.

20. Supinski G, Nethery D, Nosek TM, Callahan LA, Stofan D, and DiMarco A. Endotoxin administration alters the force vs. pCa relationship of skeletal muscle fibers. Am J Physiol Regul Integr Comp Physiol 278: R891-896, 2000.
21. Shindoh C, Dimarco A, Nethery D, and Supinski G. Effect of PEG-superoxide dismutase on the diaphragmatic response to endotoxin. Am Rev Respir Dis 145: 1350-1354, 1992.
22. Tracey KJ, Lowry SF, Beutler B, Cerami A, Albert JD, and Shires GT. Cachectin/tumor necrosis factor mediates changes of skeletal muscle plasma membrane potential. J Exp Med 164: 1368-1373, 1986.
23. Rooyackers OE, Hesselink MK, and Wagenmakers AJ. Contraction failure of skeletal muscle of rats recovering from critical illness. Clin Sci (Lond) 92: 189-195, 1997.
24. Tiao G, Hobler S, Wang JJ, et al. Sepsis is associated with increased mRNAs of the ubiquitin-proteasome proteolytic pathway in human skeletal muscle. J Clin Invest 99: 163-168, 1997.
25. Tiao G, Fagan J, Roegner V, et al. Energy-ubiquitin-dependent muscle proteolysis during sepsis in rats is regulated by glucocorticoids. J Clin Invest 97: 339-348, 1996.
26. Auclair D, Garrel DR, Chaouki Zerouala A, and Ferland LH. Activation of the ubiquitin pathway in rat skeletal muscle by catabolic doses of glucocorticoids. Am J Physiol 272: C1007-1016, 1997.
27. Hamrahian AH, Oseni TS, and Arafah BM. Measurements of serum free cortisol in critically ill patients. N Engl J Med 350: 1629-1638, 2004.
28. Hobler SC, Wang JJ, Williams AB, et al. Sepsis is associated with increased ubiquitinconjugating enzyme E214k mRNA in skeletal muscle. Am J Physiol 276: R468-473, 1999.
29. Vary TC and Kimball SR. Sepsis-induced changes in protein synthesis: differential effects on fast- and slow-twitch muscles. Am J Physiol 262: C1513-1519, 1992.
30. Vary TC, Jurasinski CV, Karinch AM, and Kimball SR. Regulation of eukaryotic initiation factor-2 expression during sepsis. Am J Physiol 266: E193-201, 1994.
31. Tiao G, Lieberman M, Fischer JE, and Hasselgren PO. Intracellular regulation of protein degradation during sepsis is different in fast- and slow-twitch muscle. Am J Physiol 272: R849-856, 1997.
32. Fang CH, James HJ, Ogle C, Fischer JE, and Hasselgren PO. Influence of burn injury on protein metabolism in different types of skeletal muscle and the role of glucocorticoids. J Am Coll Surg 180: 33-42, 1995.
33. Goodman MN and Ruderman NB. Starvation in the rat. I. Effect of age and obesity on organ weights, RNA, DNA, and protein. Am J Physiol 239: E269-E276, 1980.
34. Goodman MN, Lowell B, Belur E, and Ruderman NB. Sites of protein conservation and loss during starvation: influence of adiposity. Am J Physiol 246: E383-390, 1984.
35. Rannels SR and Jefferson LS. Effects of glucocorticoids on muscle protein turnover in perfused rat hemicorpus. Am J Physiol 238: E564-572, 1980.
36. Fitts RH, Riley DR, and Widrick JJ. Physiology of a microgravity environment invited review: microgravity and skeletal muscle. J Appl Physiol 89: 823-839, 2000.
37. Thomason DB and Booth FW. Atrophy of the soleus muscle by hindlimb unweighting. J Appl Physiol 68: 1-12, 1990.

3

Ubiquitin-proteasome-dependent proteolytic activity remains elevated after zymosan-induced sepsis in rats while muscle mass recovers

R. Minnaard, A.J.M. Wagenmakers, L. Combaret,
D. Attaix, M.R. Drost, G.P. van Kranenburg,
G. Schaart and M.K.C. Hesselink

Int J Biochem Cell Biol 37: 2217-25, 2005

Abstract

We studied the role of the ubiquitin-proteasome system in rat skeletal muscle during sepsis and subsequent recovery. Sepsis was induced with intraperitoneal zymosan injections. This model allows one to study a sustained and reversible catabolic phase, and mimics the events that prevail in septic and subsequently recovering patients. In addition, the role of the ubiquitin-proteasome system during muscle recovery is poorly documented. There was a trend for increased ubiquitin-conjugate formation in the muscle wasting phase, which was abolished during the recovery phase. The trypsin- and chymotrypsin-like peptidase activities of the 20S proteasome peaked at day 6 following zymosan injection (i.e. when both muscle mass and muscle fiber cross-sectional area were reduced the most), but remained elevated when muscle mass and muscle fiber cross sectional area were recovering (11d). This clearly suggests a role for the ubiquitin-proteasome pathway in the muscle remodeling and/or recovery process. Protein levels of 19S complex and 20S proteasome subunits did not increase throughout the study, pointing to alternative mechanisms regulating proteasome activities. Overall these data support a role for ubiquitin-proteasome dependent proteolysis in the zymosan septic model, in both the catabolic and muscle recovery phases.

Introduction

In many catabolic conditions exhibiting extensive muscle wasting (e.g. starvation, cancer, sepsis, renal failure, etc.) increased proteolysis occurs largely through the ubiquitin-proteasome (Ub-P) pathway (1, 2). This ATP-dependent proteolytic pathway can be divided into two major steps. In the first step, proteins are targeted for degradation by covalent attachment of a polyubiquitin chain (ubiquitin conjugation). Ubiquitin conjugation is achieved by the combined action of the Ub-activating enzyme (E1), Ub-conjugating enzymes (E2), and Ub-ligases (E3) (3). In the second step, ubiquitinated proteins are recognized and degraded by the 26S proteasome, a large multi-catalytic protein complex, which comprises two 19S regulatory complexes and a 20S proteolytic core. Multiple catabolic conditions, such as sepsis, cancer and diabetes, are typified by activation of a series of Ub-P related events, like increased ubiquitin conjugation rates (4, 5), increased levels of mRNA encoding for key components of the system (1, 6, 7) and increased proteasome activity (8, 9).

Acute models of sepsis like cecal ligation and puncture (CLP) and endotoxin injections, commonly used to induce experimental sepsis in animals, result either in premature death or in a very transient catabolic state. As a consequence, most of the information on the regulation of the Ub-P system during sepsis applies only to the acute phase. Therefore, it is not possible to investigate the period of recovery following acute sepsis. Intraperitoneal zymosan injections have been used in rats to investigate the effects of an acute sepsis followed by a recovery period that includes a restoration of food intake and muscle mass (10). As the muscle atrophy in this model is more sustained and reversible, this model better resembles the events that prevail in septic and subsequently recovering patients than the CLP and endotoxin models. Zymosan is a potent stimulator of the alternative pathway of the complement system and of macrophages. Intraperitoneal injections with zymosan result in an acute local inflammatory response (peritonitis), triggering a systemic response resulting in clinical sepsis. Zymosan injection results in acute sepsis followed by a prolonged recovery. Signs of catabolism (reduction of body and muscle mass) are present until 6 days after zymosan injection. For a full comprehension of the role of the Ub-P pathway during acute sepsis-induced atrophy and subsequent muscle mass recovery, it is of importance to study the time-course of the Ub-P pathway response. Therefore, the aim of this study was to measure changes

in protein content of key components of the Ub-P pathway, ubiquitin-conjugate formation and proteasome activities both during the acute wasting phase of sepsis and the subsequent recovery period.
It was anticipated that increased formation of ubiquitin-conjugates, increased (specific) proteasome activity and increased protein levels of the 19S and 20S proteasome subunits would be most prominent in the period of rapid muscle wasting in the first days after zymosan injection and would return to control levels in the period of muscle mass recovery. Comparisons were made with pair-fed control rats to discriminate between the effects of sepsis on the one hand and of reduced food-intake on the other hand.

Materials and Methods

Animals and experimental design

The experiments were approved by the institutional animal experimental committee. Rats were individually housed (12h dark-light cycle, 21-22 °C and 50-60% humidity). Zymosan was used according to Rooyackers et al. (10). In the present chapter, the same rats were used as in chapter 2. Ten-week-old, male Wistar rats with a body mass of 300 ± 24 g were randomly assigned to a zymosan-injected, a pair-fed or an *ad libitum* fed control group. Rats assigned to the zymosan group were given an aseptic intraperitoneal injection of zymosan (30 mg/ 100 g body mass, homogeneously suspended in liquid paraffin (25 mg/ml)), based on pilot studies with a mortality rate of approximately 20%. Pilot experiments testing the effect of an i.p. injection with sterile paraffin did not show any effect on food intake and body weight during an 11-day follow-up. We interpreted this as the absence of a 'vehicle' effect. Four groups of rats (n = 10) were injected with a zymosan suspension. Food intake and body mass were recorded daily. At 2h, 2d, 6d and 11d after zymosan injection rats were anaesthetized using a subcutaneous injection of ketamine (100 mg/kg body mass) and xylazine (10 mg/kg) and the main dorsal and plantar flexor muscles of the hindlimb (tibialis anterior (TA) and gastrocnemius, respectively) were carefully dissected, weighed (wet weight) and frozen in melting 2-methylbutane, after which rats were sacrificed by cervical dislocation. Since zymosan injection affects food intake, control rats were pair-fed to the 2, 6 and 11d zymosan rats. An *ad libitum* fed control group, which was sacrificed at day 11, was also included.

Muscle fiber cross-sectional area quantitation

The mean TA muscle fiber cross-sectional area (CSA) was determined as described recently (11). Briefly, transverse muscle sections were cut and incubated with a rabbit polyclonal laminin antibody (Sigma, Zwijndrecht, The Netherlands), followed by incubation with an Alexa350-conjugated goat antirabbit Ig antibody (Molecular Probes, Invitrogen, Breda, The Netherlands). Muscle fiber CSA was quantitated using a fluorescence microscope (Uvikon, Bunnik, The Netherlands) and Lucia 4.8 software (Nikon, Düsseldorf, Germany) using the laminin signal as a marker for cell boundary.

Western blot analysis

Individual tibialis anterior muscles were homogenized in 4 ml ice-cold buffer (pH 7.5), containing 50 mM Tris, 1mM EDTA, 1 mM DTT, 1 mM PMSF, 10 μg/ml pepstatin A and 10 μg/ml leupeptin. Homogenates were centrifuged at 10,000 x g, 4 °C for 10 min. and the resulting supernatants were centrifuged at 100,000 x g, 4 °C for 1h. The soluble protein concentration was determined in the supernatant using the Bio-Rad protein assay. Soluble proteins (20 μg) were subjected to routine Western blotting using 12% polyacrylamide SDS-gels and antibodies against the 14 kDa-E2 (polyclonal rabbit antibody; 1:5,000), the 19S complex subunit S6a (TBP1-19; monoclonal mouse antibody; 1:10,000; Affiniti Research Products, Exeter, UK) and the 20S proteasome subunit C8 (MCP72; mouse monoclonal; 1:10,000; Affiniti). After washing, blots were incubated with either a horseradish peroxidase-conjugated swine anti-rabbit Ig (SwARPO, DAKO, Glostrup, Denmark) or a horseradish peroxidase-conjugated rabbit anti-mouse Ig (DAKO), both diluted 1:10,000. Chemiluminescence was performed using a Super Signal West Dura extended kit (Pierce, Rockford, IL) and the blots were exposed to CL-Xposure Film (Pierce). Protein bands were quantified using optical densitometry.

Ubiquitin-conjugate formation

Soluble proteins were prepared from individual TA muscles as described in the Western blot section, after which they were pooled (n=10 per group). The ubiquitin conjugate formation was determined by incubating 50 μg of

soluble proteins for 1h at 37 °C with 5 μM [125I]-labelled ubiquitin (specific activity ~3000 c.p.m. $pmol^{-1}$), 50 mM Tris-HCl (pH7.5), 1 mM DTT, 2 mM $MgCl_2$ and 2 mM AMP-PNP, in a total volume of 20 μl. The reactions were stopped by adding 1x sample buffer according to Laemmli (12) (62.5 mM Tris-HCl (pH 6.8), 5% β-mercaptoethanol, 2% SDS, 0.1% bromophenol blue and 10% glycerol). It has been shown that conjugation rates are linear for these 60 minutes and that exogenous labelled ubiquitin was present in significant excess of any endogenous ubiquitin (i.e. addition of higher amounts of labelled ubiquitin did not increase rates of ubiquitin conjugation) (13). After stopping the reaction, the ubiquitin-conjugated proteins were separated from free ubiquitin by electrophoresis on 12% polyacrylamide SDS-gels. Subsequently, gels were dried and exposed to Hyperfilm MP (Amersham Biosciences, Roosendaal, The Netherlands). The film was scanned and both the high molecular weight conjugate band and the 70 kDa ubiquitin-conjugate band were quantified by optical densitometry.

Isolation of 20S proteasomes and measurement of peptidase activities

In all groups the 20S proteasome activities were determined in the gastrocnemius lateralis muscle, essentially according to Hobler et al. (8). Briefly, muscles were homogenized and proteasomes were isolated by sequential (ultra)centrifugation steps. Proteasome fractionation yielded similar amounts of protein (determined with the Bio-Rad protein assay) across the different experimental groups. The peptidase activities of the 20S proteasome were determined fluorometrically by measuring the hydrolysis of the fluorogenic substrates Succinyl-Leu-Leu-Val-Tyr-7-amido-4-methylcoumarin (Suc-LLVY-AMC, Sigma) and t-Butoxycarbonyl-Leu-Arg-Arg-7-amido-4-methylcoumarin (Boc-LRR-AMC, Affiniti). These substrates are preferentially hydrolyzed by the chymotrypsin-like and trypsin-like activities of the 20S proteasome, respectively. Standard curves were established for AMC, which permitted the expression of the proteasome activity as pmol AMC · μg $protein^{-1}$ · min^{-1}. Adding the proteasome inhibitor MG132 to the reaction resulted in complete inhibition of the proteasome peptidase activities.

Statistics

Results are presented as means ± SEM. To study the effects of zymosan injection and pair-feeding on the measured parameters in time a one-way ANOVA was performed using *ad libitum* fed control data as t=0 data. Differences were located using the Scheffé post-hoc test. Two-way ANOVA was performed to examine the interaction between intervention (zymosan treatment or pair-feeding) and time. Significance was set at $P < 0.05$.

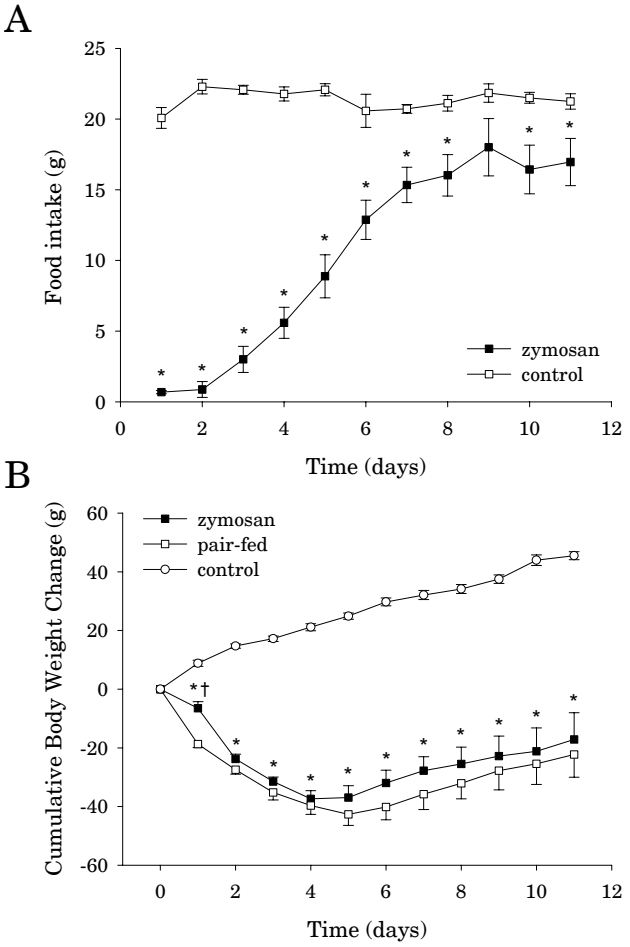

Figure 1: (A) Food intake of zymosan-treated and *ad libitum* fed control rats. **(B)** Cumulative change in body mass of zymosan treated, pair-fed control and *ad libitum* fed control rats.
* P<0.05 vs. *ad libitum* fed control rats, † P<0.05 vs. pair-fed controls.

Results

Characterization of the zymosan model

Zymosan injection induced an acute peritonitis, with symptoms of severe illness being present in all rats during the first 2 days after injection. Symptoms included lethargy, hypophagia, hyperventilation, tachycardia, fever, diarrhea and loss of hemorrhagic fluid from the nose. As anticipated, zymosan injection resulted in 20% mortality. Figure 1A shows a reduction in food intake of approximately 90% until 2 days post-injection with a gradual increase of food intake towards day 7. Hereafter, food intake remained stable, but at a significantly lower level (~18%) than in controls. The reduced food intake was almost instantaneously reflected in a decreased body mass, with a similar response being present in the zymosan and pair-fed control rats (Figure 1B).

As soon as 2 days after zymosan injection, the mass (Figure 2) and fiber CSA (Table 1) of the TA muscle declined significantly compared to both pair-fed and *ad libitum* fed controls. The most prominent decline was observed at day 6. The pair-fed group showed similar, albeit less pronounced responses for both muscle mass and fiber CSA. On day 11 TA muscle mass was increased compared to day 6 in both the zymosan-treated (P=0.008) and pair-fed groups (P=0.016). The TA fiber CSA showed the same trends in both the zymosan-treated and pair-fed groups, although the 6 day and 11 day values were not significantly different. The same pattern of wasting and recovery was observed in the gastrocnemius muscle (data not shown).

Table 1. Muscle fiber cross-sectional area (CSA) in the tibialis anterior muscle.

		Mean fiber CSA (μm^2)
	control	1469 ±70
2 d	zymosan	1108 ± 69 (-25%)*†
2 d	pair-fed	1351 ± 81 (-8%)
6 d	zymosan	1009 ± 62 (-31%) *†
6 d	pair-fed	1264 ± 83 (-14%)*
11 d	zymosan	1163 ± 70 (-21%)*†
11 d	pair-fed	1363 ± 59 (-7%)

Values between brackets indicate the relative reduction of CSA vs. *ad libitum* fed controls.
* P<0.05 vs. *ad libitum* fed control rats
† P<0.05 vs. pair-fed controls.

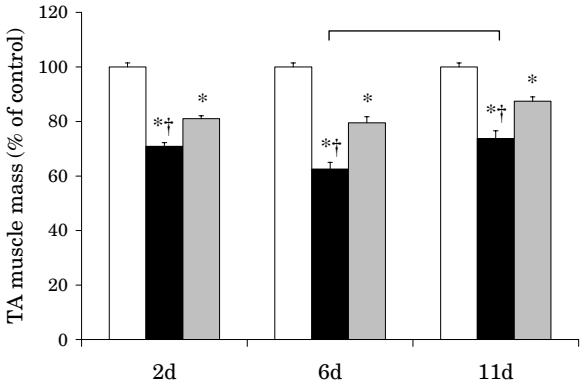

Figure 2: Tibialis anterior muscle mass (% of control absolute muscle mass) at different time points in zymosan (black bars), pair-fed (grey bars) and *ad libitum* fed control (white bars) rats. * P<0.05 vs. *ad libitum* fed control rats. † P<0.05 vs. pair-fed rats. No intervention*time effect was detected. The bracket indicates a significant difference between the 6d and 11d zymosan-treated groups.

Ubiquitin-conjugate formation

The *in vitro* formation of ubiquitin-conjugates increased (+50%) within 2 h after zymosan injection (Figure 3), transiently decreased at day 2, peaked again at day 6 (+49%) and was totally normalized at day 11. Except for day 2 (+35%), there was no increased accumulation of ubiquitin conjugates in the pair-fed rats.

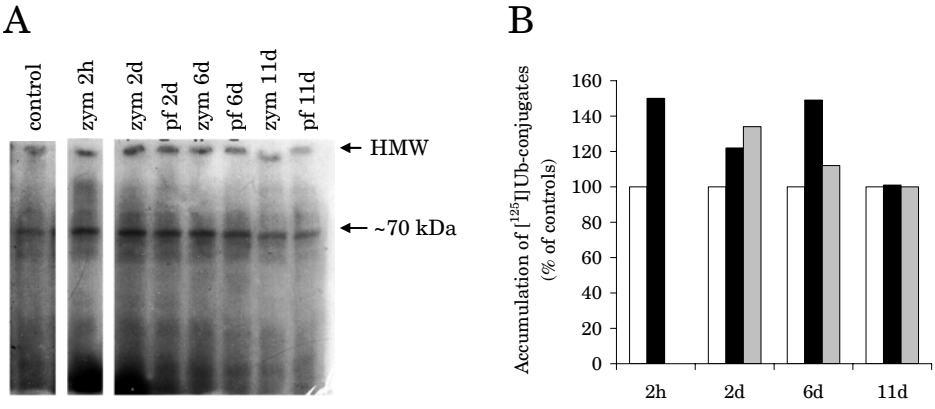

Figure 3: (A) Accumulation of soluble muscle [^{125}I]Ub-conjugates in the control, zymosan-injected (zym), and pair-fed (pf) groups. HMW denotes high molecular weight proteins. **(B)** Quantitation of [^{125}I]Ub-conjugation (% of controls) in zymosan-injected (black bars), pair-fed (grey bars) and *ad libitum* fed control (white bars) rats. Values are averages of three separate measurements.

Protein levels of components of the ubiquitin-proteasome pathway

To examine if changes in ubiquitin conjugation rates and proteasome activity can be explained by changes in protein levels of key components of the Ub-P system, we determined protein levels of the 14-kDa E2 ubiquitin conjugating enzyme, the 19S complex S6a subunit and the 20S proteasome C8 subunit at days 2, 6 and 11. A significant increase in 14-kDaE2 protein levels (compared to controls) was only observed 2 days after zymosan injection (Figure 4A). The protein levels of the 19S complex subunit S6a (Figure 4B) and 20S proteasome subunit C8 (Figure 4C) did not change in either the zymosan-injected or pair-fed rats.

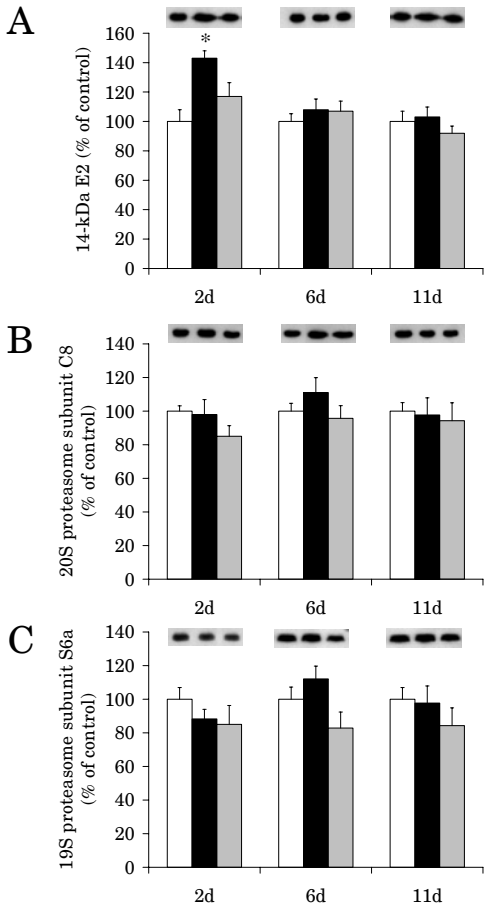

Figure 4: Protein levels (% of control) of **(A)** 14-kDa E2 ubiquitin-conjugating enzyme, **(B)** 20S proteasome subunit C8, and **(C)** subunit S6a of the 19S complex, at several time points in zymosan-injected (black bars), pair-fed (grey bars) and *ad libitum* fed (white bars) rats.
* $P<0.05$ vs. ad libitum fed control rats. No treatment*time effect was detected.

20S Proteasome activities

The trypsin-like (+47%) peptidase activity of the 20S proteasome markedly increased as early as 2 h after zymosan injection and remained elevated throughout the study (Figure 5B). The chymotrypsin- and trypsin-like peptidase activities of the 20S proteasome increased by 82% and 100% at day 6 after zymosan injection, respectively, when the decline in muscle mass was most prominent. The trypsin-like activity was markedly and significantly higher in the zymosan than in the pair-fed group at all time-points, while the chymotrypsin-like activity was markedly higher at days and 11. Notably, the peptidase activities of the 20S proteasome (either trypsin- or chymotrypsin-like) did not exceed control values in the pair-fed groups, except for the trypsin-like activity at day 11. While at day 11 muscle mass was increased in comparison to day 6 (P=0.008), the 20S proteasome peptidase activities remained high in the zymosan-injected group at this time point.

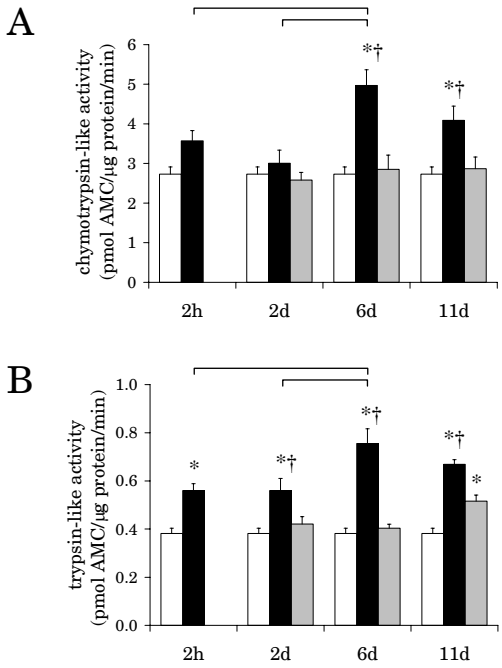

Figure 5: (A) Chymotrypsin- and **(B)** trypsin-like peptidase activities of the 20S proteasome (expressed as pmol AMC generated/μg protein/min) at several time points in zymosan-injected (black bars), pair-fed (grey bars) and ad libitum fed (white bars) rats. * P<0.05 vs. ad libitum fed control rats. † P<0.05 vs. pair-fed rats. A significant treatment*time effect was detected for the chymotrypsin (P=0.045) and trypsin-like (P=0.012) peptidase activities of the 20S proteasome. The brackets denote significant differences between the respective zymosan-injected groups.

Discussion

In the present study, sepsis-induced muscle wasting was achieved by intraperitoneal injection with zymosan, resulting in a period of acute sepsis. Although zymosan-induced sepsis is primarily caused by a non-infective stimulus rather than by the actual presence of bacteria, classical infectious responses (e.g., tachycardia, fever, increased respiratory rate, and hypophagia) were observed. Throughout the 11-day period of investigation body and muscle mass of the zymosan-injected rats had not yet returned to control values. Using this model we observed both acute (within 2 h) and prolonged effects on the Ub-P pathway, i.e. trends for increased ubiquitin-conjugate formation for up to 6 days, increased chymotrypsin-like activity at days 6 and 11, and increased trypsin-like activities of the 20S proteasome throughout the study. Notably, these changes were not paralleled by increased protein levels of subunits of both the 19S complex and 20S proteasome. These data suggest that proteasome activities may be upregulated by alternative mechanisms. At day 11, when muscle mass was clearly recovering, the 20S proteasome peptidase activities were still significantly elevated. This observation is remarkable and clearly suggests that in the recovery period, when muscle mass recovers, the degradation rate of at least a number of proteins is upregulated. Another striking observation was that the decreased muscle mass in the pair-fed rats did not require significant increases in peptidase activities of the 20S proteasome. Thus, muscle wasting during periods of reduced food intake in otherwise healthy rats was not accompanied by marked effects on the Ub-P system.

The increased ubiquitin-conjugate formation in the zymosan septic model is in agreement with previous observations in other catabolic conditions, including fasting (13), cancer (4), diabetes (14), and dexamethasone treatment (9). However, care should be taken in interpreting our results, as we measured the accumulation of Ub-conjugates at a single time point and not the rate of ubiquitination. Whereas it had been shown that following CLP rates of ubiquitin conjugation were increased within 16 hours after induction of sepsis (4), the present data suggest that the formation of ubiquitin-conjugates increased as early as 2 hours after inducing sepsis.

Increased mRNA levels of subunits of the 20S proteasome are commonly observed in multiple catabolic conditions, including sepsis, in both rat (8, 15-17) and human muscles (18). Similar observations also prevailed for 19S proteasome subunits in other catabolic conditions (6). In contrast, this study

clearly shows that changes at the protein level were absent in response to zymosan injection, suggesting that it is premature to link increased mRNA levels of proteasome subunits directly to increased proteasome activity and increased rates of proteolysis. In line with this, administering glucocorticoids to induce muscle atrophy in rats increased proteasome activity and mRNA levels of five 19S proteasome subunits, while protein levels of these subunits did not change (9). Also, CLP-induced sepsis in rats upregulated the 20S proteasome C9 subunit mRNA level without a concomitant change in protein content (8). A putative explanation for the apparent discrepancy between the response of proteasome subunits at the mRNA level and at the protein level could be an increased rate of turnover of the proteasome subunits. Alternatively, it has also been hypothesized that increased mRNA levels of proteasome subunits are required for the increased biogenesis of muscle proteasomes in acute diabetes to change the proteasome subtype pattern and modulate peptidase activities (19).

The 20S proteasome contains at least 3 peptidase activities, i.e. the trypsin-like, chymotrypsin-like and caspase-like activities (20, 21). *In vivo*, the peptidase activities of the 20S proteasome are regulated by the 19S proteasome, which serves to recognize, unfold and inject polyubiquitinated proteins into the catalytic chamber of the 20S proteasome (22). In the present study we measured peptidase activities of the 20S proteasome with established methods (23, 24). To the best of our knowledge, 20S proteasome activities measured in identical or similar conditions were always in good agreement with rates of proteolysis. These activities increased when rates of total and/or proteasome-dependent proteolysis were increased (8, 9, 23, 25). Conversely peptidase activities decreased when proteolysis was attenuated after a catabolic event (25-27), or when proteolysis decreased below basal levels (26). Increased 20S proteasome peptidase activities have been previously reported in septic muscles within 4 h after CLP (8). Within a shorter time frame (i.e. 2 h after zymosan injection) we observed a significant increase in the trypsin-like 20S proteasome peptidase activity. This very fast response suggests the involvement of a rapidly acting regulatory mechanism such as (de)phosporylation of proteasome subunits. Indeed, the proteasome has multiple phosphorylation sites with dephosphorylation reducing proteasome activity (28, 29).

While the increased proteasome activity in the acute phase was anticipated, we observed the highest activities at days 6 and 11 after zymosan injection.

This prolonged increase in 20S proteasome activity is remarkable, especially at day 11, when muscle mass and CSA were clearly improving. Assuming that the high proteasome activities during recovery indeed reflect high rates of proteolysis, protein synthesis rates must be simultaneously increased to ensure net protein anabolism. Increased protein breakdown has been previously reported during muscle hypertrophy in the fowl (30) and during compensatory growth in response to muscle overloading in the rat (31). The high proteasome activity during recovery may suggest a role for Ub-P dependent proteolysis in the remodeling of skeletal muscle. An increased proteasome activity may be needed to remove or replace remnant proteins or atrophy-related protein isoforms during recovery. A role of the Ub-P pathway in muscle remodeling has been reported previously during reloading of the unweighted soleus muscle (32, 33). Therefore, contrasting with the established role of the Ub-P system in catabolic phases, high proteasome activities may also contribute to accelerate muscle recovery. If this is the case, blocking proteasome activity for sustained periods of time could be deleterious as this may impede muscle recovery after a catabolic event.

Despite the presence of muscle atrophy, the proteasome peptidase activities and formation of ubiquitin-conjugates (except for day 2) were not increased in the pair-fed rats. This is presumably due to the stage of maturation of the rats used in this study (10 weeks at the onset of the study). Young rats exhibit a pronounced activation of the Ub-P system upon starvation (13), but this catabolic response is strongly attenuated or delayed in older (young)-adult animals (34-36).

In summary, the present study clearly shows an activation of the Ub-P pathway during the long-lasting muscle wasting in zymosan-injected septic rats. More interestingly, 20S proteasome peptidase activities remained elevated when muscle mass and CSA improved during the subsequent recovery period. This suggests that increased proteolysis plays a role in muscle recovery and/or remodeling.

Acknowledgements

We would like to thank Dr. S. Wing (McGill University, Montréal, Canada) for providing us with the 14 kDa-E2 antibody.

References

1. Attaix D, Combaret L, Kee AJ, and Taillandier D. Mechanisms of ubiquitination and proteasome-dependent proteolysis in skeletal muscle. Molecular Nutrition (J Zempleni, H Daniels eds) CAB International, Wallingford, Oxon, UK: 219-235, 2003.
2. Jagoe RT and Goldberg AL. What do we really know about the ubiquitin-proteasome pathway in muscle atrophy? Curr Opin Clin Nutr Metab Care 4: 183-190, 2001.
3. Pickart CM. Mechanisms underlying ubiquitination. Annu Rev Biochem 70: 503-533, 2001.
4. Solomon V, Baracos V, Sarraf P, and Goldberg AL. Rates of ubiquitin conjugation increase when muscles atrophy, largely through activation of the N-end rule pathway. Proc Natl Acad Sci U S A 95: 12602-12607, 1998.
5. Lecker SH, Solomon V, Mitch WE, and Goldberg AL. Muscle protein breakdown and the critical role of the ubiquitin- proteasome pathway in normal and disease states. J Nutr 129: 227S-237S, 1999.
6. Price SR. Increased transcription of ubiquitin-proteasome system components: molecular responses associated with muscle atrophy. Int J Biochem Cell Biol 35: 617-628, 2003.
7. Lecker SH, Jagoe RT, Gilbert A, et al. Multiple types of skeletal muscle atrophy involve a common program of changes in gene expression. Faseb J 18: 39-51, 2004.
8. Hobler SC, Williams A, Fischer D, et al. Activity and expression of the 20S proteasome are increased in skeletal muscle during sepsis. Am J Physiol 277: R434-440, 1999.
9. Combaret L, Taillandier D, Dardevet D, et al. Glucocorticoids regulate mRNA levels for subunits of the 19 S regulatory complex of the 26 S proteasome in fast-twitch skeletal muscles. Biochem J 378: 239-246, 2004.
10. Rooyackers OE, Saris WH, Soeters PB, and Wagenmakers AJ. Prolonged changes in protein and amino acid metabolism after zymosan treatment in rats. Clin Sci (Lond) 87: 619-626, 1994.
11. Minnaard R, Drost MR, Wagenmakers AJ, van Kranenburg GP, Kuipers H, and Hesselink MK. Skeletal Muscle wasting and contractile performance in septic rats. Muscle Nerve 31: 339-348, 2005.
12. Laemmli UK. Cleavage of structural proteins during the assembly of the head of bacteriophage T4. Nature 227: 680-685, 1970.
13. Kee AJ, Combaret L, Tilignac T, et al. Ubiquitin-proteasome-dependent muscle proteolysis responds slowly to insulin release and refeeding in starved rats. J Physiol 546: 765-776, 2003.
14. Lecker SH, Solomon V, Price SR, Kwon YT, Mitch WE, and Goldberg AL. Ubiquitin conjugation by the N-end rule pathway and mRNAs for its components increase in muscles of diabetic rats. J Clin Invest 104: 1411-1420, 1999.
15. Chai J, Wu Y, and Sheng Z. The relationship between skeletal muscle proteolysis and ubiquitin-proteasome proteolytic pathway in burned rats. Burns 28: 527-533, 2002.
16. Voisin L, Breuille D, Combaret L, et al. Muscle wasting in a rat model of long-lasting sepsis results from the activation of lysosomal, Ca2+ -activated, and ubiquitin-proteasome proteolytic pathways. J Clin Invest 97: 1610-1617, 1996.
17. Deval C, Mordier S, Obled C, et al. Identification of cathepsin L as a differentially expressed message associated with skeletal muscle wasting. Biochem J 360: 143-150, 2001.

18. Tiao G, Hobler S, Wang JJ, et al. Sepsis is associated with increased mRNAs of the ubiquitin-proteasome proteolytic pathway in human skeletal muscle. J Clin Invest 99: 163-168, 1997.
19. Merforth S, Kuehn L, Osmers A, and Dahlmann B. Alteration of 20S proteasome-subtypes and proteasome activator PA28 in skeletal muscle of rat after induction of diabetes mellitus. Int J Biochem Cell Biol 35: 740-748, 2003.
20. Orlowski M and Wilk S. Ubiquitin-independent proteolytic functions of the proteasome. Arch Biochem Biophys 415: 1-5, 2003.
21. Orlowski M and Wilk S. Catalytic activities of the 20 S proteasome, a multicatalytic proteinase complex. Arch Biochem Biophys 383: 1-16, 2000.
22. Tanaka K. Molecular biology of proteasomes. Mol Biol Rep 21: 21-26, 1995.
23. Fang CH, Li BG, Fischer DR, et al. Burn injury upregulates the activity and gene expression of the 20 S proteasome in rat skeletal muscle. Clin Sci (Lond) 99: 181-187, 2000.
24. Hobler SC, Wang JJ, Williams AB, et al. Sepsis is associated with increased ubiquitinconjugating enzyme E214k mRNA in skeletal muscle. Am J Physiol 276: R468-473, 1999.
25. Smith HJ, Mukerji P, and Tisdale MJ. Attenuation of proteasome-induced proteolysis in skeletal muscle by {beta}-hydroxy-{beta}-methylbutyrate in cancer-induced muscle loss. Cancer Res 65: 277-283, 2005.
26. Tilignac T, Temparis S, Combaret L, et al. Chemotherapy inhibits skeletal muscle ubiquitin-proteasome-dependent proteolysis. Cancer Res 62: 2771-2777, 2002.
27. Whitehouse AS and Tisdale MJ. Downregulation of ubiquitin-dependent proteolysis by eicosapentaenoic acid in acute starvation. Biochem Biophys Res Commun 285: 598-602, 2001.
28. Mason GG, Hendil KB, and Rivett AJ. Phosphorylation of proteasomes in mammalian cells. Identification of two phosphorylated subunits and the effect of phosphorylation on activity. Eur J Biochem 238: 453-462, 1996.
29. Mason GG, Murray RZ, Pappin D, and Rivett AJ. Phosphorylation of ATPase subunits of the 26S proteasome. FEBS Lett 430: 269-274, 1998.
30. Laurent GJ, Sparrow MP, and Millward DJ. Turnover of muscle protein in the fowl. Changes in rates of protein synthesis and breakdown during hypertrophy of the anterior and posterior latissimus dorsi muscles. Biochem J 176: 407-417, 1978.
31. Goldspink DF, Garlick PJ, and McNurlan MA. Protein turnover measured in vivo and in vitro in muscles undergoing compensatory growth and subsequent denervation atrophy. Biochem J 210: 89-98, 1983.
32. Taillandier D, Combaret L, Pouch MN, Samuels SE, Bechet D, and Attaix D. The role of ubiquitin-proteasome-dependent proteolysis in the remodelling of skeletal muscle. Proc Nutr Soc 63: 357-361, 2004.
33. Taillandier D, Aurousseau E, Combaret L, Guezennec CY, and Attaix D. Regulation of proteolysis during reloading of the unweighted soleus muscle. Int J Biochem Cell Biol 35: 665-675, 2003.
34. Mosoni L, Malmezat T, Valluy MC, Houlier ML, Attaix D, and Mirand PP. Lower recovery of muscle protein lost during starvation in old rats despite a stimulation of protein synthesis. Am J Physiol 277: E608-616, 1999.
35. Goodman MN, McElaney MA, and Ruderman NB. Adaptation to prolonged starvation in the rat: curtailment of skeletal muscle proteolysis. Am J Physiol 241: E321-327, 1981.

36. Dehoux M, Van Beneden R, Pasko N, et al. Role of the insulin-like growth factor I decline in the induction of atrogin-1/MAFbx during fasting and diabetes. Endocrinology 145: 4806-4812, 2004.

4

UCP3 in muscle wasting: a role in modulating lipotoxicity?

R. Minnaard, P. Schrauwen, G. Schaart and M.K.C. Hesselink

FEBS Letters (in press, 2006)

Abstract

Increased muscle UCP3 gene and protein expression has been reported in several models of cachexia, suggesting that this may contribute to muscle atrophy by modulating energy expenditure. In contrast to UCP1, however, UCP3 has not been shown to be involved in mitochondrial uncoupling, and hence energy expenditure, under physiological circumstances. Therefore, an alternative role for UCP3 has been hypothesized, implicating UCP3 in the defense against lipid-induced oxidative damage (lipotoxicity) by exporting free fatty acid (FFA) anions and derived lipid peroxide products from the mitochondrial matrix to maintain mitochondrial integrity. Indeed, UCP3 protein has been shown to be upregulated in situations of increased oxidative stress or increased supply of fatty acids to the muscle, conditions which are present in many cachectic diseases. We aimed to explore the hypothesized role for UCP3 in cachectic rats (zymosan-induced sepsis). Zymosan-treated rats lose muscle mass very rapidly, up to 35% at day 6, after which muscle mass slowly recovers. UCP3 protein content (relative to cytochrome c content) was increased 2, 6 and 11 days after zymosan injection. Interestingly, this was only accompanied by increased plasma FFA levels at day 2, while FFA levels dropped below control levels on day 6 and 11. Rats pair-fed to the zymosan rats did show increased FFA levels throughout the study, probably accounting for the increased UCP3 levels present in these rats. The increase in UCP3 protein content was smaller than in the zymosan-treated rats, however. Muscular levels of the lipid peroxidation byproduct 4-hydroxy-2-nonenal (4-HNE) were increased at days 6 and 11 in zymosan-treated rats, supporting the idea that UCP3 may serve to modulate lipotoxicity during cachexia.

Introduction

The catabolic state present in multiple models of cachexia results in a profound and massive loss of muscle mass, and reduced cellular energy charge (for review see e.g. (1)). Upon its discovery in 1997 and based on its homology with the *bona fide* uncoupling protein UCP1, UCP3 has been implicated in the regulation of energy expenditure and has thus been studied as a putative contributor to muscle wasting under cachectic conditions. Increased gene and protein expression of UCP3 has been reported in several cachectic diseases, including cancer (2-4), sepsis (5), burn-injury (6), and rheumatoid arthritis (7, 8), indeed suggesting a role of UCP3 in facilitating, or contributing to, the muscle wasting observed. In contrast, a study in pancreatic cancer patients (9) and studies in COPD patients (10, 11) reported unchanged or even decreased UCP3 levels.

If UCP3 is indeed involved in the regulation of energy expenditure, increased muscle UCP3 content under cachectic conditions could be viewed as an unjustifiable adaptive response. UCP3 knockout mice have a similar whole body energy expenditure compared to wild-type littermates, despite a 4-fold increase of *in vivo* ATP synthesis rates (12). Moreover, the lack of an apparent phenotype in UCP3 ablated mice (13), and the inability of UCP3 to affect mitochondrial coupling in humans despite a 44% high-fat diet-induced increase in UCP3 (14), have raised serious doubts on whether UCP3 has the ability to function as a native uncoupling protein under physiological circumstances (15).

Thus, the modulation of energy expenditure may not be the main physiological role of UCP3 (15). More recently, an alternative function of UCP3 has been proposed, implicating a role for UCP3 in modulating lipotoxicity (16, 17) through the efflux of mitochondrial matrix bound fatty acids and derived lipid peroxidation products (17-19). The matrix is the major site of mitochondrial reactive oxygen species (ROS) production, and matrix bound fatty acids are especially prone to lipid peroxidation. Thus, highly reactive lipid peroxides can be formed, which in turn may damage mtDNA and important electron transport protein complexes in the matrix in a process termed lipotoxicity. As mitochondrial DNA repair mechanisms are limited (20, 21) and electron transport complexes are vital to mitochondrial life, it is important to prevent the accumulation of lipid peroxides in the matrix. In this respect, increased UCP3 content and activation of UCP3 by the lipid peroxidation byproduct 4-HNE (22) could be considered important

adaptive responses to conditions of increased oxidative stress and disturbed fat oxidation. Increased oxidative stress in combination with increased UCP3 protein levels have indeed been found in experimental cancer cachexia (23, 24).
Interestingly, the cachectic state is often accompanied by increased rates of adipose tissue lipolysis (25), a reduced mitochondrial volume and aberrations in mitochondrial protein synthesis rate (26), a combination typically resulting in increased levels of UCP3 (19).
We hypothesize that a cachexia-related increased UCP3 protein content serves to modulate lipotoxicity. To investigate this, we examined UCP3 protein content in a cachectic rat model (zymosan-induced sepsis), known to induce hypophagia (27), decrease fat oxidative capacity (28) and compromise mitochondrial protein synthesis rates (26). Pair-fed controls were included to differentiate between the effects of (semi)starvation and the effect of zymosan-induced cachexia.

Methods

Animals and experimental design

Experiments were approved by the institutional animal experimental committee. Rats were individually housed (12h dark-light cycle, 21-22 °C and 50-60% humidity). The zymosan model was applied to induce a transient septic shock, as described previously (27). Ten-week-old, male Wistar rats with an average body mass of 300 g were given an aseptic intraperitoneal injection of zymosan (30 mg/ 100 g body mass) suspended in liquid paraffin (25 mg/ml). A homogeneous zymosan suspension was sterilized by incubation at 100°C for 90 minutes. Four groups of rats (n = 10) were injected with the zymosan suspension.
Food intake and body mass were recorded daily. Rats were sacrificed at 2d, 6d, and 11d after zymosan injection. Since zymosan-induced sepsis is associated with profound decreases in food intake, age-matched control rats were pair-fed to the 2, 6, and 11 d zymosan rats. An age-matched *ad libitum* fed control group, which was sacrificed at day 11, served to provide control levels of all parameters assessed.
In all groups blood was sampled by cardiac punction after 2 hours of food withdrawal and prior to dissecting the tibialis anterior muscle (TA), which

was promptly frozen in melting 2-methylbutane, after which the rats were sacrificed by cervical dislocation.

Muscle UCP3 protein content and lipid peroxidation

Skeletal muscle UCP3 protein content was determined as described previously (14). Briefly, from each sample an equal amount of protein was loaded on a polyacrylamide gel and western blotting was performed against rat UCP3 using a rabbit polyclonal UCP3 antibody (code 1338; kindly provided by LJ Slieker, Eli Lilly). Blotting was also performed for cytochrome c (CytC) as a marker of mitochondrial content. For valid inter gel comparison a standard sample was loaded on each gel and UCP3 levels were expressed relative to this standard. Values were expressed as UCP3/CytC ratios and as percentages of control values.
As marker of lipid peroxidation, protein adducts of the lipid peroxidation byproduct 4-hydroxy-2-nonenal (4-HNE) were examined by immunofluorescence using a rabbit polyclonal antibody against 4-HNE-protein adducts (Calbiochem, San Diego, CA, USA). In the present paper, protein adducts of 4-HNE are referred to as 4-HNE content or levels. Only images in which the entire field of view comprised muscle fibers were processed for quantification. Upon conversion to 8 bits grayscale, the 4-HNE derived staining was measured as integral optical density and expressed as percentage of control values. Using this approach we ensured the examination of 4-HNE in muscle cells and avoided contamination of other cell-types, as may occur in muscle homogenates.

Plasma analyses

Blood samples were collected in tubes containing EDTA and immediately centrifuged at 4,000 rpm for 10 min at 4°C. Plasma was frozen in liquid nitrogen and stored at -80°C until further analysis of free fatty acids (FFA) (Wako NEFA C test kit; Wako chemicals, Neuss, Germany) and triglycerides (glycerol kinase-lipase method Boehringer, Mannheim, Germany) was undertaken. All analyses were performed on an automated centrifugal spectrophotometer (Cobas Fara, La Roche, Basel, Switzerland).

Statistics

Results are presented as means ± SEM. For each time-point, the zymosan, pair-fed, and control group data were compared using one-way ANOVA analysis. Differences were located using the Scheffé post-hoc test. Significance was set at $P < 0.05$. For UCP3 protein analyses, three muscle pools were made per zymosan group and compared to the corresponding pair-fed and control muscle pools. The effect of zymosan on UCP3 protein was compared to the effect of pair-feeding using mixed model analysis with zymosan and time as factors.

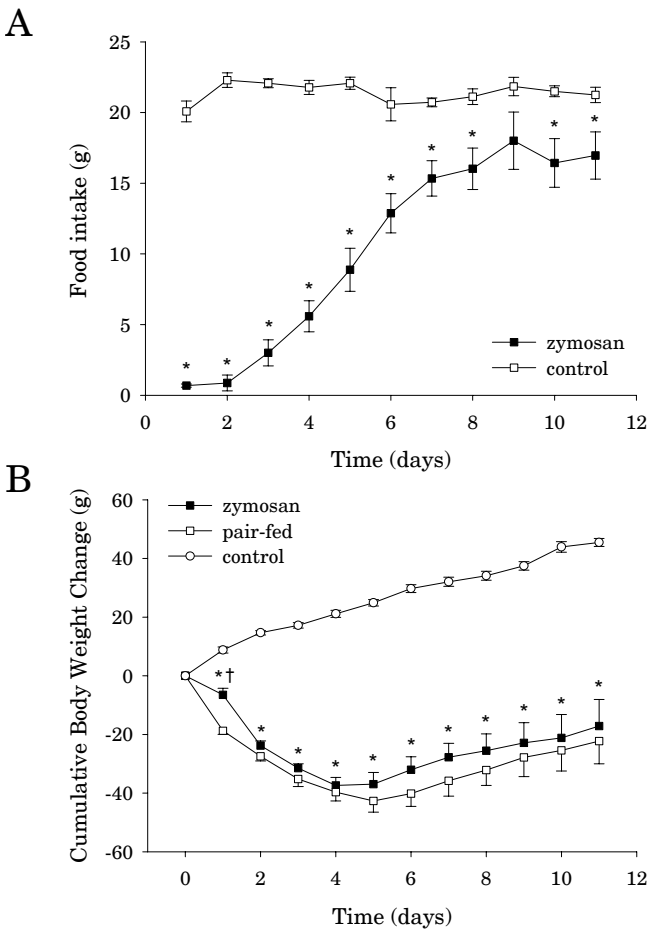

Figure 1: (A) Food intake of zymosan-treated and *ad libitum* fed control rats. **(B)** Cumulative change in body mass of zymosan-treated, pair-fed control and *ad libitum* fed control rats.
* P<0.05 vs. *ad libitum* fed control rats, † P<0.05 vs. pair-fed controls.

Results

Food intake, body mass and muscle mass

Acute peritonitis was observed during the first 2 days after zymosan injection, along with symptoms of severe illness including lethargy, hypophagia, hyperventilation, tachycardia, fever, diarrhea and loss of hemorrhagic fluid from the nose. There was a mortality of 20% in this acute phase. Food intake reduced significantly from ~20 g/day to an average of 1 g/day on day 1 and 2, after which it gradually increased to 75% of normal intake on day 8 (Figure 1A), and remained constant from then onward. Both the zymosan and pair-fed groups showed a large loss of body mass (Figure 1B); rats started to regain body mass between days 5-11. There were no significant differences in body mass between the zymosan and the pair-fed group. No catch-up growth was observed in either group.

Table 1: Tibialis anterior (TA) muscle mass in the experimental groups.

		TA muscle mass (mg)
	control	610 ± 9
2 d	zymosan	518 ± 22*†
2 d	pair-fed	604 ± 14
6 d	zymosan	444 ± 15*†
6 d	pair-fed	545 ± 11*
11 d	zymosan	522 ± 23*†
11 d	pair-fed	611 ± 12

* P<0.05 vs. *ad libitum* fed control rats
† P<0.05 vs. pair-fed controls.

Plasma analyses

In control rats, plasma triglyceride (TG) levels equaled 1142±94 μmol/l (Figure 2A). In line with the declined food intake the first 2 days after zymosan injection, plasma TG levels dropped profoundly in both zymosan-treated (230±34 μmol/l, p<0.01) and pair-fed control (301±36 μmol/l, p<0.01) rats. Six days after zymosan injection plasma TG levels (976±118 μmol/l) had restored to levels insignificantly different from control values (1142±94 μmol/l), while in pair-fed rats (492±67 μmol/l) TG content remained decreased compared to zymosan-treated (P<0.01) and *ad libitum* fed control rats (P<0.001). At day 11, when food-intake partly normalized and body

mass had started to regain, no significant differences in plasma TG levels were detected between groups (Figure 2A).

At day 2 both zymosan-treated (Figure 2B; 290±19 μmol/l) and pair-fed rats (298±27 μmol/l) showed significantly increased plasma free fatty acid (FFA) levels compared to *ad libitum* fed rats (215±189 μmol/l). At six days after zymosan injection a remarkable drop in plasma FFA was observed in zymosan-treated rats (143±7 μmol/l), whereas in pair-fed rats (350±17 μmol/l) FFA levels were significantly (P<0.01) higher compared to both zymosan-treated and control rats. At day 11, plasma FFA levels in zymosan-treated rats (171±9 μmol/l) did not differ from control values, while in pair-fed rats (295±23 μmol/l) plasma FFA levels were still significantly higher than both zymosan-treated and control levels.

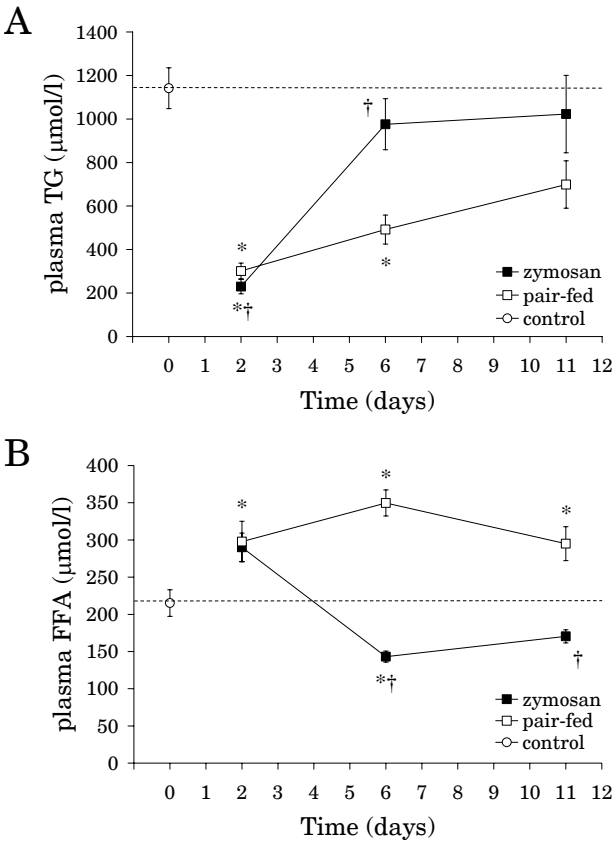

Figure 2: Plasma levels of **(A)** triglycerides (TG) and **(B)** free fatty acids (FFA) in zymosan-treated, pair-fed and *ad libitum* fed control rats (t=0 days). * P<0.05 vs. *ad libitum* fed rats. † P<0.05 vs. pair-fed rats.

Muscle UCP3 protein content and lipid peroxidation

Compared to control values (100±14%) UCP3 protein content relative to mitochondrial density, as measured by cytochrome C content, was increased in zymosan-injected rats (224±54%) as in pair-fed controls (197±32%), as shown in Figure 3. At all time points measured, UCP3/CytC content was higher in zymosan injected rats than in pair-fed controls. After an initial rise, UCP3/CytC levels seemed to stabilize at approximately 200% at days 6 and 11 in pair-feds, whereas in the zymosan condition UCP3/CytC content increased towards 262±25% at day 6 and 256±26% at day 11.

Lipid peroxidation was measured by immunofluorescence (representative 4-HNE stainings for control and zymosan-treated rats at day 11 are shown in Figure 4A and B, respectively). In control rats, 4-HNE content was set at 100 percent. In zymosan-treated rats, 4-HNE was not increased at day 2, but 4-HNE content was significantly elevated at day 6 (117±4%) and remained significantly elevated at day 11 (119±4%). Interestingly, 4-HNE was increased at day 2 in pair-fed rats (118±5 %; $P<0.05$), but the initial rise in 4-HNE returned to control values at days 6 and 11.

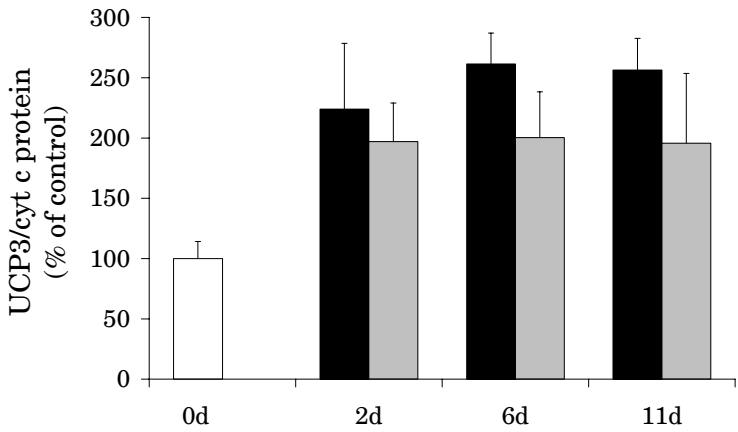

Figure 3: UCP3/Cytc protein ratios in tibialis anterior muscles from zymosan-treated (black bars), pair-fed (grey bars) and *ad libitum* fed control (white bar) rats. Ratios are expressed as percentages of control levels. When compared to pair-fed rats, mixed model analysis showed a significant zymosan effect on UCP3/CytC ratios (P=0.026) and no time (P=0.927) or time*zymosan effect (P=0.603).

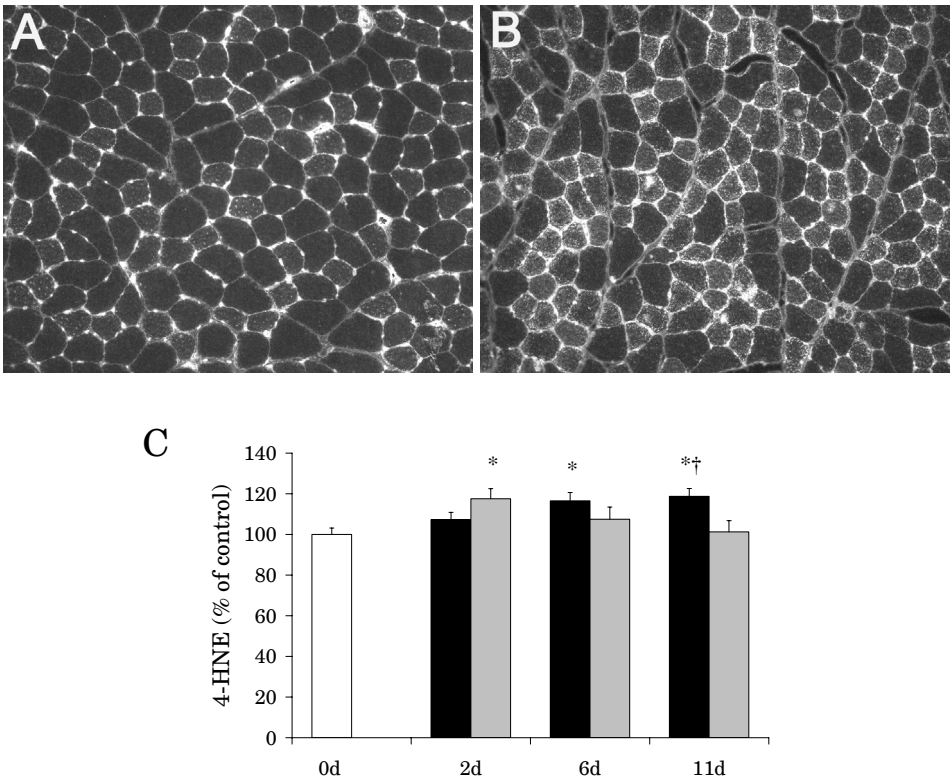

Figure 4: 4-hydroxy-2-nonenal (4-HNE) protein adduct levels in tibialis anterior muscles. **(A-B)** Representative examples of 4-HNE immunofluorescence stainings performed on tibialis anterior muscle sections of a control (panel A) and 11-day zymosan-treated (panel B) rat. **(C)** Quantification of 4-HNE protein adducts in muscles of zymosan-treated (black bars), pair-fed (grey bars) and *ad libitum* fed control (white bar) rats. * $P<0.05$ vs. *ad libitum* fed rats. † $P<0.05$ vs. pair-fed rats.

Discussion

Here we examined the hypothesis that cachexia related increased UCP3 protein content serves to modulate lipotoxicity. Compared to controls, rats rendered cachectic by injection of zymosan possessed increased muscular UCP3 protein content lasting for at least 11 days. Pair-fed control rats showed a more modest increase in UCP3 levels than cachectic rats. In zymosan-treated rats we observed an increase of the lipid peroxidation byproduct 4-hydroxy-2-nonenal (4-HNE) in TA muscle both 6 and 11 days after injection. Interestingly, after 2 days of pair-feeding, increased 4-HNE content was observed which returned to control values at days 6 and 11. This may suggest that in food restricted but otherwise healthy animals, the

increase in UCP3 protein content suffices to modulate the increased lipid peroxidation observed after 2 days of pair-feeding. In contrast to pair-fed rats, 4-HNE content was elevated in rats rendered cachectic by zymosan injection from day 6 onward, despite an increased UCP3 content. If UCP3 indeed serves to modulate lipotoxicity during cachexia, this indicates that in critically ill rats increased UCP3 protein content or its state of activation is inadequate to deal with the increased oxidative stress and concomitant lipid peroxidation products present during cachexia.

During the first 2 days after zymosan injection or pair-feeding, when food intake had reduced to virtually zero, we observed a sharp decline in plasma triglyceride levels paralleled by increased plasma FFA levels in both groups; the classical response to acute food restriction. Increased plasma FFA levels are potent activators of UCP3 gene expression (29). Conversely, the use of anti-lipolytic agents resulted in a blunted increase in UCP3 (30), even under conditions of β-adrenergic stimulated energy expenditure (31). Increased FFA levels in both zymosan-treated and pair-fed rats may trigger the initial rise in UCP3 protein content observed at day 2. In pair-fed rats, plasma FFA levels remained elevated at days 6 and 11, potentially explaining why UCP3 protein levels remained relatively high in this condition (albeit lower than in zymosan-injected rats). In contrast to pair-fed rats, plasma FFA levels of zymosan-treated rats at days 6 and 11 were lower than control and pair-fed levels. The decreased FFA levels in zymosan-treated rats are most likely accounted for by reduced tissue lipoprotein lipase (LPL) activity (32, 33). This notion is substantiated by the normalization of plasma triglyceride levels observed in zymosan-treated animals at days 6 and 11. Strikingly, in zymosan-treated rats UCP3 content remained elevated despite significant reductions in FFA levels, but in the presence of increased 4-HNE levels. Thus, although elevated plasma FFA levels may explain the relatively high UCP3 levels in pair-fed rats, high FFA levels are not involved in increasing UCP3 content in zymosan-treated rats. Interestingly, an increased UCP3 protein content in the absence of increased plasma FFA levels has previously been observed in cancer cachexia (23). This indicates that under conditions of cachectic stress other processes are involved which induce maintenance of high UCP3 levels. One such process may be an increased production of ROS and 4-HNE, although so far it has not been examined if 4-HNE is able to increase UCP3 protein content.

Not only has increased oxidative stress been reported in cachexia, but the resultant ROS have also been shown to result in lipid peroxidation products, as indicated by increased adducts of the lipid peroxidation byproduct 4-HNE in tumour-bearing cachectic rats (24). This is in line with our present observation of increased 4-HNE in zymosan-treated rats. Interestingly, 4-HNE has recently been identified as one of the few UCP3 activators (22) resulting in a reduced mitochondrial proton gradient. Reduction of the proton gradient in a process referred to as mild uncoupling results in lowered production of ROS (34). Thus, a unifying physiological role for increased UCP3 content in cachectic conditions can be hypothesized; UCP3 increases in a process at least partly driven by increased plasma FFA levels during early cachexia to deal with increased ROS and lipid peroxides. In a feed-forward loop, 4-HNE may activate and possibly upregulate UCP3 to facilitate efflux of fatty acid anions or lipid peroxides from the mitochondrial matrix. This process has a dual effect; lowering of the proton gradient serves to reduce ROS production and efflux of fatty acid anions and/or lipid peroxides serves to preserve mitochondrial integrity and mitochondrial function. In the present model, where zymosan injection induces critical illness with a 20% mortality rate during the first 2 days after injection (35), the increase in UCP3 protein content seems inadequate to properly deal with the rise in lipid peroxidation observed at days 6 and 11 after zymosan injection. This may indicate that under these extreme conditions, the rise in lipid peroxides exceeds the capacity of UCP3 to deal with this appropriately, possibly resulting in increased mitochondrial damage. In line with this, a previous study using the same model has shown mitochondrial morphological abnormalities and decreased mitochondrial protein synthesis (26).

In conclusion, the present study shows increased UCP3 protein content along with increased 4-HNE adducts in skeletal muscle of cachectic rats. These observations support the idea that increased UCP3 in cachectic conditions helps to modulate the cachexia related oxidative stress and ameliorates lipotoxicity.

Acknowledgements

Dr. M. Hesselink is supported by a VIDI Research Grant for innovative research from the Netherlands Organization for Scientific Research (Grant

917.66.359). The research of Dr. P. Schrauwen is sponsored by a fellowship of the Royal Netherlands Academy of Arts and Sciences.

References

1. Giordano A, Calvani M, Petillo O, Carteni M, Melone MR, and Peluso G. Skeletal muscle metabolism in physiology and in cancer disease. J Cell Biochem 90: 170-186, 2003.
2. Collins P, Bing C, McCulloch P, and Williams G. Muscle UCP-3 mRNA levels are elevated in weight loss associated with gastrointestinal adenocarcinoma in humans. Br J Cancer 86: 372-375, 2002.
3. Busquets S, Sanchis D, Alvarez B, Ricquier D, Lopez-Soriano FJ, and Argiles JM. In the rat, tumor necrosis factor alpha administration results in an increase in both UCP2 and UCP3 mRNAs in skeletal muscle: a possible mechanism for cytokine-induced thermogenesis? FEBS Lett 440: 348-350, 1998.
4. Sanchis D, Busquets S, Alvarez B, Ricquier D, Lopez-Soriano FJ, and Argiles JM. Skeletal muscle UCP2 and UCP3 gene expression in a rat cancer cachexia model. FEBS Lett 436: 415-418, 1998.
5. Sun X, Wray C, Tian X, Hasselgren PO, and Lu J. Expression of uncoupling protein 3 is upregulated in skeletal muscle during sepsis. Am J Physiol Endocrinol Metab 285: E512-520, 2003.
6. Hart DW, Wolf SE, Chinkes DL, et al. Determinants of skeletal muscle catabolism after severe burn. Ann Surg 232: 455-465, 2000.
7. Roubenoff R, Roubenoff RA, Cannon JG, et al. Rheumatoid cachexia: cytokine-driven hypermetabolism accompanying reduced body cell mass in chronic inflammation. J Clin Invest 93: 2379-2386, 1994.
8. Starnes HF, Jr., Warren RS, Jeevanandam M, et al. Tumor necrosis factor and the acute metabolic response to tissue injury in man. J Clin Invest 82: 1321-1325, 1988.
9. DeJong CH, Busquets S, Moses AG, et al. Systemic inflammation correlates with increased expression of skeletal muscle ubiquitin but not uncoupling proteins in cancer cachexia. Oncol Rep 14: 257-263, 2005.
10. Russell AP, Somm E, Debigare R, et al. COPD results in a reduction in UCP3 long mRNA and UCP3 protein content in types I and IIa skeletal muscle fibers. J Cardiopulm Rehabil 24: 332-339, 2004.
11. Gosker HR, Schrauwen P, Hesselink MK, et al. Uncoupling protein-3 content is decreased in peripheral skeletal muscle of patients with COPD. Eur Respir J 22: 88-93, 2003.
12. Cline GW, Vidal-Puig AJ, Dufour S, Cadman KS, Lowell BB, and Shulman GI. In vivo effects of uncoupling protein-3 gene disruption on mitochondrial energy metabolism. J Biol Chem 276: 20240-20244, 2001.
13. Gong DW, Monemdjou S, Gavrilova O, et al. Lack of obesity and normal response to fasting and thyroid hormone in mice lacking uncoupling protein-3. J Biol Chem 275: 16251-16257, 2000.
14. Hesselink MK, Greenhaff PL, Constantin-Teodosiu D, et al. Increased uncoupling protein 3 content does not affect mitochondrial function in human skeletal muscle in vivo. J Clin Invest 111: 479-486, 2003.

15. Nedergaard J, Ricquier D, and Kozak LP. Uncoupling proteins: current status and therapeutic prospects. EMBO Rep 6: 917-921, 2005.
16. Schrauwen P and Hesselink MK. Oxidative capacity, lipotoxicity, and mitochondrial damage in type 2 diabetes. Diabetes 53: 1412-1417, 2004.
17. Goglia F and Skulachev VP. A function for novel uncoupling proteins: antioxidant defense of mitochondrial matrix by translocating fatty acid peroxides from the inner to the outer membrane leaflet. Faseb J 17: 1585-1591, 2003.
18. Himms-Hagen J and Harper ME. Physiological role of UCP3 may be export of fatty acids from mitochondria when fatty acid oxidation predominates: an hypothesis. Exp Biol Med (Maywood) 226: 78-84, 2001.
19. Schrauwen P, Saris WH, and Hesselink MK. An alternative function for human uncoupling protein 3: protection of mitochondria against accumulation of nonesterified fatty acids inside the mitochondrial matrix. Faseb J 15: 2497-2502, 2001.
20. Wallace DC, Shoffner JM, Trounce I, et al. Mitochondrial DNA mutations in human degenerative diseases and aging. Biochim Biophys Acta 1271: 141-151, 1995.
21. Papa S. Mitochondrial oxidative phosphorylation changes in the life span. Molecular aspects and physiopathological implications. Biochim Biophys Acta 1276: 87-105, 1996.
22. Echtay KS, Esteves TC, Pakay JL, et al. A signalling role for 4-hydroxy-2-nonenal in regulation of mitochondrial uncoupling. Embo J 22: 4103-4110, 2003.
23. Busquets S, Almendro V, Barreiro E, Figueras M, Argiles JM, and Lopez-Soriano FJ. Activation of UCPs gene expression in skeletal muscle can be independent on both circulating fatty acids and food intake. Involvement of ROS in a model of mouse cancer cachexia. FEBS Lett 579: 717-722, 2005.
24. Barreiro E, de la Puente B, Busquets S, Lopez-Soriano FJ, Gea J, and Argiles JM. Both oxidative and nitrosative stress are associated with muscle wasting in tumour-bearing rats. FEBS Lett 579: 1646-1652, 2005.
25. Tisdale MJ. Molecular pathways leading to cancer cachexia. Physiology (Bethesda) 20: 340-348, 2005.
26. Rooyackers OE, Kersten AH, and Wagenmakers AJ. Mitochondrial protein content and in vivo synthesis rates in skeletal muscle from critically ill rats. Clin Sci (Lond) 91: 475-481, 1996.
27. Rooyackers OE, Saris WH, Soeters PB, and Wagenmakers AJ. Prolonged changes in protein and amino acid metabolism after zymosan treatment in rats. Clin Sci (Lond) 87: 619-626, 1994.
28. Rooyackers OE, Gijsen AP, Saris WH, Soeters PB, and Wagenmakers AJ. Derangement in aerobic and anaerobic energy metabolism in skeletal muscle of critically ill and recovering rats. Biochim Biophys Acta 1315: 55-60, 1996.
29. Weigle DS, Selfridge LE, Schwartz MW, et al. Elevated free fatty acids induce uncoupling protein 3 expression in muscle: a potential explanation for the effect of fasting. Diabetes 47: 298-302, 1998.
30. Busquets S, Carbo N, Almendro V, Figueras M, Lopez-Soriano FJ, and Argiles JM. Hyperlipemia: a role in regulating UCP3 gene expression in skeletal muscle during cancer cachexia? FEBS Lett 505: 255-258, 2001.
31. Hoeks J, van Baak MA, Hesselink MK, et al. Effect of beta1- and beta2-adrenergic stimulation on energy expenditure, substrate oxidation, and UCP3 expression in humans. Am J Physiol Endocrinol Metab 285: E775-782, 2003.

32. Lanza-Jacoby S and Tabares A. Triglyceride kinetics, tissue lipoprotein lipase, and liver lipogenesis in septic rats. Am J Physiol 258: E678-685, 1990.
33. Lanza-Jacoby S, Sedkova N, Phetteplace H, and Perrotti D. Sepsis-induced regulation of lipoprotein lipase expression in rat adipose tissue and soleus muscle. J Lipid Res 38: 701-710, 1997.
34. Demin OV, Kholodenko BN, and Skulachev VP. A model of O2.-generation in the complex III of the electron transport chain. Mol Cell Biochem 184: 21-33, 1998.
35. Minnaard R, Drost MR, Wagenmakers AJ, van Kranenburg GP, Kuipers H, and Hesselink MK. Skeletal Muscle wasting and contractile performance in septic rats. Muscle Nerve 31: 339-348, 2005.

5

The acute effect of high-resistance exercise on rat muscle protein breakdown and ubiquitin-proteasome pathway activity

R. Minnaard, G. Schaart, A.J.M. Wagenmakers,
H. Kuipers, M.R. Drost and M.K.C. Hesselink

Abstract

Many studies have shown that muscle protein synthesis rates are increased acutely after a high-resistance exercise bout. Very little is known about the effect of high-resistance exercise on muscle protein breakdown and the activity of the ubiquitin-proteasome (Ub-P) pathway, the major proteolytic pathway in skeletal muscle. To test this, rats were subjected to a unilateral high-resistance electrical stimulation protocol, and total protein breakdown rates of the extensor digitorum longus (EDL) and soleus muscles were measured in both legs at 2h and 4h post-exercise. Ubiquitin-conjugation rates and 20S proteasome peptidase activities were determined in the gastrocnemius muscle. We show a small decrease of total muscle protein breakdown at 2h post-exercise in the EDL muscle (-16%), but no change at 4h post-exercise. Post-exercise protein breakdown rates were not different from control in the soleus muscle. Consistent with these data, post-exercise chymotrypsin- and caspase-like 20S proteasome activities were also not different from control in the gastrocnemius muscle. Interestingly, Ub-conjugation rates were significantly increased (+73%) at 4h post-exercise, while a trend for an increase was present at 2h post-exercise (+47%). These results suggest that a specific set of muscle proteins is increasingly targeted for breakdown acutely after a high-resistance exercise bout. In conclusion, total muscle protein breakdown rates and 20S proteasome peptidase activities remained largely unchanged acutely after a high-resistance exercise bout. Ub-conjugation rates were increased acutely post-exercise, suggesting that this may be an important mechanism involved in the muscle remodeling response to high-resistance exercise.

Introduction

Skeletal muscle is a tissue with a recognized ability to adapt to mechanical (un)loading. This is exemplified by the rapid loss of muscle mass upon unloading/disuse following limb casting (1), space flight (2, 3) or in animal models of unloading, such as hindlimb suspension (4). On the other hand, frequent muscle use can bring about muscle hypertrophy and remodeling. It is the mode, duration and frequency of the exercise that determines the amount of hypertrophy and the type of proteins involved in the remodeling process. Although an increased protein synthesis is an established event occurring in response to high-resistance exercise (5-8), an increased breakdown of damaged or redundant proteins has also been suggested to be required to ensure proper muscle function and remodeling (9, 10). An example of remodeling is the change in myosin heavy chain (MHC) isoform that was reported in the medial gastrocnemius muscle in response to the repeated administration of a high-resistance electrical stimulation protocol in rats (11, 12). In these experiments it was consistently shown that resistance exercise training in rats resulted in a decreased expression of type 2B MHC and an increased expression of type 2X MHC. This isoform change may not only depend on an altered synthesis of the involved isoforms, but may also require an increased degradation of the redundant isoform.

The degradation of (myofibrillar) proteins in eukaryotic cells is believed to occur largely via the ubiquitin-proteasome (Ub-P) pathway (13, 14). An initial and obligatory step in this pathway is the covalent binding of a chain of ubiquitin molecules to target proteins, a process catalyzed by a cascade of E1, E2 and E3 enzymes. Subsequently, proteins containing a polyubiquitin chain are recognized by the 19S proteasome, which unfolds the proteins and allows them to enter the 20S proteasome, where they are degraded (14, 15).

Despite the putative importance of muscle proteolysis in remodeling and in contrast to the many studies showing increases in protein synthesis after resistance exercise (16), the acute response of muscle protein breakdown to high-resistance exercise has not been studied in detail. The available data on muscle proteolysis after exercise are mainly based on stable isotope methods. Muscle protein breakdown has been reported to increase (+31% vs. resting levels) 3 hours after a high-resistance exercise bout, with the increase persisting for at least 24 hours (18%) (17). In addition, using a different stable isotope method, muscle protein breakdown was found to

increase ~50% 3 hours post-exercise (8). Although elegant, these stable isotope models do not allow the investigation of the role of the Ub-P pathway in exercise-induced remodeling. Hints for an important role of the Ub-P pathway in exercise-induced remodeling of skeletal muscle are derived from a study showing that 28 days of chronic low-frequency stimulation (CLFS) of the rabbit tibialis anterior muscle increased the muscle proteasome concentration and activity 2-3 fold during the course of the stimulation period (18). These data suggest that after high-resistance exercise the Ub-P pathway may be an interesting target to optimize the adaptive response of the muscle. Additional data implicating the Ub-P pathway in the proteolytic response to exercise are derived from exercise protocols using eccentric contractions (recognized to induce muscle damage (19)), showing increases in several markers of Ub-P pathway activity in the exercised muscles (20-22). There are no reports, however, measuring the response of the Ub-P pathway to a non-damaging high-resistance exercise bout.

Thus, the main aim of the present study was to investigate the short term (<6 h) effect of a high-resistance exercise bout on post-exercise proteolysis in rat skeletal muscle, and the involvement of the Ub-P pathway herein. To test this, hindlimb muscles of young male Wistar rats were electrically stimulated to perform non-damaging isometric contractions *in situ*, after which proteolysis was measured *in vitro*. In addition, we determined post-exercise 20S proteasome peptidase activities against multiple substrates, and the rate of ubiquitin conjugation to muscle proteins. Based on the chosen exercise protocol, we anticipated to observe post-exercise increases in muscle proteolysis with activation of the Ub-P pathway (10).

Materials and methods

Animals

The experiments were approved by the animal experimental committee of the Maastricht University. Four-week-old male Wistar rats, weighing ~100 g, were housed in a humidity- (50%-60%), light- (12-h dark-light cycle) and temperature-controlled (21-22 °C) environment and were allowed to acclimatize for one week prior to the experiments. In a pilot study used to validate the *in vitro* proteolysis assay, two rats were subjected to unilateral denervation. The remaining rats underwent the following experimental

conditions. One hour prior to the experiments food was removed from their cages. All experiments were started at 9.00 a.m. Rats were subjected to a single-leg exercise protocol, and were sacrificed either 2 hours (n=4) or 4 hours (n=5) after completing the exercise protocol to determine the *in vitro* proteolytic rates in the extensor digitorum longus (EDL) and soleus muscles. Young rats were used, because of their thin muscles which are easily diffusible, preventing the formation of a hypoxic core during muscle incubations. Denervation, exercise and muscle dissection were all performed under isofluorane anesthesia.

Denervation

To expose the sciatic nerve, a small longitudinal incision was made in the skin of the dorsal part of the left hindleg, just below the knee. Rats were denervated by excising a segment (~2 mm) from the sciatic nerve proximal to the anatomical branching point. The incision was carefully closed with sutures, and the rats were left to recover from the anesthesia. Forty-eight hours after denervation, the EDL, soleus and gastrocnemius muscles were excised bilaterally and processed for either *in vitro* analyses of proteolysis (EDL and soleus; for details see below) or frozen in liquid nitrogen and stored at -80 °C until further analysis.

Exercise Protocol

To perform the electrical stimulation, a small longitudinal incision was made in the skin of the dorsal part of the left hindleg, just below the knee. A bipolar, platinum hook electrode was carefully attached to the sciatic nerve, proximal to anatomical branching point, to permit simultaneous stimulation of both the plantar and dorsal flexor muscle groups. To prevent dehydration of the muscles during the exercise protocol, the incision was closed with one suture. The rats were placed in a custom built rat isometric dynamometer (23). Briefly, rats were placed on a heated-platform in a sideways position with their left foot tightly fixed to the footplate. Rats were fixated at the hip using a tail fixation unit. The footplate was fixed at an ankle angle of 90°, resulting in an optimal fiber length of the dorsiflexor muscles, while approaching the resting length for the plantar flexor muscles (23).

The exercise protocol was designed based on previous protocols, proven to result in hypertrophy when applied repeatedly (24, 25). To avoid damage induced by eccentric exercise we chose isometric resistance exercise, which is also known to result in hypertrophy in humans (26). In rats we have previously shown that an intense electrical stimulation protocol involving isometric contractions does not result in muscle damage (19). After optimization of the stimulation parameters (typically 3V and 100 Hz, pulse duration 5 ms) resulting in maximal torque (representing force), rats were subjected to a supramaximal stimulation protocol. The protocol comprised 5 sets of 12 contractions (5 sec contraction, 10 sec rest) with a 5 min rest between successive sets. Upon completing the exercise protocol, the electrode was carefully removed, the incision closed with sutures, and the rats were left to recover from the anesthesia. After terminating the isofluorane anesthesia all rats regained consciousness within 5 minutes.

In vitro proteolysis assay

Either 2 or 4 hours post-exercise the muscles of both lower hindlimbs were dissected, and the tibialis anterior and gastrocnemius muscles were frozen in liquid nitrogen and stored at -80 °C until further analysis. Care was taken to dissect the EDL and soleus muscles from tendon to tendon, carefully removing any excess fascia. Directly after dissection, the EDL and soleus muscles were weighed and attached to stainless steel supports at resting length, and placed in a standard Krebs-Henseleit medium (120 mM NaCl, 25 mM $NaHCO_3$, 4.8 mM KCl, 1.2 mM $MgSO_4$, 1.2 mM KH_2PO_4, 2.5 mM $CaCl_2$, pH 7.4), supplemented with 5 mM D-(+)-glucose, 5 mM HEPES, 0.1% BSA, 0.5 mM cycloheximide, and equilibrated with O_2:CO_2 (19:1). Cycloheximide was used to block protein synthesis. After 30 min of preincubation at 37 °C, the muscles were transferred to fresh media and incubated for another 2 h. The total rate of protein breakdown was determined by measuring the rate of tyrosine release into the medium. Tyrosine was assayed by the fluorometric method of Waalkes and Udenfriend (27), as modified by Tischler et al. (28). As tyrosine is not synthesized or metabolized in the muscle, tyrosine release, in the presence of the protein synthesis blocker cycloheximide, is a measure of the total muscle protein breakdown.

20S Proteasome peptidase activity

The method used to determine 20S proteasome peptidase activities has been previously described (29, 30). Briefly, gastrocnemius lateralis muscles (GL) were homogenized and proteasomes were isolated by sequential (ultra)centrifugation steps. The protein content of the proteasome fractions was determined with the Bio-Rad protein assay, using bovine serum albumine as a standard. Proteasome fractionation yielded similar amounts of protein in all muscle fractions. The 20S proteasome peptidase activity was determined fluorometrically by measuring the activity against the fluorogenic substrates Succinyl-Leu-Leu-Val-Tyr-7-amido-4-methylcoumarin (Suc-LLVY-AMC, Sigma, Zwijndrecht, The Netherlands) and Benzyloxycarbonyl-Leu-Leu-Glu-7-amido-4-methylcoumarin (Z-LLE-AMC, BIOMOL, Exeter, UK). These substrates are preferentially hydrolyzed by the chymotrypsin-like and caspase-like peptidase activities of the 20S proteasome, respectively. Standard curves were established for AMC, which permitted the expression of the proteasome activity as pmol AMC · μg protein^{-1} · min^{-1}. Adding the proteasome inhibitor MG132 to the reaction resulted in complete inhibition of the proteasome proteolytic activity.

Ubiquitin conjugation rates

Gastrocnemius medialis muscles (GM) from both stimulated and control legs were homogenized in ice-cold buffer (pH 7.5), containing 50 mM Tris, 1 mM EDTA, 1 mM PMSF, 1 mM DTT, 10 μg/ml pepstatin A and 10 μg/ml leupeptin). Homogenates were centrifuged at 10,000 x g, 4 °C for 10 min and the resulting supernatants were centrifuged at 100,000 x g, 4 °C for 1h. The soluble protein concentration was determined in the supernatants using the Bio-Rad protein assay.

Ubiquitin (Sigma) was labeled with an infrared dye using the IRDye 800CW antibody labeling kit (LICOR Biosciences, Lincoln, NB) according to the manufacturers' instructions. Briefly, 1 mg of ubiquitin was dissolved in 1 ml PBS, after which the reactive IRDye 800CW (dissolved in 50 μl of DMSO) was added. The labeling reaction was performed in the dark for 2h at 4 °C, while continuously rotating the vial end-over-end. Subsequently, the mixture was dialyzed against PBS for 24h at 4 °C using a Slide-A-Lyzer dialysis cassette with a 7,000 MW cut-off (Pierce, Rockford, IL) to remove unbound dye from the solution. The solution containing the IRDye 800CW

labeled ubiquitin was removed from the cassette, aliquoted and stored at -20 °C. Ub-conjugation rates were determined by incubating 50 μg of soluble proteins for 15, 30, 45 and 60 min at 37 °C with 10 μM IRDye 800CW-labeled ubiquitin, 50 mM Tris-HCl (pH 7.5), 1 mM DTT, 2 mM $MgCl_2$ and 2 mM AMP-PNP, in a total volume of 20 μl. The reactions were stopped by adding 1x sample buffer according to Laemmli (31) (62.5 mM Tris-HCl (pH 6.8), 5% β-mercaptoethanol, 2% SDS, 0.1% bromophenol blue and 10% glycerol). In pilot experiments using muscles from both healthy control rats (n=4) and zymosan-treated rats (n=4) we confirmed that Ub-conjugation rates were linear for these 60 min. After stopping the reaction, ubiquitin-conjugated proteins were separated from free ubiquitin by electrophoresis on 12% polyacrylamide SDS-gels. Directly after electrophoresis the gels were scanned using a two-colour (700 and 800 nm) Odyssey Infrared Imaging System (LICOR Biosciences). The IRDye 800CW dye is detected in the green 800 nm channel, while the All-Blue molecular weight marker (BioRad) is detected in the red 700 nm channel. The total amount of Ub-conjugation was quantified in each lane (bands ranging from ~30 kDa to high molecular weight) using Odyssey application software v1.2. Ub-conjugation rates were determined by calculating the slope of Ub-conjugation for each muscle. After scanning, the gels were stained with Coomassie Brilliant Blue to confirm an equal protein loading of the gel.

Statistics

Results are represented as means ± standard deviation. Data were compared between the exercised and non-exercised legs using a paired t-test. Significance was set at $P < 0.05$.

Table 1: Body and muscle mass 48h after denervation.

	Body mass t=0h (g)	Body mass t=48h (g)	Leg	Soleus mass (mg)	EDL mass (mg)
rat 1	86	94	control	42.5	43.9
			denervated	30.5	40.6
rat 2	84	93	control	39.8	47.3
			denervated	33.2	46.8

Results

Denervation

Denervation is a recognized method to induce muscle atrophy, which has pronounced and rapid effects on the soleus muscle in particular, while these effects are much slower in the EDL muscle. Denervation atrophy is known to be accompanied by large increases in proteolysis in the soleus muscle (32, 33). In our hands, 48 hours of denervation decreased the soleus muscle mass by an average 23%, while the EDL muscle mass was not yet affected (Table 1). Corresponding with the effects on muscle mass, denervation caused a massive increase in protein breakdown in the soleus muscle, without affecting protein breakdown in the EDL muscle (Figure 1).

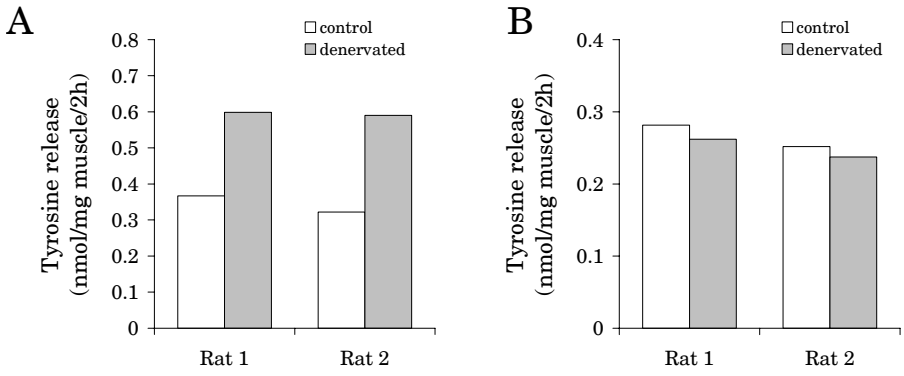

Figure 1: Total protein breakdown (nmol tyrosine·mg muscle^{-1}·2h^{-1}) measured in incubated soleus **(A)** and EDL **(B)** muscles from both legs in two unilaterally denervated rats.

Exercise

The EDL and soleus muscles responded differentially to exercise with respect to total protein breakdown rates (measured as the amount of tyrosine released into the incubation medium). Two hours post-exercise there was a 16 ± 1.0% decrease of muscle protein breakdown in the EDL muscle (Figure 2A). Of note, in every single animal at this time-point protein breakdown rates were lower in the exercised EDL muscle compared to the control EDL muscle (Figure 2B). Four hours post-exercise, however, no differences between the exercised leg and the non-exercised leg were observed (Figure 2A), with individual rats responding with either an

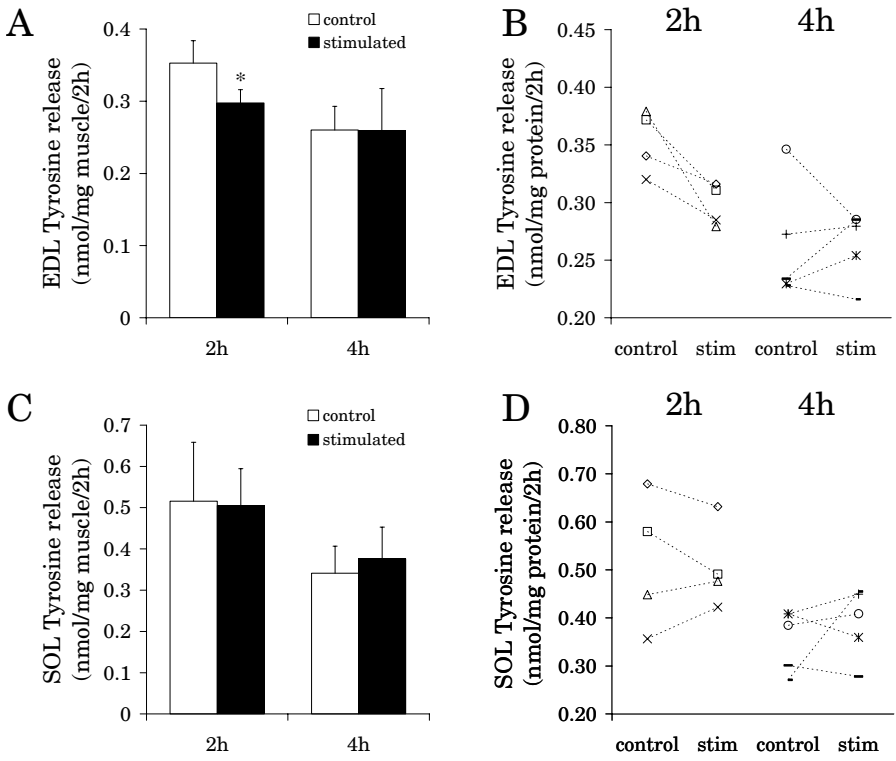

Figure 2: Total protein breakdown (nmol tyrosine·mg muscle^{-1}·2h^{-1}) in incubated EDL **(A)** and soleus **(C)** muscles from both legs, measured 2h (n=4) and 4h (n=5) after completing a unilateral, isometric resistance exercise bout (stimulated). * $P<0.05$ vs. the non-exercised control leg. Individual protein breakdown rates for each rat are displayed for the EDL **(B)** and soleus **(D)** muscles. Data represented by similar symbols are obtained from the same rat.

increased or a decreased proteolytic rate (Figure 2B). In the soleus muscle, however, protein breakdown was not affected by the exercise bout at either time-point (Figure 2C and 2D).

Overall, protein degradation in the muscles of both legs was higher in the rats sacrificed 2h post-exercise compared to those sacrificed 4h post-exercise (Figure 2).

The peptidase activities of proteasome preparations from both stimulated and control gastrocnemius lateralis muscles (GL) are shown in Figure 3. Exercise did not affect the chymotrypsin-like (Figure 3A) and caspase-like (Figure 3C) proteasome peptidase activities, either 2h or 4h post-exercise. Note that, in correspondence with protein breakdown in the EDL and soleus muscles, the proteasome peptidase activities in the GL muscles from either

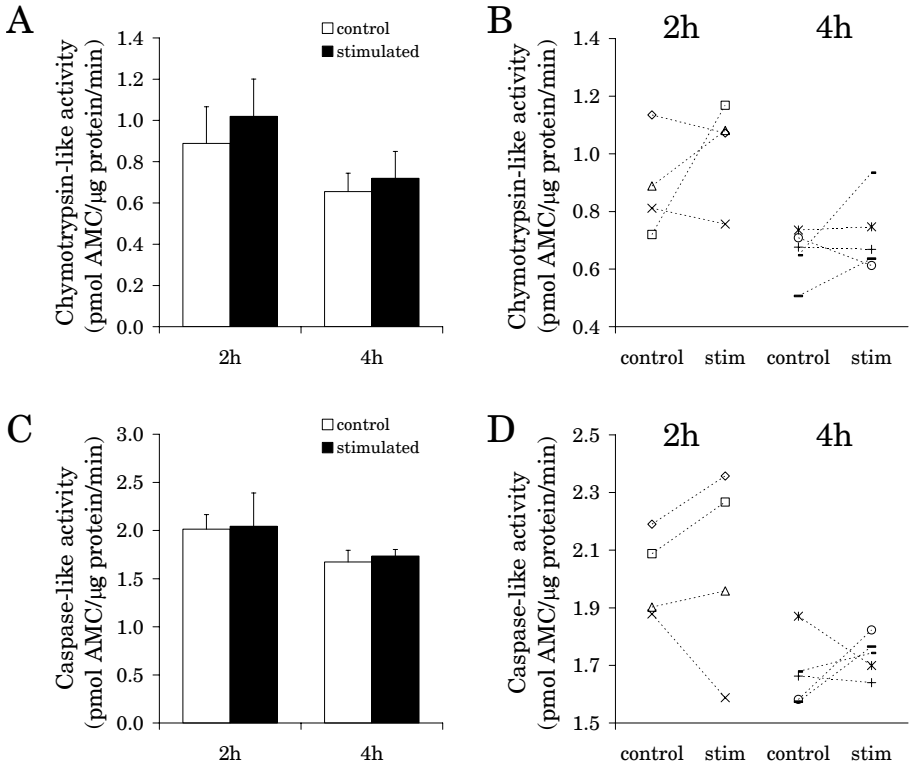

Figure 3: Chymotrypsin-like (A) and Caspase-like (C) 20S proteasome peptidase activities in gastrocnemius lateralis muscles from both legs, measured 2h (n=4) and 4h (n=5) after completing a unilateral, isometric resistance exercise bout (stimulated). Individual 20S proteasome peptidase activities are displayed in B (chymotrypsin-like) and D (caspase-like), and are expressed as the release of AMC in pmol/μg protein/min. Data represented by similar symbols are obtained from the same rat.

leg are higher in the rats sacrificed 2h post-exercise, compared to those sacrificed at 4h.

Interestingly, although we did not observe a difference in proteasome activities between exercised and control GL, Figure 4 shows a significant 73% increase in ubiquitin-conjugation rates in the gastrocnemius medialis muscle (GM) at 4h postexercise, and a trend for increased rates (+49%) at 2h postexercise. Figure 4C shows that increased Ub-conjugation rates were observed in stimulated vs. control GM in every single rat at 4h post-exercise. Although different Ub-conjugation rates were observed between specific bands (representing distinct proteins) within one muscle, an increased rate of Ub-conjugation is observed in various proteins in response to exercise (Figure 4A).

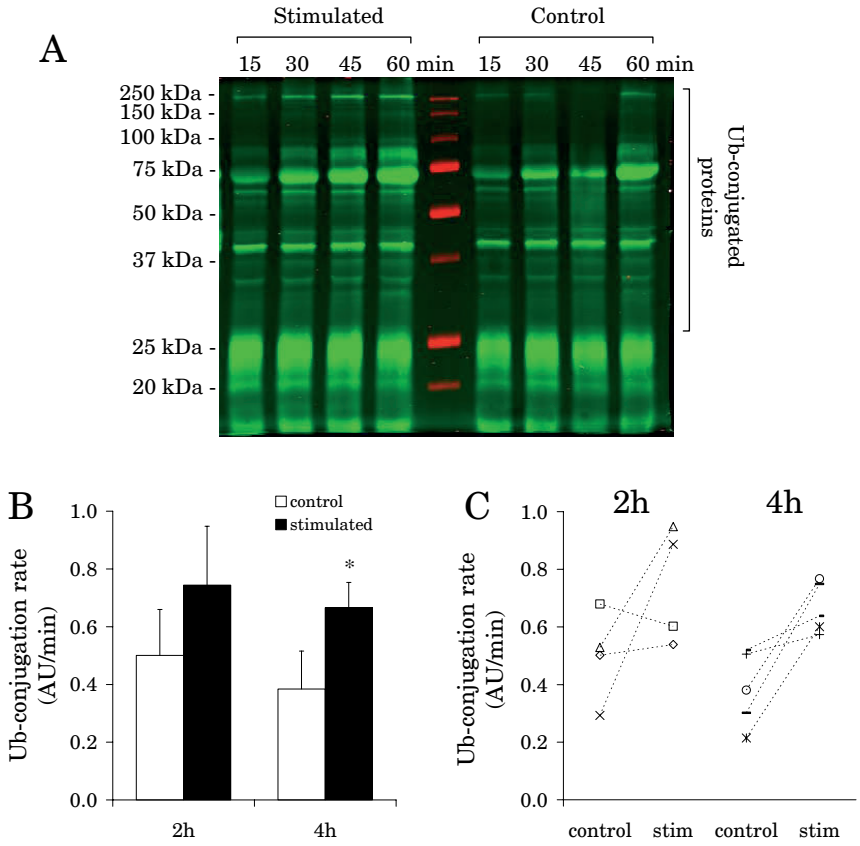

Figure 4: Ubiquitin-conjugation rates in gastrocnemius medialis muscles are increased 2h and 4h post-exercise. A representative scanned gel is shown in **A**, in which the Ub-conjugated proteins of both a stimulated and control muscle are shown in green and the molecular weight marker in red. The bracket indicates the area of each lane that is used for quantification. Ub-conjugation rates are quantified in panel **B** (* $P<0.05$ vs. the non-exercised control leg). Individual Ub-conjugation rates are displayed in **C**.

Discussion

The present study does not show evidence for an increased protein breakdown in the hours following a heavy resistance exercise protocol. This observation is not in line with our hypothesis and seems to contrast with observations made in man with stable isotopes, suggesting that mixed muscle protein degradation was increased after resistance exercise. Our data actually show a small decrease of protein breakdown in isolated EDL muscle 2h post-exercise, while no difference was present 4h post-exercise. At both time-points, total protein breakdown rates were not affected by

exercise in the soleus muscle. In contrast with the data on total proteolysis in the EDL and soleus muscles, we do show evidence for a regulation of the Ub-P pathway after high-resistance exercise in the gastrocnemius medialis muscle. Ub-conjugation rates were significantly higher in exercised vs. control muscles at 4h post-exercise, while a trend for increased rates was present at 2h post-exercise. 20S proteasome peptidase activities were not different between exercised and control gastrocnemius lateralis muscles, however. These data suggest that in the hours following a high-resistance exercise bout certain muscle proteins are increasingly targeted for breakdown by the Ub-P pathway without a concomitant increase in mixed muscle protein breakdown. Increasing the rate at which Ub-conjugation proceeds may be an important mechanism involved in the remodeling response of muscle to a high-resistance exercise bout.

Two studies reported increased mixed-muscle protein breakdown rates in humans ~3h after a standard high-resistance exercise bout (8, 17). These studies used different stable-isotope techniques to calculate muscle protein breakdown, i.e. a three pool model and an intracellular tracer-dilution technique. Both methods rely on several assumptions, which have been explained and commented upon in previous reviews (34, 35). The main concerns were that the three pool model includes more tissues than muscle only (e.g. tendon, bone and skin protein turnover), and that both methods use sets of equations for calculating protein synthesis and protein degradation that are mutually dependent. Our data in isolated rat muscles also fail to show increased total protein breakdown levels after an intense stimulation protocol, previously proven to result in muscle hypertrophy when administered repeatedly (24, 25). In fact, we even show a small decrease of total protein breakdown 2h post-exercise in the EDL muscle. The discrepancy between our results and those obtained in humans with tracer methodology may be explained by the different methods used to measure protein breakdown. Incubated muscles are always in a net negative protein balance, and therefore it may be argued that our proteolysis measurements do not accurately reflect the *in vivo* situation in humans.

Another study using a microdialysis approach also found no increase in 3-methylhistidine (3-MH) release from human skeletal muscle during a 24h period after a high-resistance exercise bout (36). These findings suggested that either total protein breakdown did not change after exercise or that myosin and actin proteolysis was not a significant component of total

proteolysis after a high-resistance exercise bout. Increased *in vitro* rates of mixed muscle but not myofibrillar proteolysis in rat soleus muscle have been described in the hours following a treadmill-running protocol (37). However, as this experiment used an endurance exercise protocol, these data cannot easily be compared to our findings in response to resistance exercise. Thus, the increase of protein breakdown after high-resistance exercise still remains to be firmly established.

Since degradation of (myofibrillar) proteins in eukaryotic cells is believed to occur largely via the ubiquitin-proteasome (Ub-P) pathway (13, 14), it is of great interest to study the acute response of this pathway to a high-resistance exercise bout. There are no reports studying the influence of high-resistance exercise (either isometric or shortening contractions) on parameters of Ub-P pathway activity, however. The only evidence implicating the Ub-P pathway in the proteolytic response to exercise is provided by studies using eccentric exercise protocols, which are known to induce muscle damage, and hence require active removal of these damaged proteins. Increased muscle levels of Ub-conjugated proteins (22), as well as increased protein levels of Ub, Ub-conjugating enzyme E2 and 20S proteasome (21) have been reported 24h after performing a bout of eccentric exercise.

Highly increased activities of the Ub-P pathway have also been observed in rabbit tibialis anterior muscles during the course of a 28-day chronic low-frequency electrical stimulation (CLFS) protocol (18). This increased activity was underpinned by increased proteasome subunit mRNA and protein levels, increased proteasome activity and increased Ub-ATP-dependent hydrolysis of the exogenous protein substrate casein (18). CLFS results in a completely different pattern of muscle activation than any mode of human exercise. This form of stimulation is a potent stimulus for the muscle to remodel its protein composition, necessary to optimize muscle function for this new type of activity. The highly increased activity of the Ub-P pathway in the present experiment implies an important role for this pathway in muscle remodeling therefore suggesting that this pathway may also be implicated in the muscle remodeling response to a bout of high-resistance exercise. The increased rates of Ub-conjugation that we observed in the hours following electrical stimulation suggest that increasing the speed of the ubiquitination process may be an early adaptive response required for muscle remodeling. Although it is unclear which proteins are specifically

ubiquitinated in our assay, increased Ub-conjugation rates are observed in various proteins of different molecular weights. This suggests that at least a subset of muscle proteins is increasingly conjugated with ubiquitin, and therefore is increasingly targeted for breakdown by the 26S proteasome. Thus, increased rates of Ub-conjugation may be necessary to facilitate the increased breakdown of certain muscle proteins after a high-resistance exercise bout. In order to gain more knowledge on the adaptive response of muscle to high-resistance exercise, it will be of great importance for future studies to identify the specific proteins that are increasingly ubiquitinated following exercise. Our data suggest that an increased proteasome activity is not implicated in the post-exercise muscle remodeling at the chosen time-points. The present study, however, does not rule out a possible involvement of increased proteasome activity at a later time-point. The discrepancy in proteasome activities between CLFS and our stimulation protocol may also be explained by the fact that the former is a more potent and prolonged trigger for muscle remodeling.

In conclusion, our data do not indicate that an increased rate of muscle protein breakdown is present in the first 4 hours following a high-resistance exercise bout. Total protein breakdown rates did not increase in the EDL and soleus muscles, both 2h and 4h post-exercise. Interestingly, we show that Ub-conjugation rates are increased post-exercise, suggesting that this may be an important early event in the muscle remodeling response to high-resistance exercise. In contrast, our data do not implicate increased proteasome activities in this remodeling. Clearly, additional work needs to be done to identify the specific proteins that are increasingly targeted for breakdown by the Ub-P pathway after high-resistance exercise.

References

1. Jones SW, Hill RJ, Krasney PA, O'Conner B, Peirce N, and Greenhaff PL. Disuse atrophy and exercise rehabilitation in humans profoundly affects the expression of genes associated with the regulation of skeletal muscle mass. Faseb J 18: 1025-1027, 2004.
2. Akima H, Kawakami Y, Kubo K, et al. Effect of short-duration spaceflight on thigh and leg muscle volume. Med Sci Sports Exerc 32: 1743-1747, 2000.
3. Tesch PA, Berg HE, Bring D, Evans HJ, and LeBlanc AD. Effects of 17-day spaceflight on knee extensor muscle function and size. Eur J Appl Physiol 93: 463-468, 2005.
4. Taillandier D, Aurousseau E, Combaret L, Guezennec CY, and Attaix D. Regulation of proteolysis during reloading of the unweighted soleus muscle. Int J Biochem Cell Biol 35: 665-675, 2003.

5. Koopman R, Wagenmakers AJ, Manders RJ, et al. Combined ingestion of protein and free leucine with carbohydrate increases postexercise muscle protein synthesis in vivo in male subjects. Am J Physiol Endocrinol Metab 288: E645-653, 2005.
6. Phillips SM, Tipton KD, Ferrando AA, and Wolfe RR. Resistance training reduces the acute exercise-induced increase in muscle protein turnover. Am J Physiol 276: E118-124, 1999.
7. Chesley A, MacDougall JD, Tarnopolsky MA, Atkinson SA, and Smith K. Changes in human muscle protein synthesis after resistance exercise. J Appl Physiol 73: 1383-1388, 1992.
8. Biolo G, Maggi SP, Williams BD, Tipton KD, and Wolfe RR. Increased rates of muscle protein turnover and amino acid transport after resistance exercise in humans. Am J Physiol 268: E514-520, 1995.
9. Taillandier D, Combaret L, Pouch MN, Samuels SE, Bechet D, and Attaix D. The role of ubiquitin-proteasome-dependent proteolysis in the remodelling of skeletal muscle. Proc Nutr Soc 63: 357-361, 2004.
10. Reid MB. Response of the ubiquitin-proteasome pathway to changes in muscle activity. Am J Physiol Regul Integr Comp Physiol 288: R1423-1431, 2005.
11. Caiozzo VJ, Haddad F, Baker MJ, and Baldwin KM. Influence of mechanical loading on myosin heavy-chain protein and mRNA isoform expression. J Appl Physiol 80: 1503-1512, 1996.
12. Caiozzo VJ, Baker MJ, and Baldwin KM. Modulation of myosin isoform expression by mechanical loading: role of stimulation frequency. J Appl Physiol 82: 211-218, 1997.
13. Rock KL, Gramm C, Rothstein L, et al. Inhibitors of the proteasome block the degradation of most cell proteins and the generation of peptides presented on MHC class I molecules. Cell 78: 761-771, 1994.
14. Hershko A and Ciechanover A. The ubiquitin system. Annu Rev Biochem 67: 425-479, 1998.
15. Glickman MH and Ciechanover A. The ubiquitin-proteasome proteolytic pathway: destruction for the sake of construction. Physiol Rev 82: 373-428, 2002.
16. Rennie MJ and Tipton KD. Protein and amino acid metabolism during and after exercise and the effects of nutrition. Annu Rev Nutr 20: 457-483, 2000.
17. Phillips SM, Tipton KD, Aarsland A, Wolf SE, and Wolfe RR. Mixed muscle protein synthesis and breakdown after resistance exercise in humans. Am J Physiol 273: E99-107, 1997.
18. Ordway GA, Neufer PD, Chin ER, and DeMartino GN. Chronic contractile activity upregulates the proteasome system in rabbit skeletal muscle. J Appl Physiol 88: 1134-1141, 2000.
19. Hesselink MK, Kuipers H, Geurten P, and Van Straaten H. Structural muscle damage and muscle strength after incremental number of isometric and forced lengthening contractions. J Muscle Res Cell Motil 17: 335-341, 1996.
20. Feasson L, Stockholm D, Freyssenet D, et al. Molecular adaptations of neuromuscular disease-associated proteins in response to eccentric exercise in human skeletal muscle. J Physiol 543: 297-306, 2002.
21. Willoughby DS, Taylor M, and Taylor L. Glucocorticoid receptor and ubiquitin expression after repeated eccentric exercise. Med Sci Sports Exerc 35: 2023-2031, 2003.
22. Stupka N, Tarnopolsky MA, Yardley NJ, and Phillips SM. Cellular adaptation to repeated eccentric exercise-induced muscle damage. J Appl Physiol 91: 1669-1678, 2001.

23. Drost MR, Maenhout M, Willems PJ, Oomens CW, Baaijens FP, and Hesselink MK. Spatial and temporal heterogeneity of superficial muscle strain during in situ fixed-end contractions. J Biomech 36: 1055-1063, 2003.
24. Diffee GM, Caiozzo VJ, McCue SA, Herrick RE, and Baldwin KM. Activity-induced regulation of myosin isoform distribution: comparison of two contractile activity programs. J Appl Physiol 74: 2509-2516, 1993.
25. Haddad F, Qin AX, Zeng M, McCue SA, and Baldwin KM. Effects of isometric training on skeletal myosin heavy chain expression. J Appl Physiol 84: 2036-2041, 1998.
26. Jones DA and Rutherford OM. Human muscle strength training: the effects of three different regimens and the nature of the resultant changes. J Physiol 391: 1-11, 1987.
27. Waalkes TP and Udenfriend S. A fluorometric method for the estimation of tyrosine in plasma and tissues. J Lab Clin Med 50: 733-736, 1957.
28. Tischler ME, Desautels M, and Goldberg AL. Does leucine, leucyl-tRNA, or some metabolite of leucine regulate protein synthesis and degradation in skeletal and cardiac muscle? J Biol Chem 257: 1613-1621, 1982.
29. Hobler SC, Williams A, Fischer D, et al. Activity and expression of the 20S proteasome are increased in skeletal muscle during sepsis. Am J Physiol 277: R434-440, 1999.
30. Minnaard R, Wagenmakers AJ, Combaret L, et al. Ubiquitin-proteasome-dependent proteolytic activity remains elevated after zymosan-induced sepsis in rats while muscle mass recovers. Int J Biochem Cell Biol 37: 2217-2225, 2005.
31. Laemmli UK. Cleavage of structural proteins during the assembly of the head of bacteriophage T4. Nature 227: 680-685, 1970.
32. Goldspink DF. The effects of denervation on protein turnover of rat skeletal muscle. Biochem J 156: 71-80, 1976.
33. Furuno K, Goodman MN, and Goldberg AL. Role of different proteolytic systems in the degradation of muscle proteins during denervation atrophy. J Biol Chem 265: 8550-8557, 1990.
34. Liu Z and Barrett EJ. Human protein metabolism: its measurement and regulation. Am J Physiol Endocrinol Metab 283: E1105-1112, 2002.
35. Wagenmakers AJ. Tracers to investigate protein and amino acid metabolism in human subjects. Proc Nutr Soc 58: 987-1000, 1999.
36. Trappe T, Williams R, Carrithers J, et al. Influence of age and resistance exercise on human skeletal muscle proteolysis: a microdialysis approach. J Physiol 554: 803-813, 2004.
37. Kasperek GJ and Snider RD. Total and myofibrillar protein degradation in isolated soleus muscles after exercise. Am J Physiol 257: E1-5, 1989.

6

Ubiquitin-proteasome pathway and NF-κB activity in skeletal muscle of patients with non-small cell lung cancer

R. Minnaard, R.C.J. Langen, M.C.M.J. Kelders,
A.C. Dingemans, M.K.C. Hesselink, A.M.W.J. Schols

Submitted

Abstract

Cancer cachexia, characterized by weight loss and a disproportionate loss of muscle mass, is a common phenomenon in non-small cell lung cancer (NSCLC), which has been associated with a systemic inflammatory response. In experimental cancer cachexia an increased proteolysis through the ubiquitin-proteasome (Ub-P) pathway has been shown to be responsible for muscle atrophy. The aim of this study was to investigate whether the Ub-P pathway was activated in newly-diagnosed NSCLC patients, and to evaluate whether this was associated with systemic inflammation and skeletal muscle NF-κB activation. For this purpose 20S proteasome peptidase activities, as well as the mRNA expression of two critical E3 Ub-ligases, MuRF1 and atrogin-1/MAFbx, and two markers of NF-κB activity (IκBα and TNFα) were determined in muscle biopsies of newly diagnosed NSCLC patients (n=11) and compared to age-matched controls (n=8). Patients were characterized by systemic inflammation and a weight loss of 4.2%, mainly reflecting a loss of fat mass. A trend towards increased mRNA levels of MuRF1 (P=0.076), but not of atrogin-1/MAFbx, was found in NSCLC patient vs. control muscle. 20S proteasome peptidase activities were not different in patient vs. control muscle. Importantly, in NSCLC patient muscle but not in control muscle mRNA levels of IκBα, an NF-κB target gene, correlated strongly with circulatory soluble TNF receptor-55 (R=0.82, P=0.002) and C-reactive protein (R=0.73, P=0.011) levels. Our data suggest that MuRF1 may be involved in initiating Ub-P dependent muscle wasting in NSCLC patients, and that systemic inflammation may induce skeletal muscle NF-κB activity in NSCLC patients.

Introduction

Cachexia reflects a progressive body weight loss, characterized by wasting of adipose and skeletal muscle tissue, and is a common complication associated with cancer, especially cancer of the upper gastrointestinal tract and the lungs. Substantial weight loss occurs in more than 60% of lung cancer patients (1). Cancer cachexia has been associated with a poor prognosis and lower responses to chemotherapy and radiation treatment (2, 3). The reduction of muscle mass hampers the patients' ability to perform activities of daily living (ADL), and contributes to increased morbidity and mortality.

Muscle wasting reflects a net loss of muscle protein, caused by an imbalance between rates of protein synthesis and degradation. In human cancer (4-6) and animal models (7-11) there is evidence for decreased muscle protein synthesis and/or increased muscle protein degradation being responsible for muscle atrophy. Because an increased proteolysis has been implicated in muscle atrophy associated with many forms of cancer (12), it is important to study early factors contributing to and mechanisms underlying muscle proteolysis. This in order to develop targeted nutritional or pharmacological strategies to prevent or reverse cancer cachexia.

In the Ub-P pathway, proteins are targeted for degradation by the covalent attachment of a polyubiquitin chain (Ub-conjugation), after which proteins are recognized and degraded by the 26S proteasome, a large multi-catalytic protein complex, which comprises two 19S regulatory complexes and a 20S proteolytic core (13). Ubiquitin conjugation occurs through a cascade of E1 (Ub-activating), E2 (Ub-conjugating) and E3 (Ub-ligating) enzymes (14). In this process the muscle-specific Ub-ligases atrogin-1/MAFbx and MuRF1 are considered rate-limiting for muscle protein degradation (15). Moreover, both ligases are consistently induced in muscles atrophying as a result of different catabolic stimuli, including cancer (15-17). Several animal studies show that an increased proteolysis through the Ub-P pathway is responsible for the bulk of muscle atrophy during cancer cachexia (9, 18, 19). In human cancer, however, there are only a few studies providing evidence for a muscular activation of the Ub-P pathway. Increased proteasome activities, as well as increased expression of certain components of the Ub-P pathway, including Ub, the 14 kDa-E2 Ub-conjugating enzyme and several proteasome subunits, have been reported (20-22). Although atrogin-1/MAFbx and MuRF1 play critical roles in determining the rate of Ub-P

dependent proteolysis, no reports have evaluated their expression in muscle of cancer patients.

Proinflammatory mediators have been implicated in the regulation of muscle proteolysis during cancer cachexia. Lung cancer patients frequently develop a systemic inflammatory response, characterized by increased circulatory proinflammatory cytokines, such as tumor necrosis factor α (TNFα), interleukin-1 (IL-1) and interleukin-6 (IL-6), and the presence of an acute phase response (23). In animal models it has been shown that repeated administration of TNFα, IL-1 and IL-6 alone is sufficient to induce skeletal muscle atrophy (24, 25). From studies using muscle cell systems or rodents it is known that cytokines like TNFα elicit a local inflammatory response in skeletal muscle by activating the transcription factor NF-κB (26, 27). In cancer patients, however, it has not been studied whether systemic inflammation is related to skeletal muscle NF-κB activity and to the expression of its target genes.

Apart from its role as an integrator of proinflammatory signals, recent experimental work shows that NF-κB activation alone is sufficient to cause skeletal muscle atrophy (28). Continuous activation of NF-κB induced profound muscle atrophy in mice, whereas an inhibition of NF-κB activity prevented muscle atrophy in several catabolic mouse models, including cancer cachexia (28). The latter study also demonstrated a continuous activation of NF-κB induced muscle atrophy by accelerating protein breakdown through the Ub-P pathway. Moreover, the findings of this study suggested that inflammatory cytokines can directly impact muscle proteolysis by activating the Ub-P pathway through an NF-κB dependent induction of MuRF1 gene expression (28).

Until now no definite intervention strategy is known to prevent or reverse cancer cachexia. A few studies have investigated molecular markers of muscle atrophy in patients with cancer. These patients varied in cancer type and nutritional status, however, making these studies difficult to compare. To understand more of the triggers and mechanisms initiating muscle wasting in lung cancer patients we considered it important to investigate if the Ub-P pathway is activated in skeletal muscle of a group of newly diagnosed non-treated NSCLC patients without evident weight loss and if this is associated with a systemic inflammatory response and muscular NF-κB activation.

Materials and methods

Patients

Twenty-one newly diagnosed and previously untreated NSCLC patients were included. All patients had histologically or cytologically proven NSCLC. At the time of inclusion all patients were expected to be eligible for lung cancer surgery. Tumor stage was assessed using the TNM international staging system for lung cancer (29). ECOG performance status was assessed at time of inclusion (30). Ten healthy, age-matched volunteers were recruited as controls from advertisements in local newspapers. Prior to inclusion, volunteers received a physical examination. This study was approved by the medical ethical committee of the Maastricht University hospital and written informed consent was obtained from all subjects.

Muscle biopsy and plasma samples

Biopsies of the m. vastus lateralis were taken from 11 patients; 8 under general anaesthesia prior to thoracic surgery and 3 under local anaesthesia. Muscle biopsies from 8 healthy individuals were taken under local anaesthesia. Muscle biopsies were immediately frozen in liquid nitrogen and stored at -80 °C until analysis.
After an overnight fast, blood was collected from an antecubital vein in evacuated EDTA blood collection tubes (Sherwood Medical, Ballymoney, N. Ireland). After collection, the EDTA tubes were placed on ice and were centrifuged for 5 minutes at 3000 g, 4 °C. Plasma samples were stored at -80 °C until analysis.

Body composition

Dual energy X-ray absorptiometry (DEXA; DPX-L, Lunar Radiation Corp., Madison, WI) was used to determine whole-body composition, i.e. bone mineral content (BMC), fat mass (FM) and lean body mass (LBM; comprising muscle, inner organs and body water) (23). DEXA measurements were performed in the morning, in the fasted state. The principles of measuring body composition with DEXA have been described extensively elsewhere (31, 32).

Plasma inflammatory markers

Plasma soluble TNF receptor 55 (sTNF-R55) and 75 (sTNF-R75) were measured by sandwich ELISA, as described elsewhere (33). Briefly, for the measurement of sTNF-R55 and sTNF-R75, the monoclonal antibodies MR1-1 and MR2-2 (33) were used for coating the ELISA plates. Specific biotin-labeled polyclonal rabbit anti-human sTNF-R IgGs were used as detector reagents. Recombinant human sTNF-R55 and sTNF-R75 were used as standards. For both assays, the detection limit was 100 pg/ml.
Albumin and pre-albumin were measured using the Bromocresol Purple method with a Synchron CX-7 instrument (Beckman, Mijdrecht, The Netherlands). C-reactive protein (CRP) was measured by turbidimetry.

20S Proteasome peptidase activities

The method used to determine 20S proteasome peptidase activities has been described previously (34, 35). This protocol was modified slightly to allow analysis of small human muscle biopsies. To isolate 20S proteasomes, muscle biopsies were homogenized in 10 vol of ice-cold buffer (pH 7.5), containing 50 mM Tris, 5 mM $MgCl_2$, 250 mM sucrose, 1 mM DTT, and protease inhibitors (10 μg/ml antipain, aprotinin, leupeptin and pepstatin A, 0.2 mM PMSF) using a Yellowline homogenizer (IKA Works, Wilmington, NC). Proteasomes were isolated by sequential (ultra)centrifugation steps and the protein concentration in the proteasome fractions was measured with the Bio-Rad protein assay (Bio-Rad, Veenendaal, The Netherlands), using bovine serum albumin as standard. The peptidase activities of the 20S proteasome were determined fluorometrically by measuring the hydrolysis of the fluorogenic substrates Succinyl-Leu-Leu-Val-Tyr-7-amido-4-methylcoumarin (Suc-LLVY-AMC, Sigma, Zwijndrecht, The Netherlands) and Benzyloxycarbonyl-Leu-Leu-Glu-7-amido-4-methylcoumarin (Z-LLE-AMC, BIOMOL, Exeter, UK). These substrates are preferentially hydrolyzed by the chymotrypsin-like and caspase-like peptidase activities of the 20S proteasome, respectively. Adding the proteasome inhibitor MG132 to the reaction resulted in complete inhibition of the proteasome peptidase activities.

RNA isolation and assessment of mRNA abundance

Muscle biopsies were homogenized using a Polytron PT1600E homogenizer (Kinematica, Littau-Lucerne, Switzerland). Total RNA was isolated using the Totally RNA™ kit (Ambion, Austin, TX) according to the manufacturer's instructions. Isolated RNA was dissolved in TE buffer and stored at -80°C. One μg of RNA was reverse transcribed to cDNA using the Reverse iT First Strand Synthesis kit (ABgene, Epsom, UK) with oligo-dT primers.
Human MuRF1, Atrogin-1, TNFα, IκBα, and β-actin mRNA were determined by quantitative RT-PCR (Q-PCR). Q-PCR primers were designed using Primer Express 2.0 software (Applied Biosystems, Foster City, CA) and obtained from Sigma Genosys (Haverhill, UK). Primers are outlined in Table 1. PCR reactions (25 μl total volume) contained 1x qPCR MasterMix Plus for SYBR green I (Eurogentec, Seraing, Belgium) and primers (300 nM). Standard curves were made in duplicate by performing serial dilutions of pooled cDNA aliquots. Real-time PCR reactions were performed in an ABI PRISM™ 7700 Sequence Detector (Applied Biosystems). Ct values were obtained for each sample and the relative DNA concentrations were derived from the standard curve. The expression of the genes of interest was normalized to β-actin (primers obtained from Ambion).
Murine TNFα and IκBα mRNA abundance were determined by semi-quantitative RT-PCR. Primers were designed using primer3 software (http://frodo.wi.mit.edu/cgi-bin/primer3/primer3_www.cgi) and obtained from Sigma Genosys (Haverhill, UK). Primers are outlined in Table 1. PCR reactions were performed using Thermostart PCR Mastermix (ABgene). TNFα or IκBα mRNA abundance was normalized to β-actin within each individual reaction using QuantumRNA™ technology (Ambion) according to manufacturers' instructions.

Statistics

The subject characteristics (Table 2) and inflammatory mediators (Table 3) are presented as means ± SD. Proteasome activities and PCR data are presented as means ± SEM. Data are compared using a two-sided independent samples t-test. Relationships between parameters were evaluated using Pearson's correlation coefficient (R). Significance was set at $P<0.05$.

Table 1. Q-PCR and RT-PCR primer info.

Gene	Genebank Acc. nr.	Forward Primer	Reverse Primer
Q-PCR			
hAtrogin-1*1	NM_148177.1	5'-GAAGAAACTCTGCCAGTACCAC TTC-3'	5'- CCCTTTGTCTGACAGAATTAA TCG-3'
hMuRF1	AJ291713	5'-GCGAGGTGGCCCCATT-3'	5'-GATGGTCTGCACACGGTCATT-3'
hIκBα	NM_020529	5'-CTACACCTTGCCTGTGAGCA-3'	5'-TCCTGAGCATTGACATCAGC-3'
hTNFα	NM_000594	5'-CTCGAACCCCGAGTGACAA-3'	5'-AGCTGCCCCTCAGCTTGA-3'
Semi-quantitative RT-PCR			
mIκBα*2	U36277	5'-GACTCCATGAAGGACGAGGA-3'	5'-GTCTCCCTTCACCTGACCAA-3'
mTNFα	X02611	5'-ATGCACCACCATCAAGGACT-3'	5'-GCACCTCAGGGAAGAGTCTG-3'

*1 h = human
*2 m = murine

Results

Subject characteristics

Subject characteristics of the NSCLC patients and healthy controls are summarized in Table 2. At the time of inclusion all patients were expected to be eligible for surgery, however upon further staging by mediastinoscopy or thoracotomy 8 patients proved inoperable.

All NSCLC patients and 80% of the healthy subjects were current or former smokers. Both groups were similar with respect to age, sex, usual body weight and height. Mean weight loss in the patient group was 4.2 ± 5.9%, which was significantly higher than in the control subjects. Nineteen patients had a weight loss ≤10% and 2 patients >10%. Muscle biopsies were taken in a subpopulation (n=11), which represented the entire population. All patients in this subpopulation had a weight loss ≤10% (mean 4.1 ± 4.8%). The patients (n=21) showed trends towards a decreased body mass index (patients 24.6 ± 3.7 kg/m^2 vs. controls 27.1 ± 3.7 kg/m^2; p=0.092) and fat mass index (p=0.068) but not lean body mass index (p=0.28). This suggests that in this early stage wasting is more prominent in the fat compartment and precedes the loss of muscle mass. Although the NSCLC patient group varied in disease stage, we did not observe a relationship between weight loss and disease stage (R=-0.006, P=0.98). Table 3 shows the plasma levels of inflammatory mediators. NSCLC patients clearly showed an elevated systemic (pro)-inflammatory status, evidenced by an increased plasma sTNF-R55 level, and elevated plasma levels of the positive acute-phase reactants C-reactive protein (CRP) and fibrinogen.

Table 2. Clinical characteristics of patients with NSCLC and healthy control subjects.

	NSCLC patients (n=21)	Healthy controls (n=10)	P-value
Age	66 ± 8	64 ± 6	0.48
Sex (M:F)	17 : 4	7 : 3	
Usual body weight (kg)	76.0 ± 14.1	76.5 ± 12.0	0.93
Current body weight (kg)	73.0 ± 15.3	77.0 ± 12.2	0.49
Weight loss (kg)	3.0 ± 3.9*	-0.50 ± 1.6	0.012
Weight loss (%)	4.2 ± 5.9*	-0.63 ± 2.0	0.019
Height (cm)	172 ± 8	169 ± 10	0.35
Body mass index (kg/m^2)	24.6 ± 3.7	27.1 ± 3.7	0.092
Lean body mass (kg)	49.5 ± 9.3	50.9 ± 10.2	0.70
Lean body mass index (kg/m^2)	16.8 ± 2.2	17.8 ± 2.2	0.27
Fat mass (kg)	18.2 ± 7.4	22.9 ± 7.6	0.13
Fat mass index (kg/m^2)	6.2 ± 2.3	8.2 ± 3.2	0.068
Muscle biopsy performed (n)	11	8	
ECOG performance status (0 (fully active) – 5 (dead))	0 (n=15), 1(n=5), 2 (n=1)		
Survival (months, 95% CI)	23 (5-42)		
Tumor stage (I-II : IIIA : IIIB : IV)	12 : 2 : 4 : 3		

* P<0.05 vs. control subjects

Table 3. Plasma inflammatory mediators in NSCLC patients and healthy controls

	NSCLC patients (n=21)	Healthy controls (n=10)	P-value
sTNF-R55 (ng/ml)	1.05 ± 0.31*	0.77 ± 0.16	0.016
sTNF-R75 (ng/ml)	1.87 ± 0.73	1.40 ± 0.60	0.088
CRP (μg/ml)	70 ± 57*	7.2 ± 5.9	0.002
Fibrinogen (g/l)	6.3 ± 1.7*	3.8 ± 0.7	< 0.001
Albumin (mg/ml)	33.1 ± 3.3*	40.1 ± 2.6	< 0.001

* P<0.05 vs. control subjects

Ubiquitin-Proteasome Pathway

To investigate ubiquitin-proteasome pathway activity in skeletal muscle of NSCLC patients, we measured 20S proteasome peptidase activities, as well as the gene expression of the critical E3-ligases atrogin-1/MAFbx and MuRF1. As is shown in Figure 1, no differences in 20S proteasome chymotrypsin-like and caspase-like peptidase activities were observed between proteasome preparations of patient and control muscles. Figure 2A shows a trend for an increase in MuRF1 mRNA in patient vs. control muscle

(+102%, p=0.076), while levels of atrogin-1/MAFbx mRNA were not significantly different (+31%, P=0.42). Our data did not show any significant correlation between skeletal muscle Ub-P pathway activity (proteasome activity and E3-ligase mRNA) and systemic inflammatory mediators (sTNF-R55, sTNF-R75, CRP and fibrinogen) in the NSCLC patients.

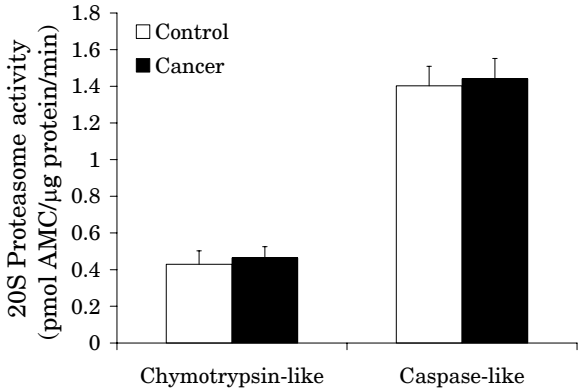

Figure 1: 20S proteasome chymotrypsin-like and caspase-like peptidase activities do not differ between NSCLC patient and healthy control muscle biopsies. 20S proteasome chymotrypsin-like and caspase-like peptidase activities were measured in muscle proteasome preparations against the fluorogenic substrates Suc-LLVY-AMC and Z-LLE-AMC, respectively. Activities are expressed as the release of AMC in pmol/μg protein/min.

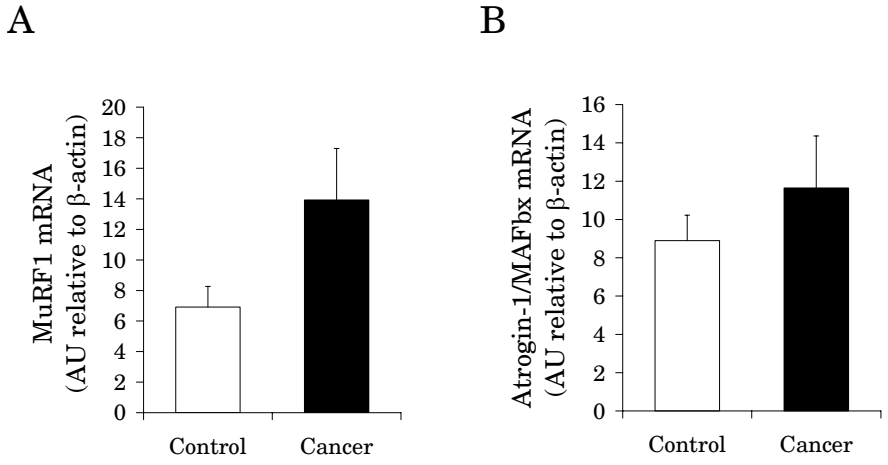

Figure 2: **(A)** MuRF1 and **(B)** Atrogin-1/MAFbx mRNA levels in muscles from NSCLC patients and control subjects. A trend for an increased MuRF1 mRNA level was observed in muscle biopsies of NSCLC patients vs. control subjects (P=0.076).

Inflammatory signaling in skeletal muscle

To determine if the elevated levels of systemic inflammatory mediators were associated with inflammatory signaling in skeletal muscle we investigated whether there was evidence of NF-κB activation in the patients. For this purpose we measured the muscle mRNA expression of IκBα and TNFα, two NF-κB target genes (36). However, to verify whether inflammatory stimuli are able to activate these NF-κB regulated genes in skeletal muscle, cultured myotubes were incubated with a prototypical inducer of NF-κB, TNFα (36, 37). Indeed, Figure 3 shows that treating fully differentiated muscle cells with TNFα for 2 hours resulted in a dramatic increase in both IκBα and TNFα mRNA expression, illustrating that an inflammatory stimulus can trigger muscular NF-κB activation. Despite an evident systemic inflammation in the patients, the mRNA expressions of both IκBα and TNFα were not significantly different in patient vs. control muscle (data not shown). Interestingly, in patient muscle IκBα mRNA levels, but not TNFα mRNA, correlated strongly with circulatory sTNF-R55 (R=0.82, p=0.002) and CRP (R=0.73, p=0.011) levels, as shown in Figure 4. In contrast, IκBα mRNA levels in control muscle did not correlate with circulatory sTNF-R55 and CRP levels.

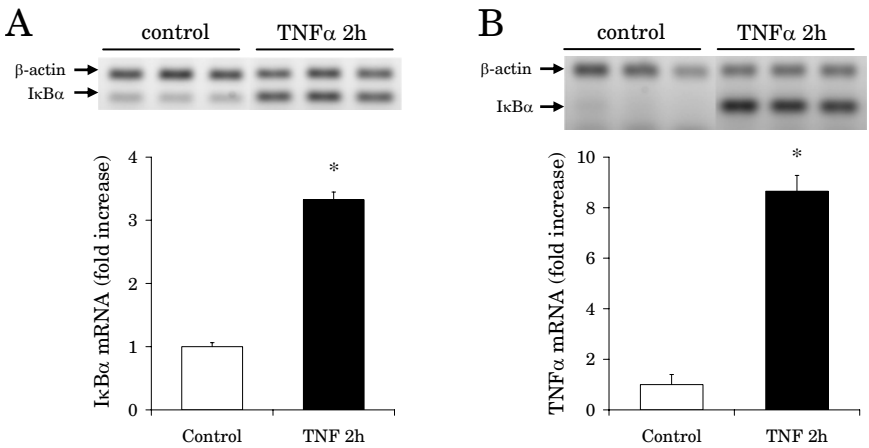

Figure 3: TNFα stimulates IκBα **(A)** and TNFα **(B)** mRNA expression in cultured skeletal muscle cells. Mouse skeletal muscle cells (C2C12, ATCC# CRL1772, Manassas, VA) were cultured as described previously (45). Murine TNFα (Calbiochem, La Jolla, CA) was added once to fully (5 day) differentiated myotubes (the *in vitro* equivalents of muscle fibers). Two hours following TNFα treatment, cells were washed, lysed and RNA was extracted as desribed previously (46). One μg of total RNA was reverse transcribed to cDNA using Superscript II RT and oligo dT primers (Invitrogen, Carlsbad, CA) according to the manufacturers' instructions. PCR reactions were performed using 2xThermo-Start PCR Master Mix (ABgene). Murine IκBα and mTNFα were amplified using the primers, outlined in Table 1. Murine mRNA abundance was normalized to a β-actin internal standard (QuantumRNA™ technology, Ambion).* P<0.05 vs. untreated C2C12 cells.

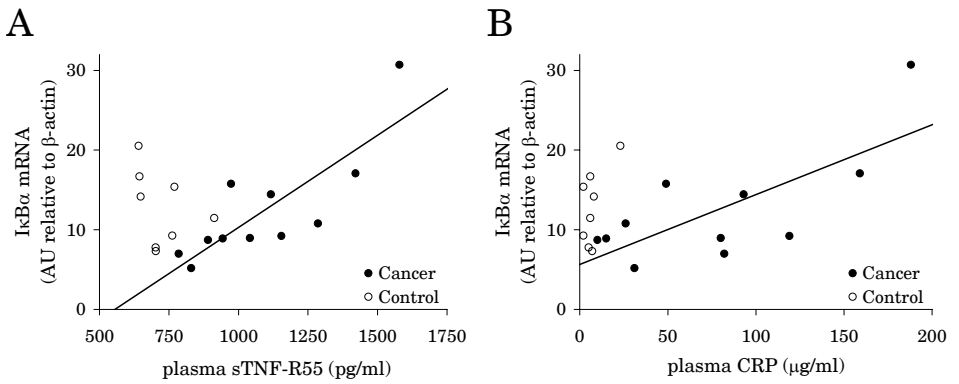

Figure 4: Skeletal muscle IκBα mRNA levels correlate strongly with circulating levels of **(A)** sTNF-R55 (R=0.82, P=0.002) and **(B)** CRP (R=0.73, P=0.011) in NSCLC patients. No correlation between muscle IκBα mRNA levels and both sTNF-R55 (R=-0.36, p=0.38) and CRP (R=0.63, P=0.097) levels was present in control subjects.

Discussion

The aim of this work was to investigate the early events that mediate cancer cachexia, and therefore a group of newly-diagnosed NSCLC patients, who were eligible for surgery, was studied. These patients had a limited body weight loss, mainly originating from a loss of fat mass. We show that the E3 Ub-ligase MuRF1 may be involved in initiating Ub-P dependent muscle wasting in NSCLC patients. In contrast, the mRNA expression of atrogin-1/MAFbx, another critical E3 Ub-ligase, as well as the chymotrypsin-like and caspase-like peptidase activities of the 20S proteasome were not significantly different. Importantly, in NSCLC patients, but not in healthy control subjects, circulating levels of the systemic inflammatory mediators sTNF-R55 and CRP correlated strongly and positively with skeletal muscle mRNA levels of IκBα, an NF-κB target gene. Since IκBα expression is controlled by the transcription factor NF-κB, these data provide a link between systemic inflammation and skeletal muscle NF-κB activity in NSCLC patients. In support of this association, we show that stimulating fully differentiated C2C12 muscle cells with TNFα induces mRNA expression of IκBα and TNFα, indicating NF-κB activation (Figure 3A).
We report no difference in 20S proteasome peptidase activities between fractions of patient and control muscle. This lack of response corresponds with a modest loss of body weight in the patients, which mainly comprises loss of fat mass and not muscle mass. Previous work in gastric cancer

patients displaying 5% weight loss, revealed an activation of the 20S proteasome in the rectus abdominis muscles (21). Notwithstanding the absence of quantitative changes in Ub-P dependent proteolysis, qualitative changes may also be important during cancer cachexia. This notion is supported by data in a mouse model of cancer cachexia, showing that myosin heavy chains were specifically targeted by the Ub-P pathway (38). These data suggested that muscle wasting during cancer cachexia does not result from a general downregulation of muscle proteins, but rather involves the targeting of specific muscle proteins.

The E3 Ub-ligases MuRF1 and atrogin-1/MAFbx have been shown to be invariably induced in experimental cancer cachexia, and many other catabolic conditions (15-17). There are no data on the expression of these ligases in muscle of cancer patients, however. In human muscle atrophy due to limb immobilization, a 4.7% decrease of quadriceps muscle mass occurred in parallel with a 67% increase in atrogin-1/MAFbx mRNA, while a trend for an increased MuRF1 mRNA level (+31%) was present (39). These findings suggest a more prominent role for atrogin-1/MAFbx in disuse atrophy. Because all patients in the present study scored well on the ECOG performance questionnaire, disuse atrophy is unlikely to play an important role, possibly explaining the lack of response in atrogin-1/MAFbx. Conversely, an increased expression of MuRF1 in the patients is in line with findings of a recent study in mice, suggesting that proinflammatory cytokines can directly impact muscle proteolysis by upregulating MuRF1 expression in an NF-κB dependent manner (28).

Several factors produced by the tumor and/or host tissues have been implicated in the regulation of muscle wasting (40). These factors include several circulating pro-inflammatory cytokines, such as TNFα, interleukin-1 (IL-1) and interleukin-6 (IL-6) (41-43), which can be produced by both the tumor and host tissues, and tumor-produced factors such as proteolysis inducing factor (PIF) (44). Interestingly, both inflammatory cytokines (26) and PIF (44) have been shown to activate NF-κB in skeletal muscle, suggesting that they share a common pathway for inducing their cachectic effects. In recent experimental work, continuous activation of NF-κB in genetically manipulated mice induced extensive muscle atrophy, whereas an inhibition of NF-κB activity prevented muscle atrophy in several catabolic models, including cancer (28). Thus, there is evidence for a pivotal role of NF-κB activation in inducing muscle atrophy. However, there is no data

available on the activity status of NF-κB in skeletal muscle of cancer patients. In the present study, we showed that skeletal muscle mRNA levels of IκBα, a target gene of NF-κB, correlated strongly with circulating CRP and sTNF-R55 levels. These correlations provide evidence for an association between systemic inflammation and skeletal muscle NF-κB activity in cancer patients. Although it is presently unknown whether these relationships are causal, they support the experimental data that proinflammatory cytokines trigger muscle atrophy through an NF-κB dependent pathway. Although we did not measure skeletal muscle NF-κB activity directly, the use of IκBα gene expression as a marker of NF-κB activity was justified by an experiment using muscle cells. In this experiment, we verified that incubation with TNFα, a prototypical activator of NF-κB, induced the gene expression of IκBα in skeletal muscle.

In summary, we show a trend towards increased mRNA levels of the critical E3 Ub-ligase MuRF1 in skeletal muscle of a group of newly diagnosed NSCLC patients. This suggests that in NSCLC patients MuRF1 may initiate an increased Ub-P pathway activity, which is known to be responsible for muscle atrophy in experimental cancer cachexia. No differences were observed in the mRNA levels of atrogin-1/MAFbx and 20S proteasome activities in patient skeletal muscle compared to control muscle. This indicates that in these patients, in contrast to common clinical practice, weight loss may be reversible and associated muscle atrophy may be delayed with nutritional and anabolic interventions. In addition, our data support an association between systemic inflammation and skeletal muscle NF-κB activity in NSCLC patients, which suggests that also in human skeletal muscle NF-κB may play a central role in causing a local inflammatory response and in inducing muscle atrophy during cancer cachexia. Longitudinal studies are however indicated involving different stages of cachexia to confirm this hypothesis in search for targeted interventions aimed at preventing or reversing muscle atrophy.

References

1. Bruera E. ABC of palliative care. Anorexia, cachexia, and nutrition. Bmj 315: 1219-1222, 1997.
2. Tisdale MJ. Cachexia in cancer patients. Nat Rev Cancer 2: 862-871, 2002.
3. Dewys WD, Begg C, Lavin PT, et al. Prognostic effect of weight loss prior to chemotherapy in cancer patients. Eastern Cooperative Oncology Group. Am J Med 69: 491-497, 1980.

4. Dworzak F, Ferrari P, Gavazzi C, Maiorana C, and Bozzetti F. Effects of cachexia due to cancer on whole body and skeletal muscle protein turnover. Cancer 82: 42-48, 1998.
5. Lundholm K, Bylund AC, Holm J, and Schersten T. Skeletal muscle metabolism in patients with malignant tumor. Eur J Cancer 12: 465-473, 1976.
6. Lundholm K, Bennegard K, Eden E, Svaninger G, Emery PW, and Rennie MJ. Efflux of 3-methylhistidine from the leg in cancer patients who experience weight loss. Cancer Res 42: 4807-4811, 1982.
7. Tessitore L, Bonelli G, and Baccino FM. Early development of protein metabolic perturbations in the liver and skeletal muscle of tumour-bearing rats. A model system for cancer cachexia. Biochem J 241: 153-159, 1987.
8. Strelkov AB, Fields AL, and Baracos VE. Effects of systemic inhibition of prostaglandin production on protein metabolism in tumor-bearing rats. Am J Physiol 257: C261-269, 1989.
9. Temparis S, Asensi M, Taillandier D, et al. Increased ATP-ubiquitin-dependent proteolysis in skeletal muscles of tumor-bearing rats. Cancer Res 54: 5568-5573, 1994.
10. Costelli P, Carbo N, Tessitore L, et al. Tumor necrosis factor-alpha mediates changes in tissue protein turnover in a rat cancer cachexia model. J Clin Invest 92: 2783-2789, 1993.
11. Beck SA, Smith KL, and Tisdale MJ. Anticachectic and antitumor effect of eicosapentaenoic acid and its effect on protein turnover. Cancer Res 51: 6089-6093, 1991.
12. Baracos VE. Regulation of skeletal-muscle-protein turnover in cancer-associated cachexia. Nutrition 16: 1015-1018, 2000.
13. Pickart CM and Cohen RE. Proteasomes and their kin: proteases in the machine age. Nat Rev Mol Cell Biol 5: 177-187, 2004.
14. Pickart CM. Mechanisms underlying ubiquitination. Annu Rev Biochem 70: 503-533, 2001.
15. Bodine SC, Latres E, Baumhueter S, et al. Identification of ubiquitin ligases required for skeletal muscle atrophy. Science 294: 1704-1708, 2001.
16. Lecker SH, Jagoe RT, Gilbert A, et al. Multiple types of skeletal muscle atrophy involve a common program of changes in gene expression. Faseb J 18: 39-51, 2004.
17. Gomes MD, Lecker SH, Jagoe RT, Navon A, and Goldberg AL. Atrogin-1, a muscle-specific F-box protein highly expressed during muscle atrophy. Proc Natl Acad Sci U S A 98: 14440-14445, 2001.
18. Llovera M, Garcia-Martinez C, Agell N, Lopez-Soriano FJ, and Argiles JM. Muscle wasting associated with cancer cachexia is linked to an important activation of the ATP-dependent ubiquitin-mediated proteolysis. Int J Cancer 61: 138-141, 1995.
19. Baracos VE, DeVivo C, Hoyle DH, and Goldberg AL. Activation of the ATP-ubiquitin-proteasome pathway in skeletal muscle of cachectic rats bearing a hepatoma. Am J Physiol 268: E996-1006, 1995.
20. Williams A, Sun X, Fischer JE, and Hasselgren PO. The expression of genes in the ubiquitin-proteasome proteolytic pathway is increased in skeletal muscle from patients with cancer. Surgery 126: 744-749; discussion 749-750, 1999.
21. Bossola M, Muscaritoli M, Costelli P, et al. Increased muscle proteasome activity correlates with disease severity in gastric cancer patients. Ann Surg 237: 384-389, 2003.
22. Khal J, Hine AV, Fearon KC, Dejong CH, and Tisdale MJ. Increased expression of proteasome subunits in skeletal muscle of cancer patients with weight loss. Int J Biochem Cell Biol 37: 2196-2206, 2005.
23. Simons JP, Schols AM, Buurman WA, and Wouters EF. Weight loss and low body cell mass in males with lung cancer: relationship with systemic inflammation, acute-phase

response, resting energy expenditure, and catabolic and anabolic hormones. Clin Sci (Lond) 97: 215-223, 1999.
24. Goodman MN. Interleukin-6 induces skeletal muscle protein breakdown in rats. Proc Soc Exp Biol Med 205: 182-185, 1994.
25. Ling PR, Schwartz JH, and Bistrian BR. Mechanisms of host wasting induced by administration of cytokines in rats. Am J Physiol 272: E333-339, 1997.
26. Langen RC, Schols AM, Kelders MC, Wouters EF, and Janssen-Heininger YM. Inflammatory cytokines inhibit myogenic differentiation through activation of nuclear factor-kappaB. Faseb J 15: 1169-1180, 2001.
27. Guttridge DC, Mayo MW, Madrid LV, Wang CY, and Baldwin AS, Jr. NF-kappaB-induced loss of MyoD messenger RNA: possible role in muscle decay and cachexia. Science 289: 2363-2366, 2000.
28. Cai D, Frantz JD, Tawa NE, Jr., et al. IKKbeta/NF-kappaB activation causes severe muscle wasting in mice. Cell 119: 285-298, 2004.
29. Mountain CF. Revisions in the International System for Staging Lung Cancer. Chest 111: 1710-1717, 1997.
30. Oken MM, Creech RH, Tormey DC, et al. Toxicity and response criteria of the Eastern Cooperative Oncology Group. Am J Clin Oncol 5: 649-655, 1982.
31. Mazess RB, Barden HS, Bisek JP, and Hanson J. Dual-energy x-ray absorptiometry for total-body and regional bone-mineral and soft-tissue composition. Am J Clin Nutr 51: 1106-1112, 1990.
32. Peppler WW and Mazess RB. Total body bone mineral and lean body mass by dual-photon absorptiometry. I. Theory and measurement procedure. Calcif Tissue Int 33: 353-359, 1981.
33. Leeuwenberg JF, Dentener MA, and Buurman WA. Lipopolysaccharide LPS-mediated soluble TNF receptor release and TNF receptor expression by monocytes. Role of CD14, LPS binding protein, and bactericidal/permeability-increasing protein. J Immunol 152: 5070-5076, 1994.
34. Hobler SC, Williams A, Fischer D, et al. Activity and expression of the 20S proteasome are increased in skeletal muscle during sepsis. Am J Physiol 277: R434-440, 1999.
35. Minnaard R, Wagenmakers AJ, Combaret L, et al. Ubiquitin-proteasome-dependent proteolytic activity remains elevated after zymosan-induced sepsis in rats while muscle mass recovers. Int J Biochem Cell Biol 37: 2217-2225, 2005.
36. Pahl HL. Activators and target genes of Rel/NF-kappaB transcription factors. Oncogene 18: 6853-6866, 1999.
37. Karin M. The beginning of the end: IkappaB kinase (IKK) and NF-kappaB activation. J Biol Chem 274: 27339-27342, 1999.
38. Acharyya S, Ladner KJ, Nelsen LL, et al. Cancer cachexia is regulated by selective targeting of skeletal muscle gene products. J Clin Invest 114: 370-378, 2004.
39. Jones SW, Hill RJ, Krasney PA, O'Conner B, Peirce N, and Greenhaff PL. Disuse atrophy and exercise rehabilitation in humans profoundly affects the expression of genes associated with the regulation of skeletal muscle mass. Faseb J 18: 1025-1027, 2004.
40. Tisdale MJ. The ubiquitin-proteasome pathway as a therapeutic target for muscle wasting. J Support Oncol 3: 209-217, 2005.
41. Strassmann G, Fong M, Kenney JS, and Jacob CO. Evidence for the involvement of interleukin 6 in experimental cancer cachexia. J Clin Invest 89: 1681-1684, 1992.

42. Fong Y, Moldawer LL, Marano M, et al. Cachectin/TNF or IL-1 alpha induces cachexia with redistribution of body proteins. Am J Physiol 256: R659-665, 1989.
43. Argiles JM, Busquets S, and Lopez-Soriano FJ. The pivotal role of cytokines in muscle wasting during cancer. Int J Biochem Cell Biol 37: 1609-1619, 2005.
44. Wyke SM and Tisdale MJ. NF-kappaB mediates proteolysis-inducing factor induced protein degradation and expression of the ubiquitin-proteasome system in skeletal muscle. Br J Cancer 92: 711-721, 2005.
45. Langen RC, Schols AM, Kelders MC, Wouters EF, and Janssen-Heininger YM. Enhanced Myogenic Differentiation by Extracellular Matrix Is Regulated at the Early Stages of Myogenesis. In Vitro Cell Dev Biol Anim 39: 163-169, 2003.
46. Van der Velden JL, Langen RC, Kelders MC, Wouters EF, Janssen-Heininger YM, and Schols AM. Inhibition of glycogen synthase kinase-3beta activity is sufficient to stimulate myogenic differentiation. Am J Physiol Cell Physiol 290: C453-462, 2006.

7

General Discussion

General Discussion

In this thesis we investigated the mechanisms that underlie muscle wasting during sepsis and cancer. During the acute phase of sepsis muscle wasting is beneficial, because it supplies amino acids for gluconeogenesis and for the production of acute phase proteins and antibodies. However, if muscle wasting is sustained during later stages the negative effects of muscle atrophy outweigh the beneficial effects most of the time. Extensive muscle wasting delays the ambulation of septic patients and, when the respiratory muscles are affected, leads to an increased risk of pulmonary complications and prolonged ventilatory support. While it is evident that an increased production of inflammatory mediators is necessary to fight invading pathogens during sepsis, cancer patients also frequently have increased levels of circulating (pro)inflammatory mediators. These (pro)inflammatory mediators are implicated in the development of cancer cachexia, a common complication in cancer patients. Cancer cachexia reflects a loss of both fat and muscle mass, and is associated with an increased mortality and morbidity.
Muscle atrophy during both sepsis and cancer has been shown to occur mainly through an increased proteolysis by the ubiquitin-proteasome pathway. Therefore, this thesis aimed to investigate the regulation and activation of this pathway during sepsis and cancer.

Muscle atrophy during sepsis

In our experiments we used zymosan injections to induce sepsis in rats. Zymosan injection rendered these rats catabolic for a period of 5-6 days, evidenced by the decrease of body and muscle mass during this period. This could be partly ascribed to a decreased food intake, as was evidenced by the apparent muscle wasting in pair-fed rats. However, muscle wasting occurred to a significantly smaller degree in these rats than in the zymosan-treated rats (**chapter 2**). The catabolic phase is followed by a prolonged recovery phase, during which body and muscle mass slowly recover. A decrease of the mean muscle fiber cross-sectional area (CSA) after zymosan injection nicely matched the observed muscle wasting. Interestingly, we showed less of a decrease in muscle fiber CSA in slow-twitch type 1 fibers compared to faster type 2A and 2B fibers. It is known that muscles

composed of fast-twitch fibers (e.g. EDL muscle) atrophy more rapidly in response to sepsis than muscles composed of slow-twitch fibers (e.g. soleus muscle) (1-3). We showed that this is a true fiber-type specific effect, present within one muscle, and suggested a differential response of proteasome activity as a potential explanation.

Because it is important for septic patients to preserve their muscle function, we addressed the question of whether zymosan injections can hamper muscle function by other mechanisms than a reduction of muscle mass. This question is based on findings in critically ill patients, suggesting that muscle weakness in these patients reflects neuropathy (critical illness neuropathy) or myopathy (critical illness, thick filament and necrotizing myopathy) in addition to muscle atrophy (4). Moreover, it has been shown in rats that endotoxin administration induces a rapid decrease of *in vitro* force generating capacity, potentially through free radical induced damage (5-7). In **chapter 2**, we indeed showed that the dorsal flexor muscles of zymosan-treated rats produced less force upon electrical stimulation. However, the lower force output was completely accounted for by the reduction of muscle mass. Thus, during the observed time-course neuropathy or a deranged excitation-contraction coupling plays a negligible role in the development of muscle weakness after zymosan injection. In critically ill patients neuropathies and myopathies have been associated with the use of steroids and muscle relaxants, possibly explaining the discrepancy with our findings (4, 8). Thus, irrespective of the presence of neuropathy or myopathy, muscle atrophy is a major factor in the development of muscle weakness and therefore it is crucial to understand the mechanisms underlying sepsis-induced muscle atrophy in order to develop interventions to preserve muscle function.

Activation of the ubiquitin-proteasome pathway in skeletal muscle during sepsis

From experiments using animal models of sepsis it is known that mainly an increased proteolysis through the ubiquitin-proteasome (Ub-P) pathway is responsible for the observed muscle atrophy, although a decreased protein synthesis also contributed in some studies (9-11). In **chapter 3** we focused on the skeletal muscle activity of the Ub-P pathway after zymosan injection. Theoretically, the rate of proteolysis can be regulated at many levels in the

pathway, because it is a complex cascade of reactions. We investigated the rate at which the two main steps in Ub-P dependent proteolysis, i.e. ubiquitin-conjugation (or ubiquitination) and actual protein degradation by the proteasome, proceeded upon zymosan injection. As most studies only investigated the Ub-P pathway during the acute catabolic phase of sepsis, we considered it important to include measurements during recovery. The zymosan model is suitable for this purpose, because in contrast to the commonly used CLP (cecal ligation and puncture) model of sepsis it produces a prolonged recovery phase (12). We showed that both an increased ubiquitination and proteasome activity are implicated in muscle atrophy during the catabolic phase after zymosan injection. However, it cannot be concluded from our experiments which process is rate-limiting for Ub-P dependent proteolysis during sepsis. Several steps in the Ub-P pathway have been suggested to be rate-limiting in various catabolic conditions. Data from mice lacking any of two crucial Ub-ligases (MuRF1 and MAFbx) support a rate-limiting role for the ubiquitination machinery (13). Ablation of these muscle-specific E3 Ub-ligases partially rescued muscles from denervation-induced muscle atrophy, suggesting a crucial role of these ligases in regulating Ub-P dependent proteolysis. For this reason, and because MuRF1 and atrogin-1/MAFbx have been shown to be invariably induced in many catabolic animal models, MuRF1 and atrogin-1/MAFbx are considered key mediators of muscle atrophy (13-15). In contrast, the accumulation of Ub-conjugates in muscles of septic and tumor-bearing rats suggested that the degradation of these conjugates by the proteasome was the limiting factor (16, 17). Our findings of increased proteasome peptidase activities upon zymosan injection support, but do not prove, this notion. The increased proteasome activities probably reflect increased specific activities, rather than increased amounts of proteasomes, for we observed no change in the protein level of a 20S proteasome subunit. Although the regulation of the proteasome active sites is largely unknown, allosteric changes and (de)phosphorylation of proteasome subunits have been suggested as potential mechanisms (18, 19). Our findings of increased proteasome peptidase activities as early as 2h after zymosan injection support the involvement of such a fast-acting regulatory mechanism. Perhaps the most striking observation was, however, that proteasome peptidase activities remained at a high level during recovery from the zymosan challenge (11d). Assuming that the increased proteasome activities reflect increased rates of

muscle proteolysis, muscle protein synthesis must be simultaneously increased to bring about the partial restoration of muscle mass at this time point. This observation may also indicate a role for the Ub-P pathway in muscle remodeling after recovery from a septic challenge.

A role for the Ub-P pathway has not only been suggested in muscle remodeling during recovery from sepsis, but may also be involved in the adaptive response of skeletal muscle to contractile activity (or exercise). Muscle fiber typology is known to adapt to periods of use and disuse. Chronic low frequency stimulation has been proven a potent model to induce shifts in muscle myosin heavy chain isoforms towards predominantly slow oxidative fibers. It has been shown that this shift is accompanied by a sharp activation of the Ub-P pathway, suggesting a role for the pathway in muscle remodeling (20). Apart from its effect on protein mass, resistance exercise also affects muscle fiber typology in rats (21, 22). In both processes, the role of proteolysis, and Ub-P dependent proteolysis in particular, has not been investigated in great detail. Thus, in **chapter 5** we aimed to explore the role of the Ub-P pathway in skeletal muscle after high-intensity activity. To this end, rat muscles were unilaterally stimulated using an isometric, high-intensity training protocol, and total protein breakdown, ubiquitin-conjugation rates and proteasome activities were measured both 2h and 4h post-exercise. Overall, we showed that protein breakdown rates, measured *in vitro* using muscle incubations, were largely unchanged in the EDL and soleus muscles post-exercise, except for a small decrease at 2h in the soleus muscle. Accordingly, proteasome activities (in the gastrocnemius lateralis muscle) were not affected by the exercise bout. Interestingly, ubiquitin-conjugation rates were increased both 2h and 4h post-exercise, indicating that at least a specific set of muscle proteins is increasingly targeted for breakdown. Our data suggest that increasing the rate of ubiquitin-conjugation to muscle proteins may be involved in muscle remodeling upon high-resistance exercise. Although our data are not conclusive because of the limited number of rats they identify the ubiquitination process as an important target for future investigations into muscle remodeling.

Mechanisms regulating muscle atrophy during cancer

Proinflammatory cytokines (TNFα most notably) have been implicated in the activation of the Ub-P pathway during muscle atrophy in both sepsis

and cancer. In addition, experimental work provided evidence for a crucial role of the transcription factor NF-κB in the intracellular signaling of Ub-P pathway activation (23, 24). In **chapter 6** we aimed to translate these findings to the human patient setting. In this chapter we investigated if the Ub-P pathway was activated in muscle biopsies of newly-diagnosed non-small cell lung cancer (NSCLC) patients, and if this was associated with an activation of muscular NF-κB and systemic inflammation. The NSCLC patients had a mean weight loss of 4%, mainly reflected in a decreased fat mass. Because of the limited weight loss of the patients, this study describes the early events that may lead to Ub-P pathway activation and muscle atrophy. From a therapeutical standpoint it is important to identify markers or triggers of muscle atrophy at this stage, because muscle atrophy may still be reversed or prevented. We showed an association between plasma inflammatory mediators and a marker of skeletal muscle NF-κB activity in the NSCLC patients. These data are the first to link systemic inflammation to muscular NF-κB activity in cancer patients, and therefore support the idea that also in patients pro-inflammatory cytokines trigger muscle atrophy in an NF-κB dependent manner. The other major finding in the NSCLC patients was a trend towards increased MuRF1 mRNA levels, while no change was observed in atrogin-1/MAFbx mRNA and proteasome activities. This suggests that MuRF1 may be involved in initiating skeletal muscle Ub-P pathway activation in an early stage of weight loss. Interestingly, in a recent paper it was shown that a continuous muscular activation of NF-κB in mice caused an upregulation of MuRF1 mRNA and no change in atrogin-1/MAFbx (24). The authors proposed a signalling scheme in which cachectic factors such as cytokines and the tumor-derived proteolysis inducing factor (PIF) induce MuRF1 expression through NF-κB activation, resulting in increased Ub-P dependent proteolysis and muscle atrophy. Our findings support the presence of this cytokine signaling scheme in NSCLC patients. However, it is unlikely that this is the only signaling route for increasing Ub-P pathway activity, because atrogin-1/MAFbx has been shown to be induced in skeletal muscle in several models of cancer cachexia (14). In addition, p38 MAPK has recently been proposed as the trigger for upregulation of MAFbx in skeletal muscle upon stimulation with TNFα (25).

Although the mechanisms that cause muscle atrophy during cancer cachexia are beginning to be unraveled in studies using animals or cell

systems, it is still a challenge to translate these findings to the patient setting. Our data contribute to this translation by showing an association between systemic inflammation and muscular markers of NF-κB, and by showing that the upregulation of MuRF1 may be an early event involved in muscle atrophy in NSCLC patients. A pitfall of including a group with no apparent cachexia is that it is not known which of these patients will actually develop cachexia when the disease progresses. Sixty percent of NSCLC patients eventually develop substantial weight loss (26). Longitudinal studies, involving different stages of cachexia, are therefore indicated to confirm the role of NF-κB and the Ub-P pathway in the development of muscle atrophy during NSCLC. An understanding of these fundamental processes can then be used to design targeted interventions to prevent or reverse muscle atrophy in cancer patients.

Future directions

Many issues still remain to be addressed regarding the role of the Ub-P pathway in muscle atrophy. Probably the most important issue is to translate the findings from experiments using cell systems or animals to the human catabolic patient. While there is some evidence associating an activation of the Ub-P pathway with muscle atrophy in patients, a key role of this pathway in human muscle atrophy still remains to be firmly established. In addition to this, there are several mechanistic issues that need to be solved. Insight into the precise mechanisms of ubiquitination and proteasomal degradation is necessary to invent new drugs or therapies to prevent or reverse muscle atrophy during several catabolic diseases. Because the Ub-P pathway is also involved in other important processes such as cell-cycle regulation, antigen presentation and transcriptional regulation, these therapies should be aimed at specific sites of the pathway or at specific protein targets to prevent toxicity. The first important mechanistic issue regards the specificity of the Ub-P pathway. Although the E3 Ub-ligases are thought to confer the pathway its specificity, their target proteins remain largely unknown. With respect to muscle atrophy, it would be very important to know which E3 ligases are responsible for the degradation of the major myofibrillar and cytoskeletal proteins, but also of important growth and transcription factors. Moreover, identifying the substrates of MuRF1 and atrogin-1/MAFbx will provide crucial information,

because these E3 ligases have been implicated in many conditions of muscle atrophy. In contrast to the key role of these ubiquitinating enzymes, relatively little is known about the role of deubiquitinating enzymes in muscle atrophy. More information is also needed about the signals that mark proteins for degradation and the mechanisms that increase proteasome activity during conditions of muscle atrophy.

It should also be emphasized that Ub-P associated muscle wasting not only occurs in diseases classically related to loss of muscle mass (sepsis, cancer cachexia, COPD, quadriplegia, etc.), but also in, for instance, type 2 diabetes. In type 2 diabetes maintenance of muscle mass is critical as muscle is the major organ for post-prandial glucose uptake, the defective process in type 2 diabetes. Hence, it is also of importance for type 2 diabetics to do the utmost to maintain muscle mass. So far, little is known about the involvement of the Ub-P pathway in the slow but progressive loss of muscle mass in type 2 diabetic patients. As this population of patients is readily growing, further studies are required to identify powerful targets for intervention with the aim to prevent the loss of muscle mass. The elderly constitute another large population characterized by slow but progressive muscle wasting, and therefore it is also critical to study the role of the Ub-P pathway in aging-induced muscle atrophy.

It has been emphasized many times in this thesis that several conditions of muscle atrophy share common mechanisms for activating the Ub-P pathway. However, to be able to develop targeted interventions, it is important to identify the triggers and signaling routes that are specific for each catabolic condition.

References

1. Hasselgren PO, James JH, Benson DW, et al. Total and myofibrillar protein breakdown in different types of rat skeletal muscle: effects of sepsis and regulation by insulin. Metabolism 38: 634-640, 1989.
2. Tiao G, Lieberman M, Fischer JE, and Hasselgren PO. Intracellular regulation of protein degradation during sepsis is different in fast- and slow-twitch muscle. Am J Physiol 272: R849-856, 1997.
3. Vary TC and Kimball SR. Sepsis-induced changes in protein synthesis: differential effects on fast- and slow-twitch muscles. Am J Physiol 262: C1513-1519, 1992.
4. Hund E. Neurological complications of sepsis: critical illness polyneuropathy and myopathy. J Neurol 248: 929-934, 2001.

5. el-Dwairi Q, Comtois A, Guo Y, and Hussain SN. Endotoxin-induced skeletal muscle contractile dysfunction: contribution of nitric oxide synthases. Am J Physiol 274: C770-779, 1998.
6. Supinski G, Nethery D, Stofan D, and DiMarco A. Comparison of the effects of endotoxin on limb, respiratory, and cardiac muscles. J Appl Physiol 81: 1370-1378, 1996.
7. Supinski G, Nethery D, Nosek TM, Callahan LA, Stofan D, and DiMarco A. Endotoxin administration alters the force vs. pCa relationship of skeletal muscle fibers. Am J Physiol Regul Integr Comp Physiol 278: R891-896, 2000.
8. Wagenmakers AJ. Muscle function in critically ill patients. Clin Nutr 20: 451-454, 2001.
9. Tiao G, Fagan JM, Samuels N, et al. Sepsis stimulates nonlysosomal, energy-dependent proteolysis and increases ubiquitin mRNA levels in rat skeletal muscle. J Clin Invest 94: 2255-2264, 1994.
10. Voisin L, Breuille D, Combaret L, et al. Muscle wasting in a rat model of long-lasting sepsis results from the activation of lysosomal, Ca2+ -activated, and ubiquitin-proteasome proteolytic pathways. J Clin Invest 97: 1610-1617, 1996.
11. Jagoe RT and Goldberg AL. What do we really know about the ubiquitin-proteasome pathway in muscle atrophy? Curr Opin Clin Nutr Metab Care 4: 183-190, 2001.
12. Rooyackers OE, Saris WH, Soeters PB, and Wagenmakers AJ. Prolonged changes in protein and amino acid metabolism after zymosan treatment in rats. Clin Sci (Lond) 87: 619-626, 1994.
13. Bodine SC, Latres E, Baumhueter S, et al. Identification of ubiquitin ligases required for skeletal muscle atrophy. Science 294: 1704-1708, 2001.
14. Gomes MD, Lecker SH, Jagoe RT, Navon A, and Goldberg AL. Atrogin-1, a muscle-specific F-box protein highly expressed during muscle atrophy. Proc Natl Acad Sci U S A 98: 14440-14445, 2001.
15. Glass DJ. Skeletal muscle hypertrophy and atrophy signaling pathways. Int J Biochem Cell Biol 37: 1974-1984, 2005.
16. Baracos VE, DeVivo C, Hoyle DH, and Goldberg AL. Activation of the ATP-ubiquitin-proteasome pathway in skeletal muscle of cachectic rats bearing a hepatoma. Am J Physiol 268: E996-1006, 1995.
17. Tiao G, Fagan J, Roegner V, et al. Energy-ubiquitin-dependent muscle proteolysis during sepsis in rats is regulated by glucocorticoids. J Clin Invest 97: 339-348, 1996.
18. Mason GG, Hendil KB, and Rivett AJ. Phosphorylation of proteasomes in mammalian cells. Identification of two phosphorylated subunits and the effect of phosphorylation on activity. Eur J Biochem 238: 453-462, 1996.
19. Orlowski M and Wilk S. Ubiquitin-independent proteolytic functions of the proteasome. Arch Biochem Biophys 415: 1-5, 2003.
20. Ordway GA, Neufer PD, Chin ER, and DeMartino GN. Chronic contractile activity upregulates the proteasome system in rabbit skeletal muscle. J Appl Physiol 88: 1134-1141, 2000.
21. Haddad F, Qin AX, Zeng M, McCue SA, and Baldwin KM. Effects of isometric training on skeletal myosin heavy chain expression. J Appl Physiol 84: 2036-2041, 1998.
22. Caiozzo VJ, Haddad F, Baker MJ, and Baldwin KM. Influence of mechanical loading on myosin heavy-chain protein and mRNA isoform expression. J Appl Physiol 80: 1503-1512, 1996.

23. Li YP, Lecker SH, Chen Y, Waddell ID, Goldberg AL, and Reid MB. TNF-alpha increases ubiquitin-conjugating activity in skeletal muscle by up-regulating UbcH2/E220k. Faseb J 17: 1048-1057, 2003.
24. Cai D, Frantz JD, Tawa NE, Jr., et al. IKKbeta/NF-kappaB activation causes severe muscle wasting in mice. Cell 119: 285-298, 2004.
25. Li YP, Chen Y, John J, et al. TNF-alpha acts via p38 MAPK to stimulate expression of the ubiquitin ligase atrogin1/MAFbx in skeletal muscle. Faseb J 19: 362-370, 2005.
26. Bruera E. ABC of palliative care. Anorexia, cachexia, and nutrition. Bmj 315: 1219-1222, 1997.

Summary – Samenvatting

Summary

Muscle wasting occurs as a result of several diseases, including sepsis and cancer. When this loss of muscle mass is extensive it is very detrimental to the patient. Extensive muscle wasting is associated with an impaired prognosis and increased mortality rates. Moreover, muscle wasting limits patients in performing the activities of daily living and prolongs recovery. Since muscles are mainly built from proteins, it is the muscle protein mass that determines muscle mass and function. Muscle proteins are continuously synthesized and degraded (protein turnover). A continuous turnover is necessary to replace damaged or dysfunctional proteins. In healthy persons, muscle protein synthesis and breakdown are balanced and muscle protein mass does not change. During disease, muscle protein degradation can become larger than protein synthesis, causing the muscle protein mass to decrease. It is now known that during several diseases an increased protein breakdown is largely responsible for the observed muscle wasting. Although several molecular mechanisms exist to degrade proteins, muscle proteins are mainly degraded by the ubiquitin-proteasome (Ub-P) pathway. This pathway is an intricate network of different enzymes and protein structures that work together to specifically degrade many different muscle proteins. Basically, protein degradation by this pathway can be divided in two main steps. Firstly, muscle proteins are bound with a chain of ubiquitin molecules, 'marking' them for degradation. A large protein structure called the proteasome recognizes the 'marked' proteins, after which the proteins enter the proteasome where they are degraded to small pieces (peptides). This pathway of protein breakdown is active in muscle continuously, providing a constant rate of protein breakdown. However, during for example infectious diseases (like sepsis) or cancer the Ub-P pathway is activated beyond the normal level, leading to an increased protein breakdown and muscle wasting. Thus, to develop interventions to prevent muscle wasting during these diseases, it is crucial to understand the exact mechanisms activating the Ub-P pathway. In this thesis we therefore aimed to study the regulation and activation of the Ub-P pathway during sepsis and cancer, two diseases in which muscle wasting is a common problem.

In our experiments we used zymosan injections in rats as an experimental model of sepsis. In **chapter 2** we characterized the zymosan sepsis model with respect to muscle wasting and function. Zymosan injection caused a

large drop in both body and muscle mass in these rats, 5-6 days after which body and muscle mass slowly started to recover. Muscle wasting occurred very rapidly after zymosan injection with a maximum loss of 35-40% measured on day 6 in both the tibialis anterior and gasctrocnemius muscles (two lower leg muscles). Not surprisingly, we found that these muscles had a lower functional capacity. Strikingly, muscle quality did not change as a result of sepsis, an observation which has been described during sepsis. In **chapter 2**, we also studied the effect of sepsis on muscle fibers. Muscles are composed of bundles of these small fibers. Several types of muscle fibers exist, each with different functional capacities. Roughly, type 1 fibers are slow, develop a low maximal force, but have great endurance, whereas type 2 fibers are fast, develop a high maximum force, but fatigue rapidly. As expected, we found that muscle wasting led to a decrease of cross-sectional area in both fiber types. In type 2 fibers, this decrease was much larger than in type 1 fibers. Thus, type 1 fibers are more resistant to muscle wasting during sepsis than type 2 fibers. To explain this phenomenon we compared the activity of the proteasome during sepsis between muscles with mainly type 1 fibers and muscles with mainly type 2 fibers. We showed an increased activity during sepsis in the type 2 fiber muscle but not in the type 1 fiber muscle, showing that probably sepsis increases protein breakdown more in type 2 muscle fibers than in type 1 muscle fibers.

In **chapter 3**, we studied the activation of the Ub-P pathway in rat skeletal muscle after zymosan injection. As explained above, the two main steps in muscle protein degradation by the Ub-P pathway are the binding of ubiquitin molecules to muscle proteins, and the degradation of these proteins by the proteasome. We found that after zymosan injection, both processes were activated. Muscle proteins were increasingly bound with ubiquitin, implying an activation of the cascade of 'ubiquitination'-enzymes after zymosan injection. In addition, muscle proteasomes were more active (faster protein degradation) after zymosan injection. Our experiments showed that an increased Ub-P pathway activity is likely to play a role in causing muscle wasting during sepsis and that this pathway is activated at different levels.

Several animal studies show that the Ub-P pathway is also involved in muscle wasting observed during cancer. The condition in which cancer patients lose body weight (both muscle mass and fat mass) very rapidly is called cachexia. In animal experiments it has been suggested that the

transcription factor NF-κB is activated in the muscle and that this triggers muscle wasting by activating muscle protein breakdown by the Ub-P pathway. In **chapter 6**, we aimed to study this hypothesis in muscle biopsies of lung cancer patients. Cachexia is a common problem in lung cancer patients and therefore it is crucial to understand the underlying mechanisms to develop interventions to prevent this condition. We showed that one of the key ubiquitinating enzymes, Muscle Ring-Finger protein 1 (MuRF1), may be involved in muscle wasting at an early stage. A limited decrease of body and muscle mass is likely to explain why we did not observe additional evidence for an activation of the Ub-P pathway in the lung cancer patients. Cancer patients commonly show a low-grade systemic inflammation, which has been implicated as a cause of cachexia. Interestingly, we showed an association between markers of NF-κB activity and the inflammatory state of the patients. This observation provides the first link between inflammation and muscle NF-κB activity in cancer patients, and suggests that also in humans NF-κB may play a central role in causing muscle wasting during cancer.

Another factor that has been implicated in causing cachexia is an increased energy expenditure. The uncoupling protein 3 (UCP3) has been studied for its effect on energy expenditure. However, it is now clear that UCP3 is not involved in regulating energy expenditure during cachexia, and alternative hypotheses about its role have been postulated. In **chapter 4**, we investigated the hypothesized role for UCP3 in the defense against oxidative damage during muscle wasting. We show that during muscle wasting induced by zymosan injections UCP3 protein content in the muscle is increased together with an increased abundance of the highly reactive substance 4-hydroxy-2-nonenal (4-HNE). 4-HNE is a highly reactive substance which can cause muscle damage. This shows that UCP3 indeed may fulfill the hypothesized function during periods of muscle wasting and oxidative stress.

A lot of research has been done on the role of protein breakdown and the Ub-P pathway during periods of muscle wasting. In contrast, protein breakdown has been hardly investigated during periods of gain of muscle mass. Resistance exercise has been shown to lead to an increase of muscle mass. There is a lot of evidence showing that an increased rate of protein synthesis in the muscle after this type of exercise is the main cause for the increased muscle mass. However, to get a complete picture more should be

known about the response of protein breakdown. In **chapter 5**, we therefore investigated the short-term effect of high-resistance exercise on protein breakdown and the activity of the Ub-P pathway in rat muscles. We showed that protein breakdown was largely unchanged shortly after a high-resistance exercise protocol, as was the activity of the proteasome. Interestingly, however, we showed that the binding of ubiquitin to muscle proteins was increased after the exercise bout. This implicates that at least some muscle proteins are increasingly 'tagged' to be broken down by the proteasome. We suggest that this may be a mechanism of the muscle to adapt its protein composition to the exercise.

To summarize, our data show that the Ub-P pathway is involved in muscle wasting during sepsis and cancer and that this pathway can be activated at different levels in the cascade of reactions leading to protein degradation by the proteasome. In future studies, however, more information is needed about the triggers activating the Ub-P pathway in each disease. Moreover, to be able to develop targeted interventions more effort is needed to identify the exact muscle proteins that are targeted by the Ub-P pathway during conditions of muscle wasting.

Samenvatting

Spiermassaverlies kan optreden als gevolg van verschillende ziektes, waaronder sepsis en kanker. Als dit massaverlies grote vormen aanneemt, heeft dit ernstige gevolgen voor de patiënt. Deze patiënten hebben een slechtere prognose en een hogere mortaliteit als gevolg van hun ziekte. Spiermassaverlies leidt tot problemen in het uitvoeren van de activiteiten van het dagelijkse leven en vertraagt het herstel van de patiënt.
Omdat spieren hoofdzakelijk opgebouwd zijn uit eiwitten, is het de eiwitmassa van de spier die de totale spiermassa en -functie bepaalt. In de spier is er sprake van een constante aanmaak en afbraak van eiwitten (eiwit turnover). Deze constante turnover houdt de spier als het ware 'gezond' door ervoor te zorgen dat beschadigde of niet functionele eiwitten vervangen worden. In gezonde personen houden de eiwitaanmaak en -afbraak in de spier elkaar in balans, wat betekent dat de spiermassa constant blijft. In geval van ziekte kan de eiwitafbraak groter worden dan de eiwitaanmaak, waardoor de spiermassa afneemt. Uit verschillende studies is gebleken dat dit spiermassaverlies voornamelijk veroorzaakt wordt door een toename van de eiwitafbraak in de spier. Hoewel de spier beschikt over verschillende moleculaire mechanismen om eiwitten af te breken, wordt kwantitatief de grootste hoeveelheid eiwitten afgebroken via het ubiquitine-proteasome (Ub-P) systeem. Dit systeem is een ingewikkelde cascade van enzymen en andere eiwitstructuren die samenwerken om specifiek een groot aantal eiwitten af te breken. Ruwweg kan het Ub-P systeem onderverdeeld worden in 2 stappen. In de eerste stap wordt er een keten van ubiquitine moleculen gebonden aan een spiereiwit, waardoor dit eiwit gemarkeerd wordt om afgebroken te worden. Een grote eiwitstructuur genaamd het proteasoom herkent de gemerkte eiwitten, waarna de eiwitten opgenomen worden in het proteasoom, waar ze vervolgens afgebroken worden tot kleine stukken (peptiden). Het Ub-P systeem is continu actief in de spier, waardoor er een constante afbraak van eiwitten plaatsvindt. Tijdens infecties (sepsis) of kanker wordt dit systeem geactiveerd, waardoor de spiereiwitafbraak verhoogd wordt en er spiermassaverlies optreedt. Om dit spiermassaverlies tegen te gaan, is het daarom cruciaal om de exacte mechanismen te begrijpen die leiden tot een activatie van het Ub-P systeem tijdens deze aandoeningen. De studies beschreven in dit proefschrift hebben daarom als doel de regulatie en de activatie van het Ub-P systeem te bestuderen tijdens

sepsis en kanker, twee aandoeningen waarin spiermassaverlies een veel voorkomend probleem is.
In de studies beschreven in dit proefschrift is gebruik gemaakt van een proefdiermodel voor sepsis, namelijk het injecteren van ratten met een zymosan-suspensie. In **hoofdstuk 2** wordt beschreven wat het effect van sepsis is op de spiermassa en -functie van deze ratten. Injectie met zymosan had een groot verlies van lichaamsgewicht en spiermassa tot gevolg, gevolgd door een langzaam herstel hiervan vanaf dag 5-6 na injectie. Een maximaal verlies van 35-40% van de spiermassa werd gemeten in de tibialis anterior en gastrocnemius spieren, 2 onderbeenspieren, op dag 6 na injectie. Tevens werd een groot verlies van functie gemeten in deze spieren. Opvallend echter was dat de spierkwaliteit intact bleef na zymosan injectie. Een verlies van spierkwaliteit en problemen met de aansturing van de spier zijn namelijk beschreven tijdens sepsis. In **hoofdstuk 2** zijn ook de effecten van sepsis op afzonderlijke spiervezels bestudeerd. Spieren zijn opgebouwd uit bundels van deze kleine vezels. Spiervezels zijn onder te verdelen in verschillende types, elk met verschillende kenmerken. In het algemeen zijn type 1 spiervezels langzaam, ontwikkelen een geringe maximale kracht, maar hebben een groot uithoudingsvermogen, terwijl type 2 spiervezels snel zijn, een grote maximale kracht ontwikkelen, maar een gering uithoudingsvermogen hebben. Zoals verwacht leidde het spiermassaverlies na zymosan injectie tot een afname van de dwarsdoorsnede van de spiervezels. Deze afname bleek echter veel groter in type 2 spiervezels, wat er op duidt dat type 1 vezels meer bestand zijn tegen spiermassaverlies tijdens sepsis dan type 2 vezels. Als verklaring voor dit fenomeen laten we zien dat in type 2 spiervezels de activiteit van het proteasoom toeneemt tijdens sepsis, terwijl dit niet het geval lijkt in type 1 spiervezels.
Vervolgens wordt in **hoofdstuk 3** dieper ingegaan op de manier waarop het Ub-P systeem geactiveerd wordt in de spier tijdens sepsis. Zoals hierboven beschreven staat, zijn de twee belangrijkste stappen in de eiwitafbraak door het Ub-P systeem de binding van ubiquitine moleculen aan spiereiwitten, gevolgd door de afbraak van deze eiwitten door het proteasoom. We laten zien dat tijdens sepsis beide processen versneld worden. Tijdens sepsis werden ubiquitine moleculen in grotere mate gebonden aan spiereiwitten, wat betekent dat de cascade van 'ubiquitinatie'-enzymen verhoogd actief is. Ook bleek dat het proteasoom geactiveerd werd (snellere eiwitafbraak) tijdens sepsis. Onze experimenten laten zien dat het Ub-P systeem een

belangrijke rol speelt in het spiermassaverlies tijdens sepsis en dat dit systeem op verschillende niveaus geactiveerd wordt.
Proefdierstudies laten zien dat het Ub-P systeem ook betrokken is bij het spiermassaverlies dat optreedt als gevolg van kanker. Het proces waarin kankerpatiënten als het ware uitgemergeld raken als gevolg van een groot verlies van lichaamsgewicht (zowel spier- als vetmassa) wordt cachexie genoemd. In proefdierstudies wordt gesuggereerd dat de transcriptiefactor NF-κB geactiveerd wordt in de spier tijdens kanker, dat op zijn beurt het Ub-P systeem activeert en zodoende spiermassaverlies veroorzaakt. In **hoofdstuk 6** hebben we deze hypothese getest in een groep longkankerpatiënten. Cachexia is een veelvoorkomend probleem bij longkanker en daarom is het cruciaal om de achterliggende mechanismen hiervan te bestuderen, teneinde interventies ter preventie van cachexie te ontwikkelen. We laten zien dat één van de sleutelenzymen in de ubiquitinatie van spiereiwitten, genaamd Muscle Ring-Finger protein 1 (MuRF1), mogelijk in een vroeg stadium betrokken is bij het spiermassaverlies. Een gering verlies van lichaamsgewicht en spiermassa verklaart waarschijnlijk waarom we geen additionele bewijzen vonden voor een activatie van het Ub-P systeem in de patiënten. Onderzoek heeft aangetoond dat bij kankerpatiënten bepaalde ontstekingsstoffen vrijkomen, die een rol spelen bij de ontwikkeling van spiermassaverlies. Interessant in dit opzicht is de aanwezigheid van een associatie tussen de aanwezigheid van deze ontstekingsstoffen in de patiëntengroep en de activiteit van NF-κB in de spier. Dit verband suggereert dat NF-κB mogelijk ook in kankerpatiënten een centrale rol speelt in het ontwikkelen van spiermassverlies.
Een toename van het energiegebruik is ook een factor die een rol speelt bij de ontwikkeling van cachexie. Het uncoupling protein 3 (UCP3) eiwit werd in eerste instantie een rol toebedeeld in het veroorzaken van het hoge energiegebruik tijdens cachexie. Uit experimenten bleek echter dat UCP3 niet betrokken is in de regulatie van het energiegebruik en daarom zijn er alternatieve hypotheses opgesteld die de rol van UCP3 beschrijven. In **hoofdstuk 4** hebben we de hypothese getest waarin UCP3 een belangrijke functie heeft in de bescherming tegen oxidatieve schade tijdens spiermassaverlies. We laten zien dat tijdens spiermassaverlies als gevolg van sepsis de hoeveelheid UCP3 eiwit in de spier toeneemt, samen met een toename van de stof 4-hydroxy-2-nonenal (4-HNE). 4-HNE is een stof met

een grote reactiviteit die spierschade kan veroorzaken. Onze experimenten sluiten aan bij de gehypothetiseerde functie van UCP3 tijdens spiermassaverlies en oxidatieve stress.

Veel onderzoek is verricht naar de rol van eiwitafbraak en het Ub-P systeem tijdens condities die gekarakteriseerd worden door spiermassaverlies. Eiwitafbraak is echter nauwelijks bestudeerd tijdens condities waarin de spiermassa juist toeneemt. Van krachttraining is bekend dat het de spieraanwas stimuleert. Tevens blijkt uit vele studies dat een stimulatie van de spiereiwitaanmaak grotendeels verantwoordelijk is voor deze toename van spiermassa. Het effect van krachttraining op de eiwitafbraak is echter nauwelijks bestudeerd. In **hoofdstuk 5** beschrijven we daarom het korte termijn effect van krachttraining op eiwitafbraak en activiteit van het Ub-P systeem in de rattenspier. De resultaten van deze studie laten zien dat kort na een enkele krachttrainingsinspanning er geen toename van de eiwitafbraak in de spier is. Overeenkomstig hiermee vonden we ook geen effect van krachttraining op de activiteit van het proteasoom in de spier. Een interessante bevinding in deze studie was dat één enkele krachttraining leidt tot een toename van de binding van ubiquitine aan spiereiwitten. Dit impliceert dat tenminste een aantal spiereiwitten verhoogd 'gemerkt' wordt om afgebroken te worden door het proteasoom. Dit gegeven suggereert mogelijk dat dit een mechanisme van de spier is om zijn eiwitcompositie aan te passen aan de gevraagde belasting.

Samenvattend kan gesteld worden dat het Ub-P systeem betrokken is bij spiermassaverlies tijdens sepsis en kanker en dat dit systeem geactiveerd wordt op meerdere punten in de cascade van reacties die leidt tot afbraak van spiereiwitten door het proteasoom. Om gerichte interventies te ontwikkelen om dit spiermassaverlies tegen te gaan, is meer kennis nodig over de specifieke triggers die het Ub-P systeem activeren in verschillende aandoeningen. In dit opzicht is het ook cruciaal dat geïdentificeerd wordt welke spiereiwitten doelwit zijn van het Ub-P systeem tijdens spiermassaverlies.

Dankwoord

Dankwoord

Na heel wat werk ligt mijn proefschrift eindelijk voor jullie. Weliswaar is mijn naam de enige die prijkt op de kaft van dit boekje, maar zonder de hulp van velen was dit proefschrift nooit geworden tot wat het nu is. Daarom wil ik iedereen bedanken die een bijdrage heeft geleverd aan dit proefschrift, hetzij praktisch, wetenschappelijk, maar vooral ook mentaal. Een aantal mensen wil ik in het bijzonder noemen.

Ten eerste wil ik mijn co-promotor Matthijs bedanken. Matthijs, bedankt in de eerste plaats voor het vertrouwen dat je in me hebt gehad. Voor ons allebei voelde dit project denk ik een beetje als een sprong in het diepe, omdat het voor ons allebei een relatief nieuw onderzoeksgebied was. Je praktische instelling en je enorme enthousiasme zijn onmisbaar geweest om dit project van de grond te krijgen. Dank voor de vele discussies, het geduld bij onze eerste metingen samen op het dierenlab en je altijd kritische houding. Ondanks dat je vaak hebt gezegd een aantal zaken bij een tweede AIO anders te gaan aanpakken, geloof ik niet dat iemand zich een betere co-promotor kan wensen. Ook wil ik de overige leden van het promotieteam bedanken. Maarten, Ton, Harm, bedankt voor jullie bijdrage!

Vervolgens wil ik de leden van de beoordelingscommissie, Edwin Mariman, Wim Saris, Cees Dejong, Olav Rooyackers en Miel Wouters, bedanken voor het kritisch lezen van het manuscript.

Gert, ook jou ben ik veel dank verschuldigd. Op het lab heb ik veel van je geleerd en op de momenten dat het even tegenzat kon je altijd wel inspringen om de boel over het dode punt heen te trekken. Wat ik erg waardeer is dat ik bij jou eigenlijk voor vanalles en nog wat terecht kan: van labhulp tot wijn/restaurantadvies, of om gewoon alles eens goed te relativeren. Gerrit, ook jij bedankt voor de hulp bij het opzetten van een aantal technieken. Je praktische tips en niet te evenaren handigheid zijn van grote waarde geweest.

Reinout, bedankt voor de plezierige tijd in het begin van mijn AIO-periode. Bedankt voor de discussies, het gezelschap tijdens de verschillende loopjes en je vermogen om op wat voor manier dan ook leven in de brouwerij te brengen. Dank ook voor een leuke tijd samen in Clermont. Kenneth, als oud-kamergenoot heb je zeker bijgedragen aan een fijne AIO-periode. Bedankt voor de voortdurende interesse in mijn onderzoek, de discussies, maar vooral je geweldige nuchterheid en directheid. Ik ben blij dat ik je straks bij de verdediging als paranimf achter me heb staan! Dank ook aan de andere

(oud-)collega's, die de afgelopen jaren hebben gezorgd voor een prettige werksfeer: Ellen, Sofie, Lex, Klien, Mireille, Jantine, Herman, Hans K., Desiree, Jos, Ron, Henk, Lars, Gerard, Fred, Frans, Annette, Jons, Paul, Harry, Leon, Hans S., Eric, Milou, Ellen L., Ruth, Esther P., Esther K., Ali, Wendy, Miranda, René, Ralph, Luc, Gijs, Joris, Johan, Patrick, Vera, Marco en al die personen die ik vergeten ben te vermelden.
Ook wil ik de mensen van Pulmonologie, Ramon, Marco, Anne-Marie en Annemie, heel erg bedanken. Ik denk dat onze samenwerking een extra dimensie heeft toegevoegd aan dit proefschrift. Dank voor de stimulerende discussies en de hulp bij het uitvoeren van de PCR's.
I also would like to thank the people at the Protein Metabolism lab at the INRA instute in Clermont-Ferrand. Didier, thank you for giving me the opportunity to work at your lab together with Reinout, which increased my understanding of the ubiquitin-proteasome pathway enormously. Your help and expert advice have contributed greatly to this thesis. Lydie, thank you for showing us around in the lab and for your expert help with setting up many of the techniques used in this thesis. Daniel B., Daniel T., Sophie, Marie-Noel, Agnes and Amina, thank you for a great time in Clermont!
Als laatste en allerbelangrijkste rest mij nog om mijn familie te bedanken. Pa en Ma, heel erg bedankt voor al jullie steun gedurende al die jaren. Jullie hebben er voornamelijk voor gezorgd dat ik ben wie ik nu ben en dit uiteindelijk heb bereikt. Ik ben er trots op dat ik jullie door middel van dit boekje en straks tijdens de promotie eindelijk kan laten zien wat ik de laatste jaren heb gedaan. Ook René, tweelingbroerje, heel erg bedankt. We trekken al heel ons leven samen op en ik hoop dat dat ook zo zal blijven. Hoewel we in onze studies ieder onze eigen weg zijn gegaan, ben ik er ontzettend blij mee dat je na je studie toch in Maastricht bent gebleven. Het is erg fijn om de steun van iemand die je bijna net zo goed kent als jezelf in de buurt te weten.
Ook mijn schoonouders, Jan en Riet, wil ik bedanken voor het feit dat jullie altijd voor ons klaar staan. Jullie steun is in vele opzichten onmisbaar geweest.
Als laatste wil ik Kirsten bedanken. Niet alleen bedankt voor het corrigeren van dit proefschrift, maar meer nog voor de geweldige tijd samen de laatste 11 jaar. Bedankt voor je geduld, je liefde en je onvoorwaardelijke steun. Ik ben er trots op dat we samen met Viggo nu een gezinnetje vormen! Je bent een supermama!

Curriculum Vitae

Ronnie Minnaard was born on July 12th 1977 in Goes, The Netherlands. In 1995, he completed his pre-university education at the "Buys Ballot College" in Goes. In the same year, he started his study Health Sciences with specialization Movement Sciences at Maastricht University, where he graduated in 2000. His master thesis entitled "The influence of elevated training intensity and frequency on total body glucose uptake and skeletal muscle GLUT4 expression in type II diabetics (NIDDM)" was awarded with the NSK Boymans encouragement prize for young researchers. After completing his master thesis he worked for 6 months as a research assistant at the department of Movement Sciences (Maastricht University), where he worked on the development of an *in vitro* method to measure the uptake of substrates in muscle cells.
In February 2001, he started his PhD at the department of Movement Sciences, Maastricht University, where he accepted a position as a lecturer in July 2005. In August 2006, he is appointed as a post-doctoral fellow at the department of Movement Sciences, Maastricht University.

List of publications

Full papers

1. Minnaard R, Drost MR, Wagenmakers AJM, van Kranenburg GP, Kuipers H, Hesselink MKC. Skeletal muscle wasting and contractile performance in septic rats. Muscle & Nerve 31: 339-348, 2005.

2. Minnaard R, Wagenmakers AJM, Combaret L, Attaix D, Drost MR, van Kranenburg GP, Schaart G, Hesselink MKC. Ubiquitin-proteasome-dependent proteolytic activity remains elevated after zymosan-induced sepsis in rats while muscle mass recovers. Int J Biochem Cell Biol 37: 2217-2225, 2005.

3. Minnaard R, Schrauwen P, Schaart G, Hesselink MKC. UCP3 in muscle wasting, a role in modulating lipotoxicity? Febs Lett (in press, 2006).

4. Minnaard R, Langen RCJ, Kelders MCMJ, Dingemans AC, Hesselink MKC, Schols AMWJ. Ubiquitin-proteasome pathway and NF-κB activity in skeletal muscle of patients with non-small cell lung cancer. Submitted for publication.

5. Ottenheijm CAC, Heunks LMA, Li YP, Ji B, Minnaard R, van Hees HWH, Dekhuijzen PNR. Diaphragm dysfunction in chronic obstructive pulmonary disease: role for the ubiquitin-proteasome pathway. Am J Respir Crit Care Med (in press, 2006).

6. Hesselink MKC, Minnaard R, Schrauwen P. Eat the meat or feed the meat; protein turnover in remodeling muscle. Curr Opin Clin Nutr Metab Care (in press, 2006).

Abstracts

1. Minnaard R, Drost MR, Wagenmakers AJM, Kuipers H, Hesselink MKC. The decrease of muscle fiber cross-sectional area following 2 days of critical illness is fiber type specific. J Muscle Res Cell Motil 24: 376.

2. Minnaard R, Hesselink M. Activation of the skeletal muscle ubiquitin-proteasome system after induction of sepsis. International Biochemistry of Exercise Conference, Maastricht, The Netherlands, 2004.

3. Minnaard R, Hesselink M. Ub-proteasome pathway and muscle wasting in critically ill rats. 2nd Cachexia Conference, Berlin, Germany, 2003.

4. Minnaard R, Langen RCJ, Kelders MCMJ, Hesselink MKC, Schols AMWJ. Ub-proteasome pathway and NF-κB activity in mildly weight-losing cancer patients. 3rd Cachexia Conference, Rome, Italy, 2005.